GPS/INS GENERALIZED EVALUATION TOOL (GIGET) FOR THE DESIGN AND TESTING OF INTEGRATED NAVIGATION SYSTEMS

A DISSERTATION

SUBMITTED TO THE DEPARTMENT OF AERONAUTICS AND ASTRONAUTICS

AND THE COMMITTEE ON GRADUATE STUDIES

OF STANFORD UNIVERSITY

IN PARTIAL FULFILLMENT OF THE REQUIREMENTS

FOR THE DEGREE OF

DOCTOR OF PHILOSOPHY

Jennifer Denise Gautier

June 2003

I certify that I have read this dissertation and that, in my opinion, it is fully adequate in scope and quality as a dissertation for the degree of Doctor of Philosophy.

Professor Bradford W. Parkinson, Principal Advisor

I certify that I have read this dissertation and that, in my opinion, it is fully adequate in scope and quality as a dissertation for the degree of Doctor of Philosophy.

Professor Per K. Enge

I certify that I have read this dissertation and that, in my opinion, it is fully adequate in scope and quality as a dissertation for the degree of Doctor of Philosophy.

Professor Claire J. Tomlin

Approved for the University Committee on Graduate Studies.

Abstract

GIGET, the GPS/INS Generalized Evaluation Tool, experimentally tests, evaluates, and compares navigation systems that combine the Global Positioning System (GPS) with Inertial Navigation Systems (INS).

GPS is a precise and reliable navigation aid but can be susceptible to interference, multipath, or other outages. An INS is very accurate over short periods, but its errors drift unbounded over time. Blending GPS with INS can remedy the performance issues of both. However, there are many types of integration methods, and sensors vary greatly, from the complex and expensive, to the simple and inexpensive. It is difficult to determine the best combination for any desired application; most of the integrated systems built to date have been point designs for very specific applications. GIGET aids in the selection of sensor combinations for any *general* application or set of requirements; hence, GIGET is the generalized way to evaluate the performance of integrated systems.

GIGET is a combination of easily re-configurable hardware and analysis tools that can provide real-time comparisons of multiple integrated navigation systems. It includes a unique, five-antenna, forty-channel GPS receiver providing GPS attitude, position velocity, and timing. An embedded computer with modular real-time software blends the GPS

measurements with sensor information from a Honeywell HG1700 tactical grade inertial measurement unit. GIGET is quickly outfitted onto a variety of vehicle platforms to experimentally test and compare navigation performance.

In side-by-side experiments, GIGET compares loosely coupled and tightly coupled integrated navigation schemes blending navigation, tactical, or automotive grade inertial sensors with GPS. These results formulate a trade study to map previously uncharted territory of the GPS/INS space that trades accuracy and expense versus complexity of design. These GIGET results can be used to determine acceptable sensor quality in these integration methods for a variety of dynamic environments.

As a demonstration of its utility as a hardware evaluation tool, GIGET is used to design a navigation system on the DragonFly Unmanned Air Vehicle (UAV). The DragonFly UAV is a test-bed for autonomous control experiments. It is a small, lightweight, highly maneuverable aircraft that requires smooth, continuous navigation information. GIGET was flown on the DragonFly to evaluate different integrated navigation combinations in the UAV's dynamic environment. GIGET shows that a loosely coupled, single-antenna GPS system with a moderately priced inertial unit will provide the consistent navigation currently needed on the DragonFly.

Acknowledgements

Special thanks go to my thesis advisor, Professor Brad Parkinson, for his direction and encouragement throughout my graduate research here at Stanford University. I especially thank him for his leadership. I believe great leadership involves the ability to teach and instill confidence in other to lead themselves. Prof. Parkinson has helped me to develop my own leadership skills through mentoring and through the inspiration of his own great accomplishments.

The faculty and staff of Stanford University and the Department of Aeronautics and Astronautics have provided a wonderful environment for graduate study. I am also particularly grateful for the advice and guidance of Professors Claire Tomlin, Per Enge, and Dave Powell. Each has provided me with tremendous opportunities and inspiration.

It has been a privilege to work with the students of the GPS Lab and the Hybrid Systems Lab. I am sincerely grateful for all the many friends I have at Stanford. Special thanks go to: Sharon Houck, Demoz Gebre-Egziabher, Roger Hayward, Paul Montgomery, Jung Soon Jang, Rodney Teo, and Gokhan Inalhan.

Many thanks go to Trimble Navigation and Honeywell Labs for their contributions and support. In particular, I thank Scott Smith, Bruce Peetz, Brian Schipper, Larry Vallot, Scott Snyder.

I am also very grateful for my friends and communities of support: St. Mark's Episcopal Church, and Women in Science and Engineering.

Table of Contents

List of Tables

List of Figures

Chapter 1: Introduction

The integration of navigation systems is a common technique to mitigate the errors associated with any single navigation aid. For instance, the Global Positioning System (GPS) blends well with Inertial Navigation Systems (INS); the short-term accuracy of INS allows for coasting between GPS outages. However, there are many methods to blend GPS with INS, and results depend on sensor quality and vehicle dynamics. Most of the integrated systems built to date have been point designs for very *specific* applications. There is a need for a *generalized* tool to aid in the design and selection of GPS/INS combinations. This work describes the development, testing and application of GIGET, the GPS/INS Generalized Evaluation Tool.

1.1 History

GPS and INS are complimentary navigation systems. There exists a long history of blending GPS with INS to remedy the performance issues of both; and there are many methods of GPS/INS integration. This section will briefly introduce the two navigation systems, describe general methods of blending, and present previous research and tools to evaluate integrated systems.

1.1.1 GLOBAL POSITIONING SYSTEM

The NAVSTAR Global Positioning System (GPS) is a satellite navigation system developed as a US Department of Defense joint program in 1973. It became fully operational in 1995 with a minimum of 24 satellites orbiting in six planes at an altitude of approximately 11,000 nmi.

GPS is a ranging system; it provides accurate time-of-arrival measurements for users to calculate position in three dimensions. GPS accuracy for civilian users is on the order of 10 m. If used differentially--requiring a reference station at a known location--GPS accuracies can be better than 10 cm.

As an external navigation aid, GPS error sources include signal path delay through the ionosphere and troposphere, satellite clock and ephemeris errors. Multipath and receiver clock errors contribute further to a GPS user's error budget.

GPS users benefit from very precise, long-term position and velocity information that is available worldwide. However, users may experience short-term GPS outages if there is signal interference, or if the view to satellites is blocked.

Figure 1.1. Global Positioning System

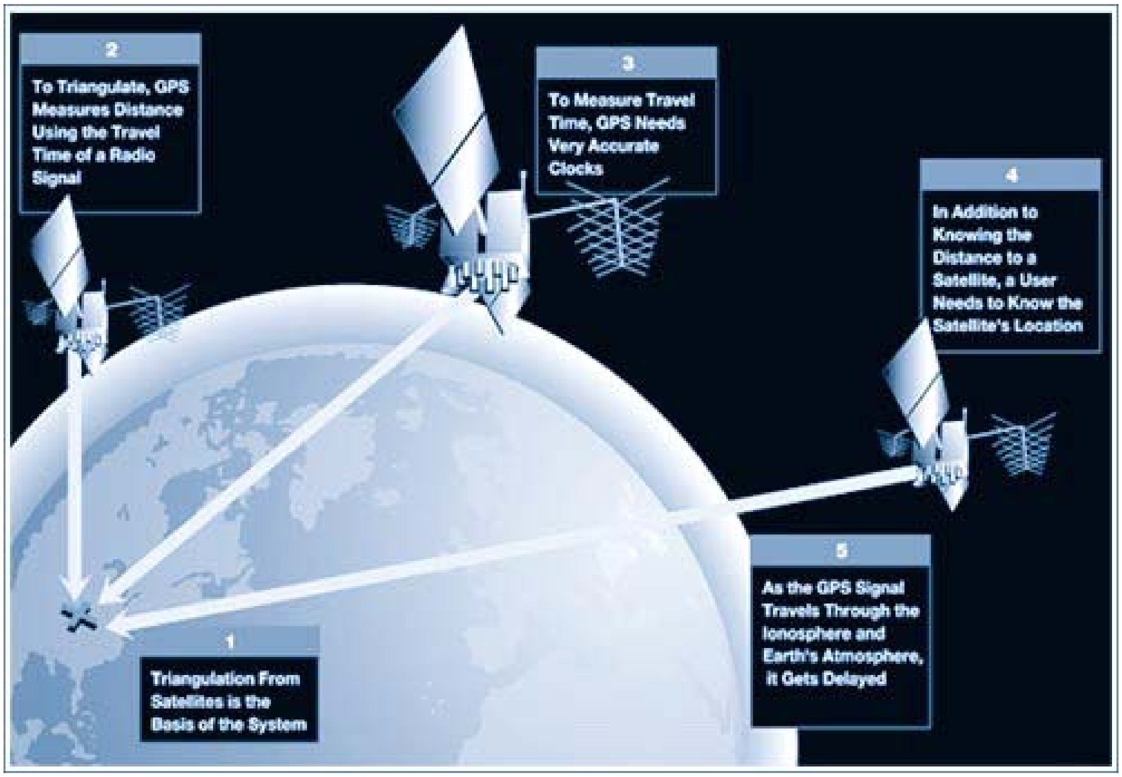
2
To Triangulate, GPS Measures Distance Using the Travel Time of a Radio Signal
3
To Measure Travel Time, GPS Needs Very Accurate Clocks
4
In Addition to Knowing the Distance to a Satellite, a User Needs to Know the Satellite's Location
5
As the GPS Signal Travels Through the Ionosphere and Earth's Atmosphere, it Gets Delayed
1
Triangulation From Satellites is the Basis of the System

Courtesy FAA

1.1.2 Inertial Navigation Systems

Inertial navigation is based on the implementation of Newton's laws of motion. Inertial Navigation Systems (INS) determine position, velocity and attitude by measuring and integrating a user's acceleration and angular velocity. Inertial sensors--accelerometers and gyroscopes--were first used for guidance and navigation in the early twentieth century.

Inertial navigators are self-contained, non-jammable systems, providing information at high data rates and bandwidth. All INS position and velocity information degrades with time; its accuracy is limited by the quality of its inertial sensors and knowledge of the Earth's gravity field and rate.

Figure 1.2 shows the range of quality in inertial sensors. The most accurate systems used in military, and high-end commercial aviation can cost over $100,000. Much less expensive sensors, used in automotive and consumer equipment, can drift by more than 200 deg/hr.

Figure 1.2. Chart of Accuracy and Expense

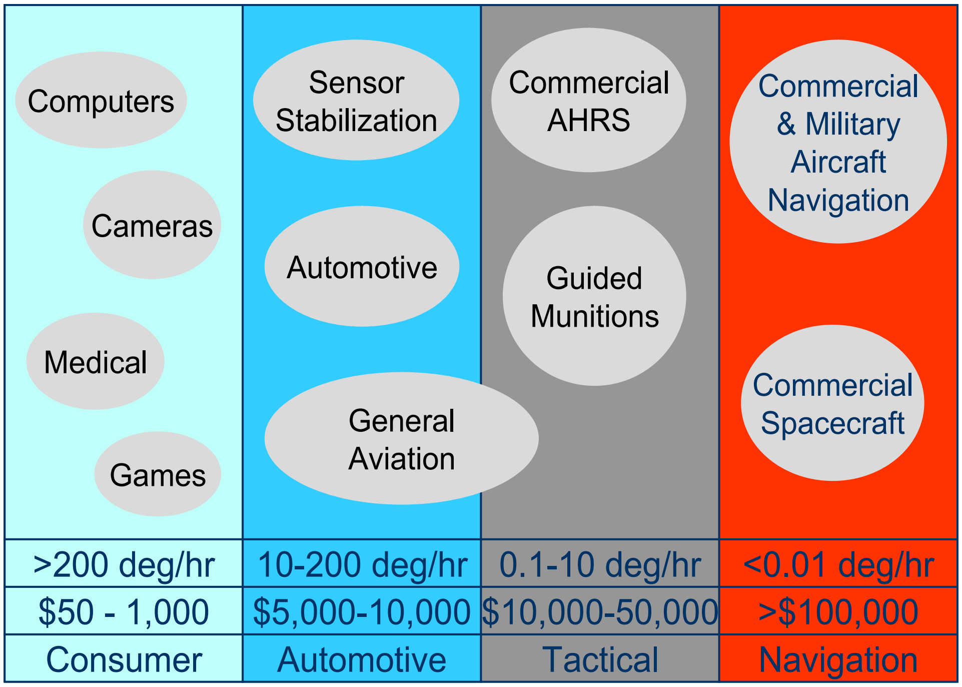

>200 deg/hr	10-200 deg/hr	0.1-10 deg/hr	<0.01 deg/hr
$50 - 1,000	$5,000-10,000	$10,000-50,000	>$100,000
Consumer	Automotive	Tactical	Navigation

Courtesy Demoz Gebre-Egziabher

Figure 1.3 shows and example of a “navigation” grade INS used in spacecraft; its errors drift no more than 0.01 deg/hr.

Figure 1.3. Example of Inertial Navigation System--Honeywell SIGI

Courtesy Honeywell

1.1.3 Integrated Navigation Systems

The blending of GPS with INS was anticipated very early on in the development of GPS. In fact, INS aiding was conceived as a way to mitigate the effects of interference and jamming even before the first GPS receivers were tested [1].

Indeed, GPS and INS have been combined and blended for so long, and in so many ways, that it is difficult to summarize all the possible methods and results. However, throughout this document, I separate GPS/INS integration into two categories: GPS aiding of INS; and INS aiding of GPS. GPS aiding of INS describes the use of GPS to aid and calibrate an inertial navigation system. This category can be broken down further to describe the degree of GPS blending: loosely coupled or tightly coupled.

INS aiding of GPS describes the use of inertially derived information to aid GPS receiver signal tracking and acquisition. These methods are usually referred to as “ultra-tightly coupled” or “deep integration.”

1.1.3.1 Levels of Integration

Figure 1.4 shows a loosely coupled GPS/INS integration. A navigation processor inside the GPS receiver calculates position and velocity using GPS observables only. An external navigation filter computes position, velocity and attitude from the raw inertial sensor measurements and uses the GPS position and velocity to calibrate INS errors.

A benefit of a loosely coupled system is that the GPS receiver can be treated as a "black box." The blended navigation filter design is simpler if using GPS pre-processed position and velocity measurements. However, if there is a GPS outage, the GPS stops providing processed measurements, and the inertial sensor calibration from the GPS/INS filter stops as well. See Chapter 4, Section 4.2.4 for more details on loosely coupled systems.

Figure 1.4. Loosely Coupled GPS/INS Integration

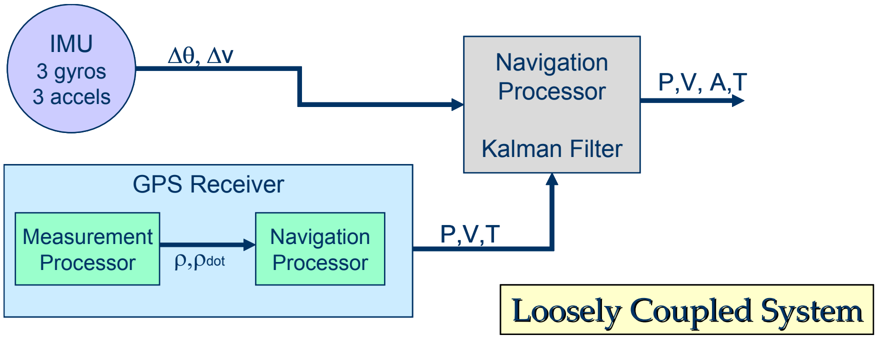

A more complicated GPS/INS filter design limits the problems due to GPS satellite blockage; Figure 1.5 shows a tightly coupled GPS/INS integration. In this system, the external navigation filter receives *raw* GPS measurements of pseudo-range and Doppler or delta-range. The tightly coupled GPS/INS filter benefits from GPS measurement updates even if there are less than four satellites available for a complete GPS navigation solution. Chapter 4, Section 4.2.5 describes the tightly coupled system in more detail.

Figure 1.5. Tightly Coupled GPS/INS Integration

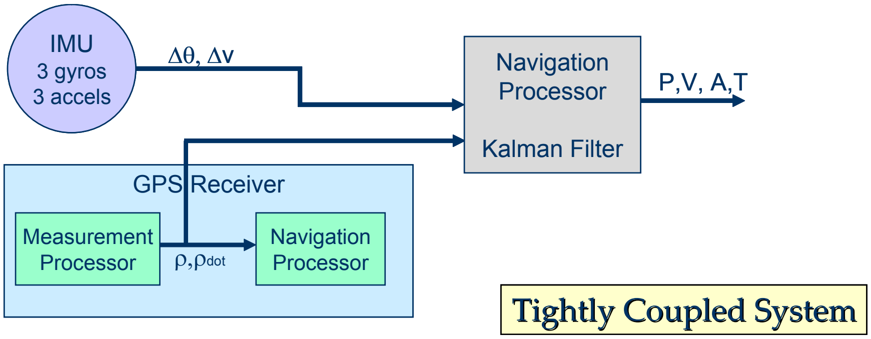

Figure 1.4 and Figure 1.5 illustrate two common methods of GPS/INS integration in the category of GPS aiding of INS. Figure 1.6 shows a method of INS aiding of GPS: ultra-tightly coupled or deep integration.

Figure 1.6. Ultra-Tightly Coupled or Deeply Integrated GPS/INS Integration

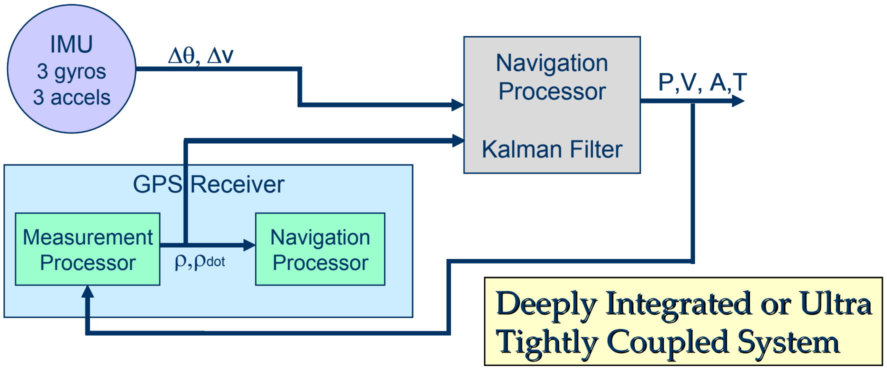

An INS can aid a GPS receiver on a variety of different levels. INS outputs of position, velocity and attitude, used as external inputs to a GPS receiver, aid in pre-positioning calculations for faster signal acquisition and in interference rejection during signal tracking. See Chapter 4, Section 4.3 for a more detailed description of ultra-tightly coupled systems.

1.1.3.2 Prior Art

Because there is such a long history of GPS/INS integration, I limit the discussion of previous research to: prior work to develop evaluation tools; research combining multi-antenna GPS with inertial sensors; and research on multi-level blending and aiding of GPS receivers. GIGET combines each of these elements to create the most general evaluation tool possible.

Evaluation Tools

In 1996, Knight at Knight Systems developed a software tool for evaluating tightly coupled GPS/INS system, GPS/INS Navigation Integrator (GINI) [2].

The University of Calgary has developed a software tool for managing GPS/INS integrated system data. In 2000, Schwarz and El-Sheimy created KINGSPAD (Kinematic Geodetic System for Position and Attitude Determination) to process GPS/INS information from a user's selected hardware set-up [3].

In 2001, CAST Navigation released a GPS simulator and testing tool, the CAST-4000, which can process off-line, integrated INS data from an Embedded GPS/INS (EGI), a high-cost, navigation grade system [4].

GPS Attitude with Inertial Sensors

Honeywell has developed Space Integrated GPS/INS (SIGI), an integrated navigation system for spaced-based operations that combines a navigation grade, ring-laser gyroscope INS with a four-antenna, GPS attitude system. Prior to SIGI, Honeywell researched GPS/INS attitude systems through IGADD (INS/GPS Attitude Determination Demonstration) in 1996. [5]

Several researchers at Stanford University have combined GPS attitude with inertial sensors or inertial measurement units. In particular, in 1996, Montgomery flew an autonomous unmanned aircraft using GPS attitude and automotive grade gyroscopes [6].

Also at Stanford, from 1998 through 2000, Gebre-Egziabher and Hayward combined short-baseline GPS attitude with very-low cost (automotive grade) gyroscopes to form an attitude heading reference system (AHRS) for General Aviation (GA) applications [7][8]. In 2001, Bevly automatically steered farm tractors with GPS attitude, position, velocity and inertial sensors [9].

More recently at Stanford, Alban, in 2002, combined automotive grade gyroscopes with GPS attitude as a navigation system for cars in urban environments [10].

Inertial Aiding: Ultra-Tightly Coupled/Deep Integration

Early GPS designers anticipated that GPS receivers may be subject to jamming, and considered the aiding of receivers with inertial information as a potential method of jamming and radio frequency interference (RFI) mitigation. Several researchers studied inertial aiding including the following: Martin [11] in 1976, at Magnovox; Carroll and Mickelson [12] in 1977, at Rockwell-Collins; Jones and MacDonald [13] in 1978, at the Analytic Sciences Corporation; and Widnall [14] in 1979, at Intermetrics. This early research primarily consisted of theoretical or conceptual results.

Many other researchers have since studied varying forms of receiver aiding with inertial information for jamming resistance and cycle-slip prevention, namely: Ward [15] in 1994;

Sennott and Senffner in 1994, [16][17]; and Phillips and Schmidt in 1996, at the Charles Stark Draper Laboratory [18].

More recently, research into receiver aiding has continued due to the DARPA sponsored project, the GPS Guidance Package (GGP). Vallot [19] in 1996, and Bye and Hartmann [20] in 1998, at Honeywell, completed several studies of inertial aiding and developed a prototype system. Similar studies at Litton, now Northrop Grumman, have led to the development of the LN-270 INS/GPS System [21].

The above research considers the use of inertial aiding primarily for military receivers. There has been renewed interest in jamming and RFI mitigation for non-military users now that GPS will be used for precision approach and landing systems.

Also, with the cost of inertial sensors dropping, research at Stanford University has been done to determine the benefits and feasibility of using inertial aiding in low-cost commercial systems [22].

1.2 Purpose Statement

The previous sections highlight some of the difficulties of past GPS/INS integration. In particular, the high cost of hardware and engineering has limited very advanced GPS/INS designs--with tightly coupled blending, inertial aiding, or GPS attitude--to military, space and high-end commercial aviation applications. Some tactical military systems use lower-cost inertial systems, but these are still relatively expensive systems, and are not generally available for consumer or commercial use.

Commercial and consumer systems use very low-cost inertial sensors, but only a few system have even been tested with very advanced blending algorithms or GPS methods [7][8][9]. In fact there exist a "gap" in the GPS/INS domain that describes the use of lower-cost sensors in advanced or complex integration techniques.

Figure 1.7 is a graphical representation of the trade space that charts GPS/INS accuracy and expense versus complexity of design and integration. The yellow boxes represent the GPS/INS designs covered in the previous section on prior art. The blue circle shows the the previously uncharted territory, the gap, in the GPS/INS space. As the cost of inertial sensors continues to decrease, this gap needs to be explored.

However, it has been very difficult to explore this space because GPS/INS integration can be so dependent on a particular application's environment and dynamics. In addition, GPS/INS project funding usually restricts the testing of integration methods and hardware to a single system and point design. There is a need for a relatively inexpensive tool that is easy to integrate onto a variety of hardware platforms, and capable of exploring many software blending techniques to test, evaluate, and compare GPS/INS integrated systems. That tool, of course, is GIGET. This work discusses the development, testing, and application of GIGET as a generalized performance evaluation tool. GIGET is a combination of easily re-configurable hardware and analysis tools to provide real-time comparisons of multiple integrated navigation systems.

Figure 1.7. GPS/INS Trade Space

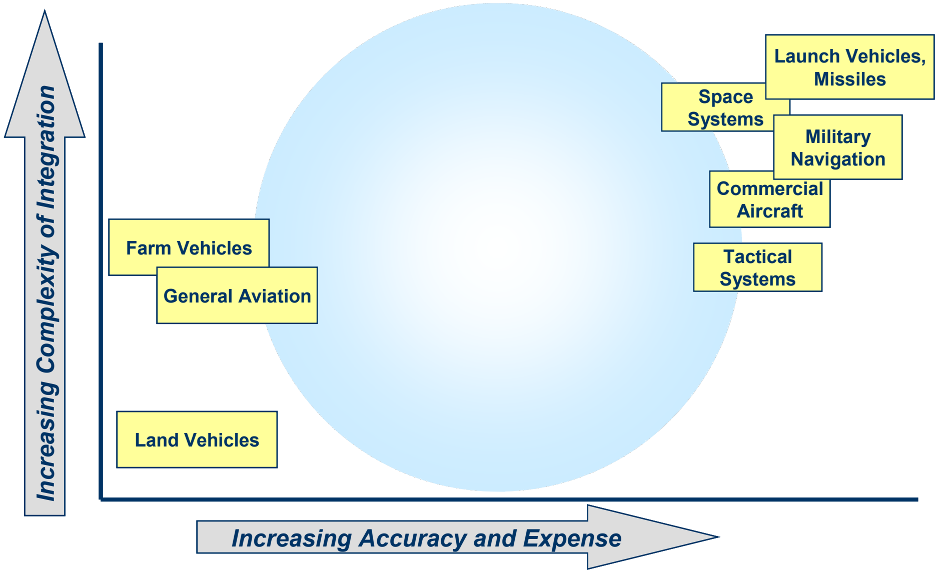

1.3 Contributions

The following is a list of my research contributions through the development, testing, and application of GIGET. References to locations in the document where each contribution is discussed in detail also follows.

- I designed, built, integrated and tested a software and hardware architecture for a re-configurable, generalized performance evaluation tool of GPS/INS systems.

  I built a five antenna, 40-channel, single-board, and common-clock GPS receiver as an enabling technology for GPS/INS performance evaluation. *See Chapter 2*.

  I developed the real-time software architecture to provide precise timing and fast re-configuration of multiple systems, data, and sensors. *See Chapter 3*.

- Using GIGET, I performed hardware and software comparisons of tightly coupled and loosely coupled navigation platforms to formulate a trade study to map previously uncharted territory of the GPS/INS space that trades accuracy and expense versus complexity of design. *See Chapter 5*. I tested and compared these results in a case study for the DragonFly UAV to determine an appropriate navigation package. *See Chapter 6*.

- I analyzed the performance limits and feasibility of using low-cost inertial sensors for deeply integrated GPS receiver aiding, including acquisition aiding, pre-positioning, and tracking loop aiding in GIGET. *See Chapter 4*.
- I developed software for the seamless real-time switching of antenna inputs for roving master GPS attitude solutions providing on-the-fly GPS attitude baseline re-configuration, and multiple-antenna GPS for INS integration for side-by-side navigation system testing. *See Chapter 3 and Chapter 4*.

1.4 Overview

The development of GIGET can be broken down into three distinct levels. Figure 1.8 graphically depicts the three GIGET tiers. Throughout the first four chapters of this document, the highlighted block in a similar illustration indicates the GIGET level being disccussed.

The first tier involves the building and assembly of the innovative hardware that creates the foundation for the remaining GIGET levels. It is this enabling technology that gives the underlying modularity and flexibility of GIGET. Chapter 2 discusses the first tier of GIGET.

The second tier covers GIGET's flexible software architecture that delivers the real-time capability to support the multiple GIGET, GPS/INS applications. Chapter 3 discusses the second tier of GIGET.

The third tier of GIGET is the application level where algorithms are chosen to demonstrate various uses of GIGET. Chapter 4 discusses the third tier of GIGET.

Figure 1.8. Three Tiers of GIGET

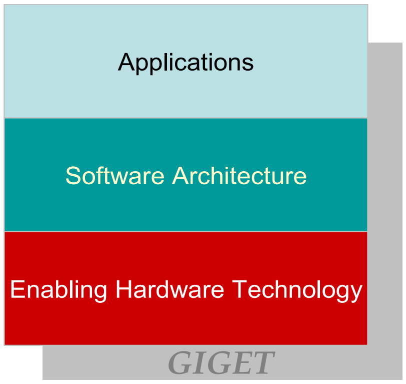

Chapter 5 discusses the use and application of GIGET in a trade study. The study results demonstrate how GIGET explores the gap in the GPS/INS trade space of accuracy and expense versus complexity of design.

As a demonstration of its utility as a *hardware* evaluation tool, GIGET was flown on the DragonFly Unmanned Air Vehicle (UAV), a test-bed for autonomous controls experiments. The DragonFly is shown in Figure 1.9. GIGET's DragonFly testing aids in the design of the UAV's navigation system. The GIGET recommendations for the DragonFly address some of the UAV specific challenges for a navigation system that only could have been evaluated with a hardware tool set, such as GIGET, flown in the exact UAV environment. Chapter 6 discusses the DragonFly case study.

Chapter 7 summarizes GIGET conclusions and discusses the future work and applications of GIGET.

Figure 1.9. DragonFly Unmanned Air Vehicle

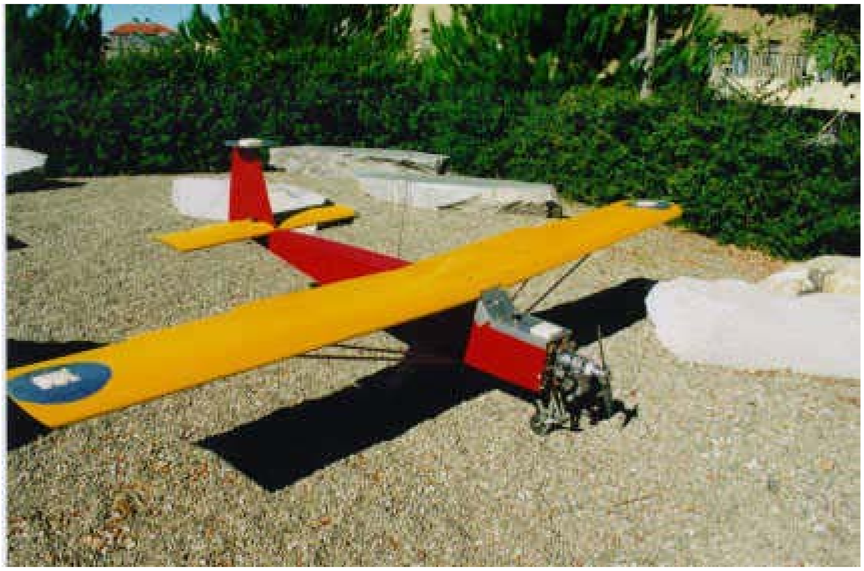

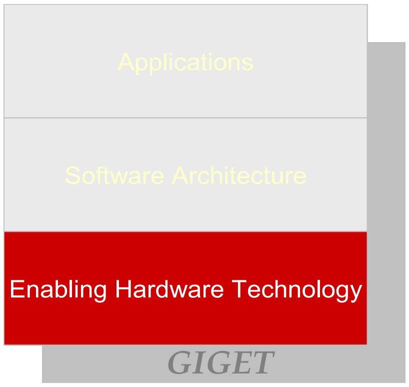

Chapter 2:
GIGET Components

Chapter 2 describes the hardware components that make up the first tier of GIGET, the enabling hardware technology. It is this innovative hardware that creates the foundation for the remaining GIGET levels; and therefore enables the underlying modularity and flexibility that this generalized evaluation tool offers.

2.1 GPS Receiver

GIGET is a tool for comparing many different navigation schemes from the complicated and highly accurate, to the simple and less accurate. The GIGET GPS receiver needs to be capable of high performance at each of these levels. Because it is a *hardware* evaluation tool, which will be transported from vehicle to vehicle, GIGET requires a GPS receiver system that is compact, low-power, lightweight, highly-accurate, and with a flexible architecture. It needs multiple antennas, not only to support GPS attitude determination, but also to support multiple and simultaneous GPS receiver experiments. It needs high-speed communications to reduce latency for time-critical navigation applications, as well as for external high-speed receiver aiding.

However, receivers on the market at the time of the GIGET development lacked several of these key requirements. For example, many popular embedded GPS systems have been designed for automotive applications that have much lower accuracy requirements and are not suited for attitude determination.

The GPS attitude systems available were more accurate, but were rigid in design and lacked the required flexibility. They also did not have the necessary high-speed communications.

In order to supply GIGET with a receiver that met all of these requirements, in collaboration with Trimble Navigation, I designed, developed, built, and tested a customized GIGET GPS receiver.

Figure 2.1. GIGET Receiver Schematic

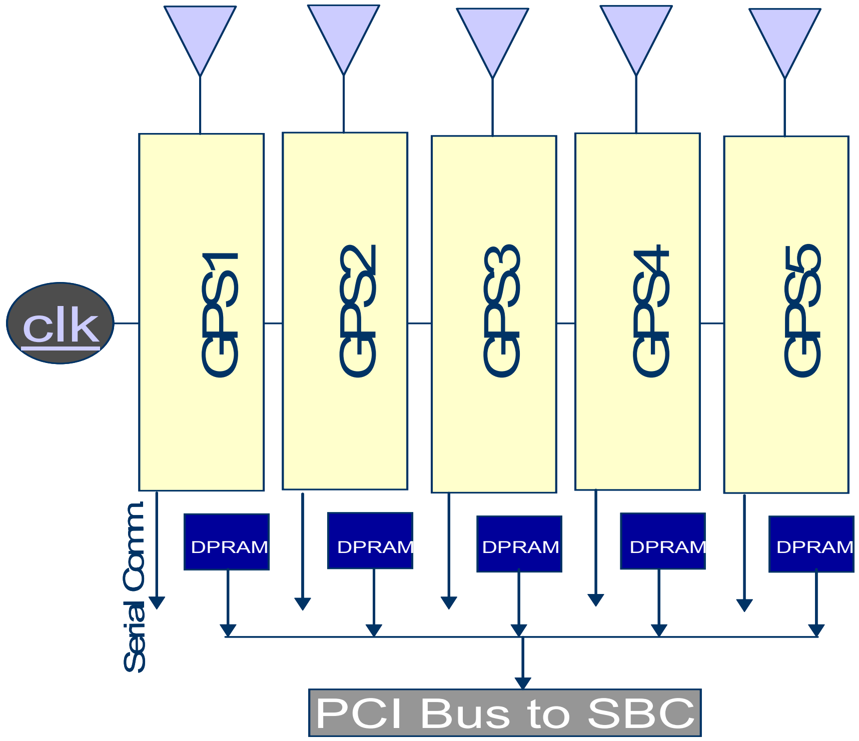

2.1.1 Trimble Receiver Design

The GIGET receiver fits on one printed circuit board which allows it to be easily embedded in a small, low-power, avionics package. GIGET needs at least three different antenna inputs to enable GPS attitude; more antennas are included to add redundancy, additional flexibility, and the ability to run side-by-side, simultaneous testing of many different navigation schemes. For example, three antennas can be used to provide attitude for a tractor, while additional antennas can be used to determine the position or heading of an implement being dragged behind the tractor. Moreover, for an aircraft, multiple antennas on the top of the fuselage provide attitude and position, while antennas on the bottom of the airplane can track pseudolites, or become primary satellite tracking antennas during aerobatic maneuvers. Ultimately, five receiver front-ends fit on a single, eight-inch square circuit board. The GIGET architecture is flexible enough to use these five antenna inputs together for attitude determination or individually for comparison testing.

Each of the five analog sections has a two-bit A/D converter providing precise GPS carrier phase measurements with reduced interference. These sections are well isolated and shielded to prevent interference between the receiver sections, as noted by Cohen [23].

Each of the five front-end sections drives a separate digital section with eight channels each. All the sections share a common reference oscillator. The handling and trace of this clock signal is carefully designed and placed to prevent some of the difficulties of previous multi-antenna, attitude receiver designs [23]. The common oscillator synchronizes all GPS measurements, making the GIGET receiver perform as if it had 40 parallel tracking channels. In addition, the carefully designed common clock allows for accurate single difference attitude determination (discussed in Chapter 4) with minimal phase noise and line bias drift.

Each receiver section provides position, velocity, timing, and raw GPS observables (phase measurements, etc.) to a central processor on a single board computer (SBC). The GPS board communicates to the SBC either through a serial bus connection or through a high rate, PCI data bus. Communications are transmitted back and forth through the PCI bus to dual-ported RAM on the GIGET receiver.

The receiver is DGPS ready and seamlessly accepts differential corrections from a ground station through a radio modem.

Figure 2.1 is a simplified schematic of the DragonFly receiver, and Figure 2.2 is a picture of the GIGET receiver.

Figure 2.2. Trimble Navigation's GIGET Receiver

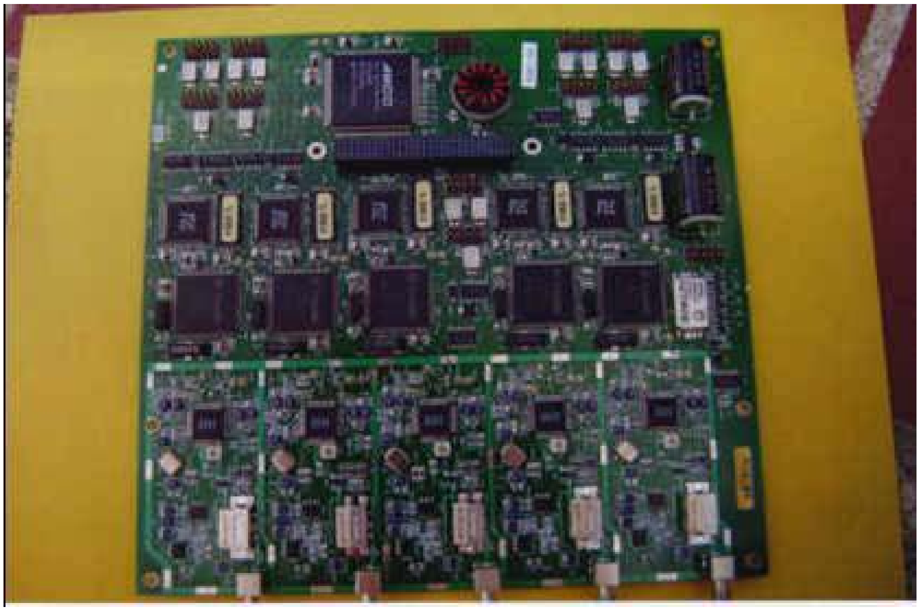

2.1.2 Unique GIGET Receiver Attributes

In summary, the GIGET receiver is a unique and flexible platform that acts as the enabling technology for many navigation experiments. The multiple antennas and the common clock provide a flexible hardware architecture for both GPS attitude determination and simultaneous experiment comparisons. The GIGET receiver provides position, velocity, timing, raw phase and range measurements at a rate of up to 10 Hz to the single board computer through a serial port or through a PCI data bus.

The PCI bus allows for very high speed communications in and out of the GPS receiver sections. The PCI bus is 32 bits wide and runs at a 33 MHz rate. This is a tremendous increase in bandwidth compared to the standard serial interfaces on most GPS receivers, which allow only 115 Kbaud communications. This high-speed communications link becomes critical for the inertial aiding applications discussed in Chapter 4. The latency involved in standard serial receiver communications would prohibit any external aiding into the GPS tracking loops.

In addition to external aiding, another unique benefit of the GIGET receiver is its ability to provide aiding between receivers through the same common PCI bus. This is essentially a "boot-strapping" of one receiver's channels to another's.

2.2 Inertial Measurement Unit

An inertial measurement unit (IMU) with the highest possible accuracy would be the best choice for GIGET. With a high accuracy inertial solution, it would be easier to compare all possible navigation schemes from the expensive, high-end combinations to the cheaper solutions. GIGET could either collect and use the raw, high quality data or intentionally degrade the raw data to emulate a poorer quality system. The highest quality inertial systems would be navigation grade units. However, besides being very expensive (~$100K), these units are also very large with high power consumption, making it very hard to embed GIGET in a small avionics box or port from vehicle system to system.

As a compromise, GIGET uses a tactical grade inertial measurement unit. These units are small and compact, with low power consumption, but output higher quality sensor data than many less expensive automotive and commercial grade units.

Also, as shown later in Chapter 4, the tactical unit is of high enough quality to be used for deep integration and the aiding of the GPS tracking loops.

2.2.1 Honeywell HG1700

The actual inertial measurement unit GIGET uses is a Honeywell HG1700 supplied by Honeywell Labs in Minneapolis, Minnesota. This IMU is tactical grade, and of moderate cost (between $10K and $20K), with three ring-laser gyroscopes and three accelerometers. It has gyroscope rate biases of around 1 deg/hr and accelerometer biases of around 1 milliG. The unit is nicely contained, aligned, and isolated in a small case weighing less than four pounds and approximately five inches cubed.

The unit consumes less than ten watts of power and supplies one Mbit/second data rate. It has an RS-422 SDLC communications protocol for the 600 Hz autopilot outputs and 100 Hz raw inertial outputs (Δv and $\Delta\theta$).

Figure 2.3. Honeywell HG1700

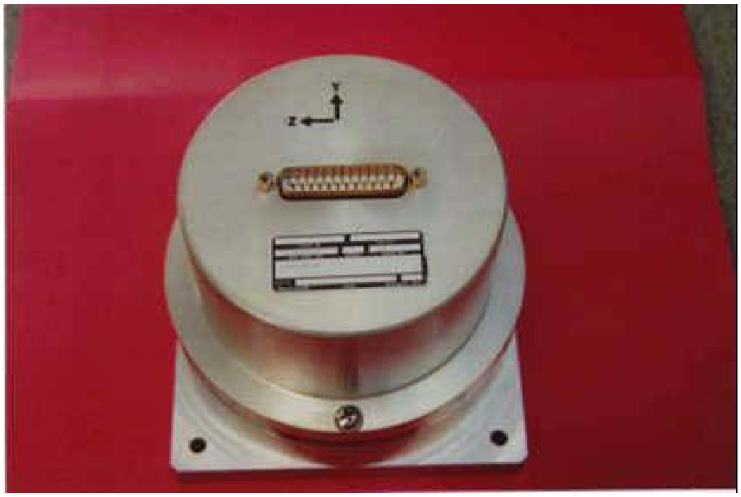

2.2.2 IMU PERFORMANCE

The HG1700 performs very well in GIGET. It has been very rugged, reliable, and consistent throughout the project testing. Figure 2.3 is a picture of the Honeywell HG1700 IMU.

2.3 Single Board Computer

The GIGET system needs a powerful, but flexible, central processing unit that is easily integrated and expanded for use with different sensors and vehicle platforms. This embedded computer gathers and processes all the information from the GPS receiver, IMU and other sensors. An off-the-shelf embedded single board computer (SBC) developed by Versalogic Corporation serves as the GIGET processor.

2.3.1 VERSALOGIC SBC

The SBC has a 5x86 processor with 2 Mbytes of on-board flash memory. It uses a PC-104+ bus system. The "+" means it uses an embedded version of both the ISA and PCI bus standards. Through this PC-104+ connector, the SBC stacks on top of the GIGET GPS receiver to create a very compact and rugged two-board system.

Figure 2.4 shows the Versalogic SBC.

Figure 2.4. Versalogic SBC

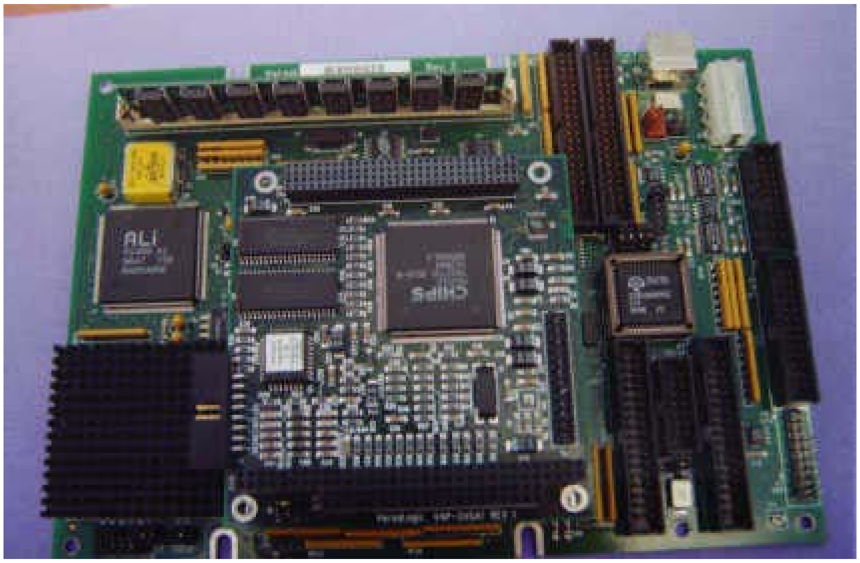

2.3.2 Expansion

Many standard expansion cards are available on the market that use the PC-104 interface. This makes it quite easy to expand the GIGET system to include wireless communications, data acquisition, and other functionality.

Expansion boards include a Real Time Devices data acquisition card to collect analog data from various other sensors such as wind speed and direction indicators, temperature probes, etc.

The ACB-104, a high-speed, synchronous serial communications expansion card made by SeaLevel Systems, serves as the interface to the Honeywell HG1700.

Figure 2.5 shows a typical PC-104 expansion board.

Figure 2.5. PC-104 Expansion Board

2.4 GIGET Avionics Box

For portability of the test equipment, GIGET components are housed in an avionics package that consists of a 1/16-inch thick aluminum box and measures 14x4x8 inches. Included in the avionics package is a cooling fan and shock mounts for vibration isolation. Figure 2.6 presents a close-up view of the avionics box.

Figure 2.6. GIGET Avionics Box

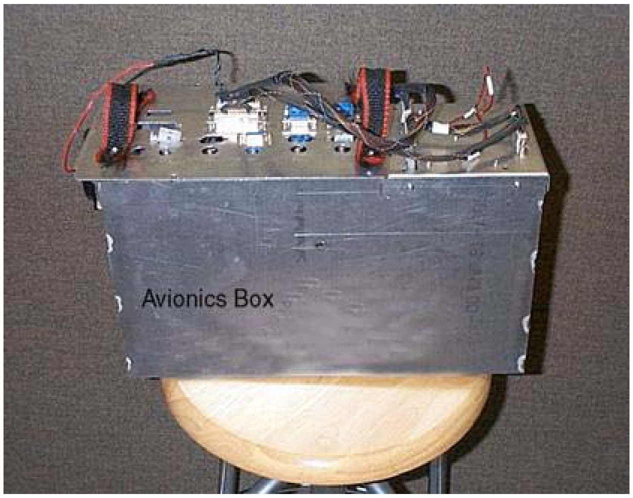

The avionics box includes the multi-antenna GPS receiver, single board computer, several expansions boards as an interface to other sensors, a radio modem for DGPS and telemetry, and the HG1700 IMU. Figure 2.7 shows the approximate layout of these components inside the avionics box.

Figure 2.7. Avionics Box Layout

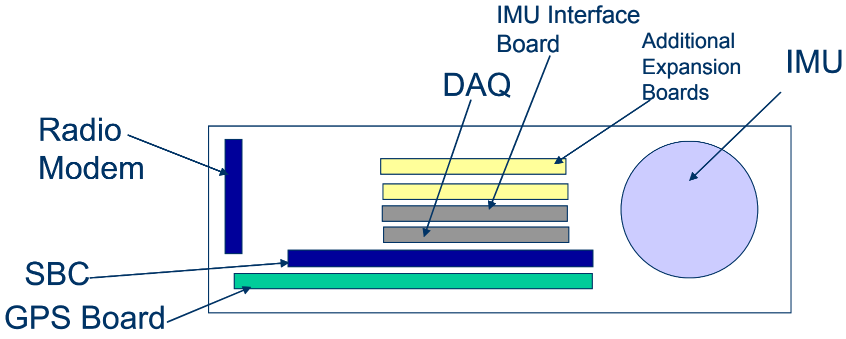

2.5 Ground Systems

GIGET communicates wirelessly to other lab and ground computers through a Freewave radio modem. The Freewave DGRO-115 is a wireless transceiver module with a frequency range of 902 to 928 MHz. It has a range of up to 20 miles with a 115 KBaud RS-232 interface. Figure 2.8 shows the Freewave modem.

Figure 2.8. Freewave Radio Modem

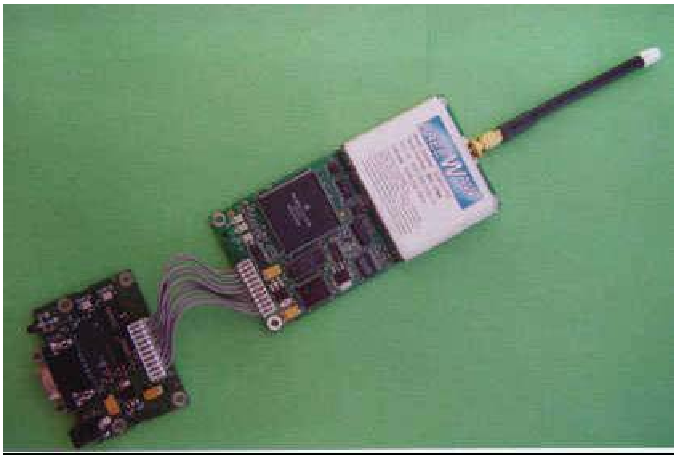

GIGET sends collected data through the avionics radio modem to a ground station. The telemetered data include inertial measurement unit data, raw GPS observables, computed navigation and attitude solutions, timing information, and other sensor packets. The ground station consists of a Pentium 133 MHz ruggedized laptop, ground radio modem, and Trimble DSM GPS reference receiver. The ground reference receiver sends code-based, differential GPS corrections to GIGET through the radio modem link at a 1 Hz rate.

All ground components are packaged in a large portable suitcase with a battery and power distribution system for easy transport and use in the field. Figure 2.9 shows the ground station suitcase and ruggedized laptop.

Figure 2.9. Ground System Suitcase and Laptop

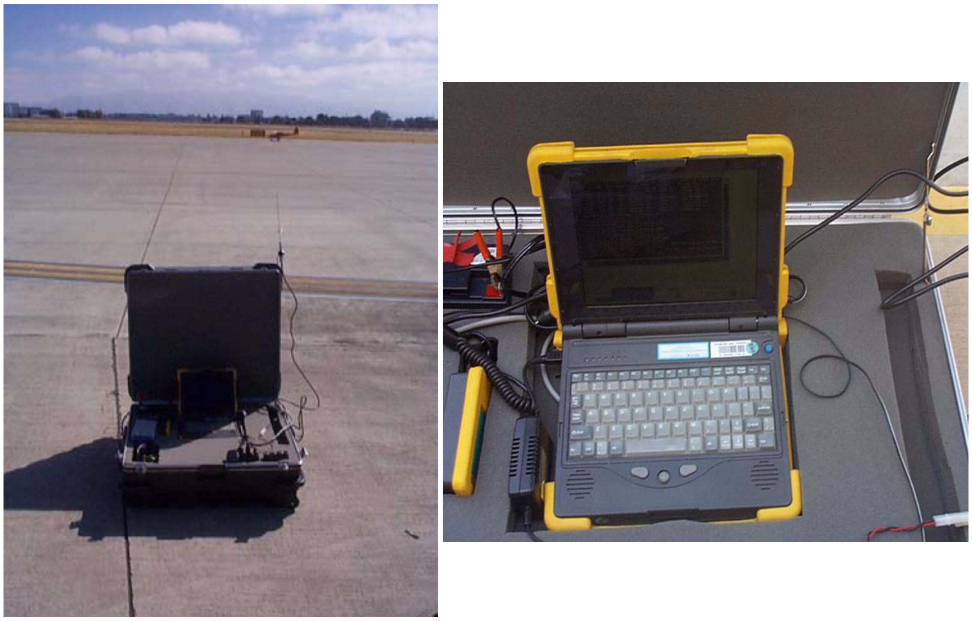

The re-configurable nature of the entire GIGET system stems from a collection of unique hardware and software components. This concludes the discussion of the enabling hardware technology, GIGET's first tier. The next chapter discusses the unique software architecture of GIGET, the second GIGET tier.

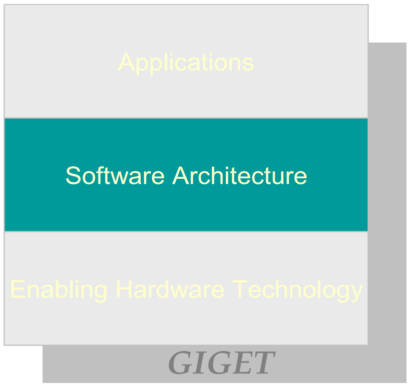

Chapter 3: System Software Development

The complete set of tools that comprises GIGET not only includes the avionics hardware and ground systems, but also a vast array of lab equipment and computers for testing, simulation, and analysis. GIGET's software architecture enables the transparent networking between all these components, and it delivers the real-time capability to support the multiple GIGET applications. The flexible nature of the software architecture allows for the seamless real-time switching of antenna inputs for roving master GPS attitude solutions and multiple-antenna GPS for INS integration. Chapter 3 discusses these features through the formulation of this second tier of GIGET, the software architecture.

3.1 GIGET System View

Figure 3.1 shows a diagram of the complete GIGET system including avionics, ground and lab development systems. The diagram illustrates the networking and communications links between all the components.

3.1.1 Lab Development Systems

The lab development systems include a web server, desktop computers for code development and simulation, and a replica of the avionics systems, used for bench testing modifications before testing with GIGET in the field. All are networked together through ethernet or serial links (wired or wireless).

Figure 3.1. GIGET System

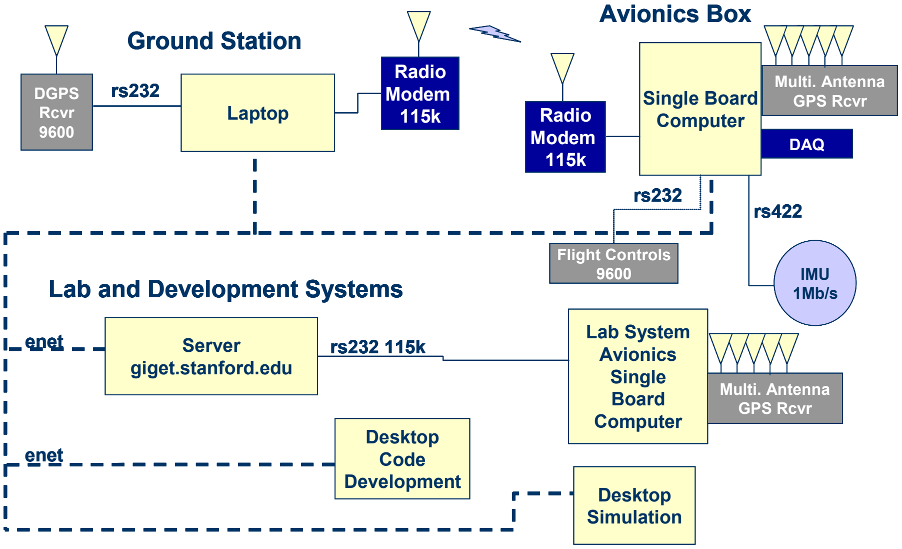

3.1.2 Operating System

GIGET's requirements for real-time applications and its large data collections demand a real-time operating system. GIGET runs the QNX real-time operating system, a posix-compliant, hard real-time operating system with a very small micro-kernel. QNX easily adapts from the embedded system of the GIGET avionics to the larger lab and development systems. Each supporting lab computer, ground or flight system is networked together as nodes on a larger system using this operating system. QNX also enables the flexible client/server software architecture described in the next section.

3.2 Software Architecture

GIGET requires a software system that is as modular and flexible as its hardware systems. It also demands a real-time operating system to manage its time-critical, multiple applications with large data collections. A client/server software architecture delivers the utility that GIGET requires; it allows for multiple GPS/INS applications, running simultaneously, for side-by-side, real-time comparisons. This section describes the client/server architecture and resulting GIGET system configuration.

3.2.1 CLIENT/SERVER ARCHITECTURE

A client/server software architecture is a message-based, modular infrastructure designed to improve flexibility and interoperability between the suppliers of services (the servers--hardware, data), and requestors of services (the clients--user applications) [24].

For GIGET, the servers are low-level applications that interface directly with the hardware components: GPS receivers, IMU, SBC, etc. Server modules collect and preprocess raw sensor data and deliver them to the clients through a "data dispatcher" interface. Clients dynamically configure the process in which the servers report the data. For instance, a server can supply data to a client as soon as available from the hardware, or it can buffer data until a client requests them to be delivered. This delivery flexibility allows for timing and data resource management. For example, data loggers capture high-bandwidth data, but have no low-latency requirements; therefore, servers store data in buffers and download to data loggers after GIGET experiments. However, for more time-critical applications, such as the navigation clients, data are transported to clients as soon as available. In both cases, the server is the same. In fact, GIGET servers support multiple data-flow types simultaneously and can change dynamically as experiments are reconfigured "on-the-fly". For example, a client can reconfigure on-the-fly to capture 600 Hz Flight Control packets from the IMU server after an initial configuration to capture 100 Hz Inertial packets.

GIGET clients include the navigation applications, attitude applications, data loggers, etc. The diagram in Figure 3.2 shows the client/server interface. Client applications connect to servers and register their interest in data by configuring latency and priority restrictions. Servers set up data "queues" for all interested clients. All servers have similar "glue" libraries to provide a uniform functional interface to the clients. Clients collect queued data when requested or when a "proxy" trigger, acting as a interrupt, is received [25].

Figure 3.2. Client/Server Interface

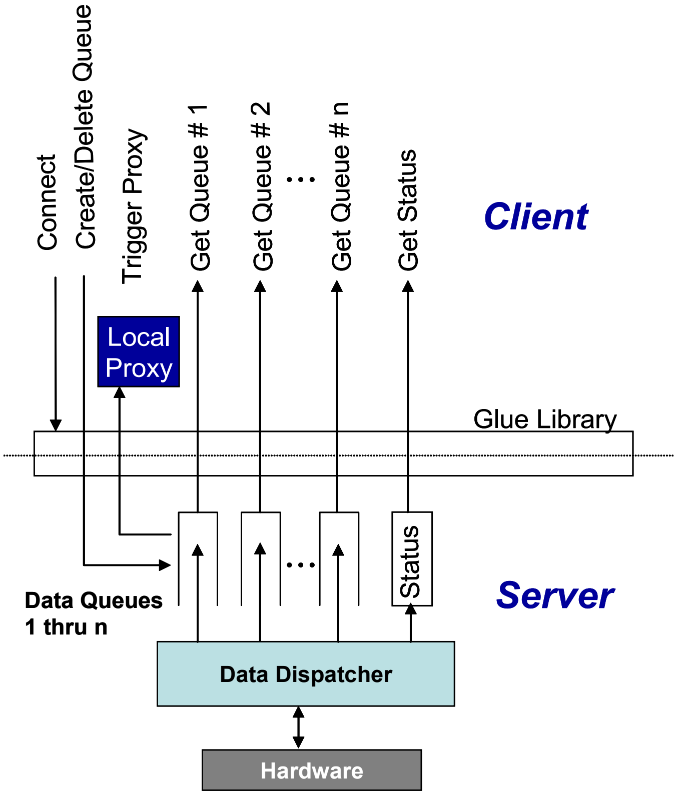

3.2.2 System Configuration

A typical GIGET experiment invokes several servers on the avionics computer and a several servers on the ground computer. These computers act as nodes on the GIGET network. QNX allows for node transparent networking; a client, hosted on any one node, can connect to any number of servers on any number of different nodes. In addition, any number of clients can run simultaneously while connected to any of these servers. This further improves modularity by allowing for multiple processes on multiple nodes, all connected to each other, processing data at various rates. A client data logger hosted on the ground connects to the avionics GPS server as easily as it connects to a GPS server located on the GIGET ground station.

This node transparent system configuration allows GIGET to run several simultaneous experiments, in real-time, for side-by-side comparisons. For example, multiple instances of the navigation client seamlessly process data from multiple GPS receivers by connecting to one GPS server. Figure 3.3 shows the typical system configuration for a GIGET experiment. The next section will discuss the individual GIGET software modules.

Figure 3.3. GIGET System Configuration and Software Modules

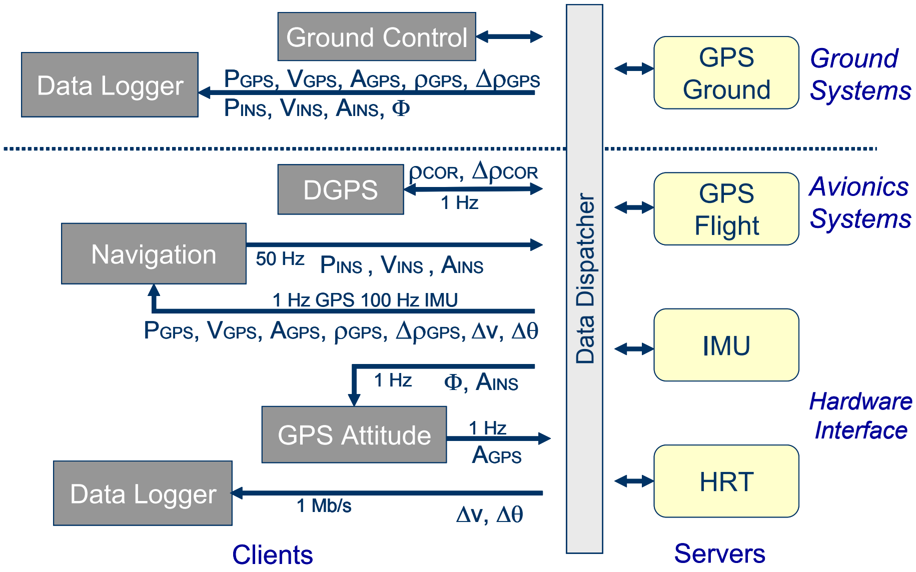
Ground Control
Data Logger
P_{GPS}, V_{GPS}, A_{GPS}, ρ_{GPS}, $\Delta\rho_{GPS}$
P_{INS}, V_{INS}, A_{INS}, Φ
DGPS
ρ_{COR}, $\Delta\rho_{COR}$
1 Hz
Navigation
50 Hz
P_{INS} , V_{INS} , A_{INS}
1 Hz GPS 100 Hz IMU
P_{GPS}, V_{GPS}, A_{GPS}, ρ_{GPS}, $\Delta\rho_{GPS}$, Δv, $\Delta\theta$
1 Hz
Φ, A_{INS}
GPS Attitude
1 Hz
A_{GPS}
Data Logger
1 Mb/s
Δv, $\Delta\theta$
Clients
Data Dispatcher
GPS Ground
Ground Systems
GPS Flight
Avionics Systems
IMU
Hardware Interface
HRT
Servers

3.3 Software Modules

GIGET runs three primary servers: the GPS server, to connect with several GPS receivers; the IMU server, to collect data from the inertial measurement unit; and the high resolution timer, to synchronize the SBC master clock. The GIGET clients include the navigation and GPS attitude modules, data loggers, ground controllers, and differential GPS clients. Although the navigation and attitude modules act as clients since they connect to the low-level servers, they also act as servers. The attitude client "serves" up the GPS attitude solution to the navigation client, while the navigation client "serves" up the INS solution to the attitude client. The following describes the functions and dependencies of each module.

3.3.1 GPS Server

The GPS server connects to the GPS hardware via a 19.2 Kbaud serial connection or through the PCI bus to the GPS dual-ported RAM. At a rate of up to 10 Hz, the receivers transmit standard Trimble TSIP binary data packets containing raw GPS observables, ephemeris, position, velocity and timing information. One server can connect to, and process data from, any number of GPS receivers. The receivers may be physically connected to any computer on the GIGET node network. All five GIGET GPS receivers in the avionics box are managed by one “flight” GPS server hosted on the avionics SBC. In a typical experiment, a separate instance of the GPS server, hosted on the ground computer, will manage data from the GIGET ground reference receiver.

Once the GPS data are received, the GPS server dispatches them to interested clients. The client determines the rate, type, and origin of the GPS packets. For instance, the attitude client connects to the flight GPS server and collects GPS carrier phase measurements from each of four GPS receivers in GIGET’s avionics box. Simultaneously, however, a navigation client can connect to the same GPS server, and collect raw measurements and position data packets from the same set of receivers. The flight GPS server delivers the data to both based on priority and latency requirements as registered by the clients.

3.3.2 Inertial Measurement Unit (IMU) Server

The IMU server connects to the inertial measurement unit via a high-speed, synchronized serial data link--SDLC, Synchronized Data Link Communication. SDLC is a standard interface for most tactical grade inertial measurement units. The IMU outputs vehicle rate and acceleration information in a “Flight Control” binary packet at a rate of 600 Hz to the IMU server. At 100 Hz, the IMU server receives “Inertial” packets, containing the raw inertial data of delta-velocity and delta-angles. GIGET primarily uses the less noisy, raw

100 Hz IMU packets; however, the IMU server is designed to deliver either packet format at the prescribed rate, or decimated data at a slower output rate.

3.3.3 High Resolution Timer (HRT) Server

The high resolution timer server, or HRT server, synchronizes GIGET's system time to GPS time. The server monitors the time stamps reported by the GPS receivers while phase locking the system time to a one pulse-per-second GPS hardware signal. The server adjusts and calibrates the master clock bias on the single board computer accordingly [25]. The HRT maintains system time to GPS time within a few microseconds of offset.

By synchronizing system time, all applications, clients and servers, time-tag and coordinate system events with GPS time, by accessing standard system timer services available through the QNX operating system. The time synchronization of the inertial sensor packets with the GPS packets is critical in all the navigation applications.

3.3.4 DGPS Client

The differential GPS client, the DGPS client, transmits GPS differential correction data from the ground reference station to each of the GPS receivers in GIGET's avionics box. This client connects to the ground GPS server and registers an interest in TSIP differential correction packets, available from the Trimble ground reference receiver. The client then connects to the flight GPS server and transmits any received differential packets, through the radio modem, to the flight GPS server. Because the GIGET receivers are DGPS ready, each automatically applies the DGPS packets when received by the flight GPS server.

3.3.5 ATTITUDE CLIENT/SERVER

Figure 3.4 shows the three basic functional blocks that form the attitude client/server. The first block is the data receive function; the attitude client/server connects to the navigation server and to four GIGET GPS receivers through the flight GPS server. The application also starts a timer function to act as a periodic interrupt.

The attitude client/server waits until it receives a series of possible messages. When a carrier phase packet arrives, the attitude application checks if it has received all four antenna phase measurements for that GPS time epoch. If so, the application proceeds to the phase processing functional block. If it receives a GPS ephemeris or position message, the application updates the satellite line-of-sight calculations. A message from the navigation client/server includes an INS attitude solution used for GPS attitude integer resolution. Because the attitude application acts as a server as well as a client, it periodically receives commands to send GPS attitude packets to the navigation client/server. The attitude application eventually moves to the phase processing functional block when it receives a timeout message from its interrupt timer, or when all four carrier phase measurement packets have been received.

In the second functional block, the GPS carrier phase measurements are processed and prepared for the GPS attitude computation. Given a baseline vector configuration (see Chapter 4, Section 4.1.1.3), the phase measurements are carefully differenced and checked to formulate the delta-phase measurements. If the attitude client/server receives only a sub-set of the four possible antenna measurements, or receives a command to process with new baselines, it will re-configure its baseline measurements, including its initial line bias estimation and integer solutions. This re-configuration is a unique functionality of GIGET that allows for on-the-fly baseline vector configuration and enables a roving master antenna. Chapter 4 describes the process of line bias estimation and integer resolution in greater detail.

Once the baseline delta-phase measurements are determined and checked for cycle-slips and satellite changes, the application proceeds to the attitude computation block. The attitude solution algorithms are described in Chapter 4. The line biases are also re-checked and updated in a background process. Once the solution is computed, the attitude application sends out the GPS attitude to all interested clients.

Figure 3.4. Attitude Client/Server Process Flow

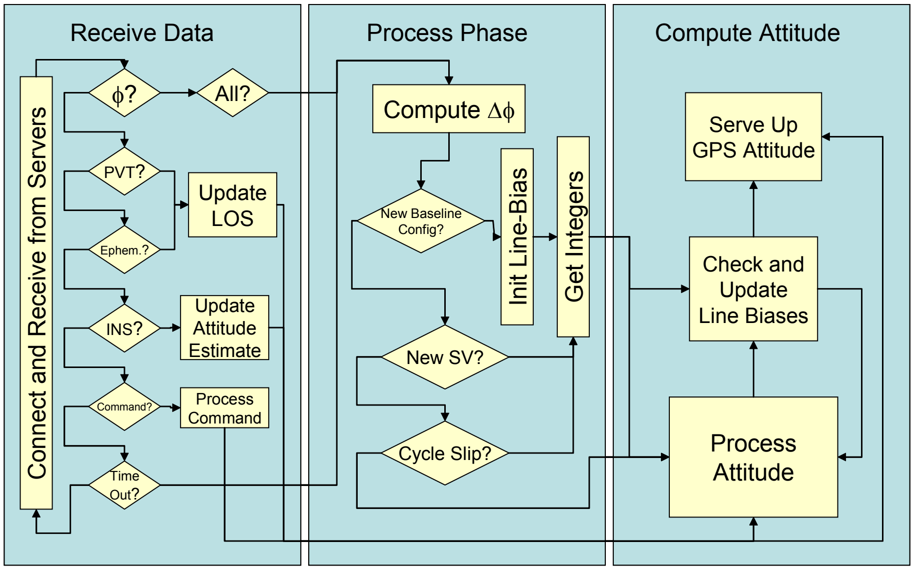

Because the attitude application acts as a client and as a server to the navigation application, the possibility of process block can occur. That is, the attitude application may stop processing if waiting for a navigation message, while at the same time, the navigation application may have stop processing if waiting for an attitude message--neither process can move forward. The attitude application's periodic timer interrupt prevents the blockage. Eventually the attitude application will continue processing once it receives a timeout message. Likewise, the navigation application continues to process whether it receives a GPS attitude message or not.

3.3.6 Navigation Client/Server

The navigation client/server is also described in three distinct functional blocks. Figure 3.5 shows the three processing functions. Similar to the attitude client/server, the first block is the data receive function. The navigation client/server connects to the IMU server, the attitude server, and the flight GPS server. Because of the unique flexibility of the GIGET architecture, the navigation application can connect to one, several, or all five GIGET GPS receivers through the flight GPS server. When a GPS packet arrives, the navigation application can select or switch which antenna/receiver message to process in the INS based on signal strength or external commands. This seamless, real-time switching of antenna inputs allows for multiple-antenna GPS updates for INS integration.

Figure 3.5. Navigation Client/Server Process Flow

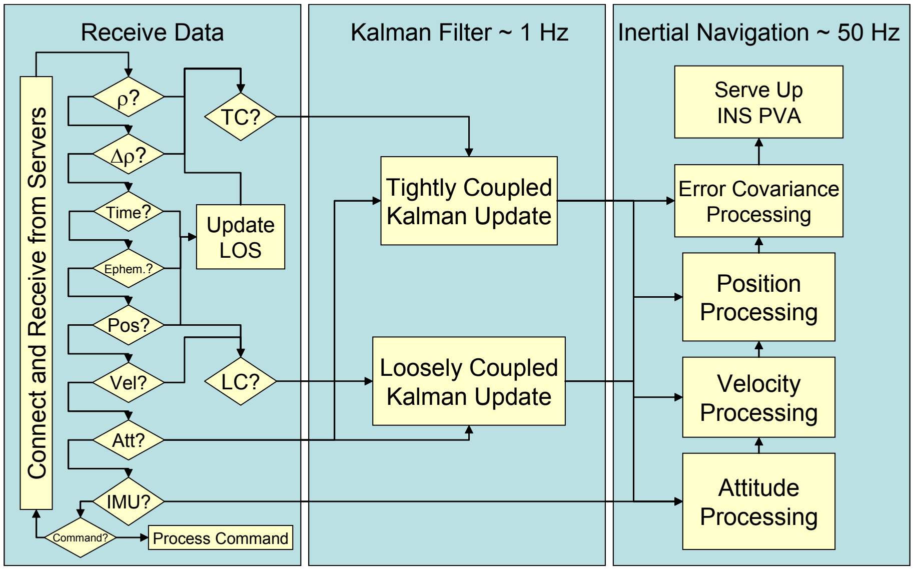

When the navigation application receives a raw GPS measurement (range or delta-range), if the navigation application is in a tightly coupled mode (see Chapter 4), it passes the measurement (and GPS attitude if available) to the Kalman filter module for a tightly coupled Kalman measurement update. If in the loosely coupled mode, the navigation application will pass a received position, velocity, or attitude packet to the Kalman filter module for a loosely coupled Kalman measurement update. A received time and ephemeris packet updates the satellite line-of-sight vectors. Any received IMU messages get passed directly to the inertial navigation process module.

In the inertial navigation process, the INS attitude is calculated first by using the IMU delta-angle measurements (see Chapter 4). Next the IMU delta-velocity measurements are integrated to update the INS velocity and position. The error covariance and estimates are next updated and the final INS solution is sent out to interested clients.

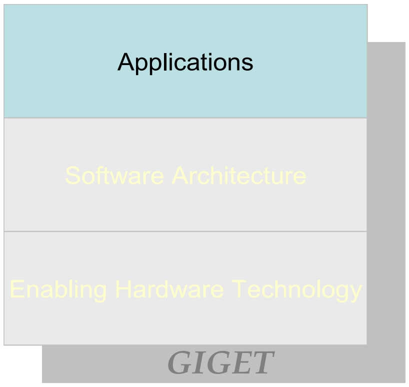

Chapter 4: Navigation Algorithms and Applications

Chapter 4 describes the third tier of GIGET development, the application level. The following sections detail the algorithms chosen to demonstrate various uses of GIGET. GIGET implements navigation algorithms used throughout industry; these very standard and conservative navigation and attitude algorithms provide a *baseline* for trade study results and comparison with future, more advanced techniques. Chapter 5 will discuss the results of a trade study using these algorithms. Although GIGET is flexible and powerful enough to demonstrate many techniques for integration, this chapter limits the scope to best demonstrate the functionality of GIGET, while still keeping the results readable and compact.

A unique feature of GIGET is that it is not limited to these baseline algorithms. In fact, with its flexible software architecture and hardware set-up, GIGET can be used for the side-by-side and real-time comparisons of several navigation algorithms in addition to the ones described in this chapter. The navigation and attitude client/servers described in

Chapter 3 implement the algorithms described here, but other software modules can easily be included and even compared simultaneously with these versions.

In addition to the navigation and attitude client/server algorithms, this chapter also discusses the application of GIGET for deep integration or ultra-tightly coupled techniques. GIGET hardware and software is uniquely designed to support these inertial aiding methods. An analysis of the benefits and difficulties of these techniques are discussed, as well as the implementation possibilities and performance limitations.

4.1 GPS Attitude Determination

The biggest benefit of having multiple antennas with the GIGET system is enabling GPS attitude determination. GPS measurements from an antenna pair, essentially, are used to find the direction of the vector connecting the two antennas. The attitude solution combines a series of these vectors to observe the full orientation of the vehicle or platform on which the antennas lie. GIGET provides highly accurate (<0.2 degrees for baselines of 36 cm and 50 cm), real-time, attitude and heading information.

As covered in Chapter 3, the GIGET attitude client/server and unique GPS server software modules allow for these vectors or antenna pairs to be either defined and calibrated rigidly before testing, or switched and re-calibrated on-the-fly. This is useful if one antenna fails and a better attitude solution can be achieved with another antenna pair configuration.

This section discusses how the attitude is determined from the antenna pair GPS measurements, and the difficulties that arise such as line bias calibration and integer resolution.

4.1.1 ATTITUDE FUNDAMENTALS

Attitude is the orientation of a vehicle relative to a known set of directions or reference frame. Section 4.2.1 includes a description of the reference frames used in the Chapter 4 algorithm development. In particular, the attitude of a vehicle is usually expressed as the orientation of the vehicle's body frame to the local level inertial reference frame. Attitude can be expressed in terms of Euler angles (roll (Φ), pitch(Θ), and yaw(Ψ)) or in terms of quaternions. There are numerical reasons why quaternion expressions are preferable; however, the following discussion is expressed in Euler angles for a more intuitive interpretation.

4.1.1.1 Attitude Determination.

The attitude matrix is the direction cosine matrix or transformation matrix that defines the orientation of the local level frame (L) to the body frame (B). (Section 4.2.1 defines these reference frames.) Attitude determination describes the search for this orthogonal matrix, $\mathbf{C}_L^B$, which satisfies the equation

$$\mathbf{C}_L^B\ \mathbf{v}^L{}_i = \mathbf{v}^B{}_i \quad (i = 1,..., n). \tag{4.1}$$

Where $\mathbf{v}^B{}_i$ and $\mathbf{v}^L{}_i$ are a collection of n observed vectors, located on the vehicle, expressed in the both the body frame and the local level frame. There have been many methods developed and presented in the literature for solving this problem [26][27][23]. These methods use GPS observables to determine these vectors, or to solve for the attitude matrix directly. The following section describes how these measurements are defined and gathered.

4.1.1.2 GPS Measurements

Figure 4.1 illustrates the GPS signal as planar wave fronts approaching two separate GPS antennas, A and B. The vector connecting the two antennas is the "baseline" vector, **b**. The unit vector from the GPS antenna to the GPS satellite is the line-of-sight vector, **e**. Δr is the difference in range to the satellite from each antenna, referred to as the delta-range. The true range from each antenna to the satellite is designated by ρ.

$$\Delta r = \rho_A - \rho_B \tag{4.2}$$

Figure 4.1. Two-Dimensional View of GPS Measurements and Baseline Vectors

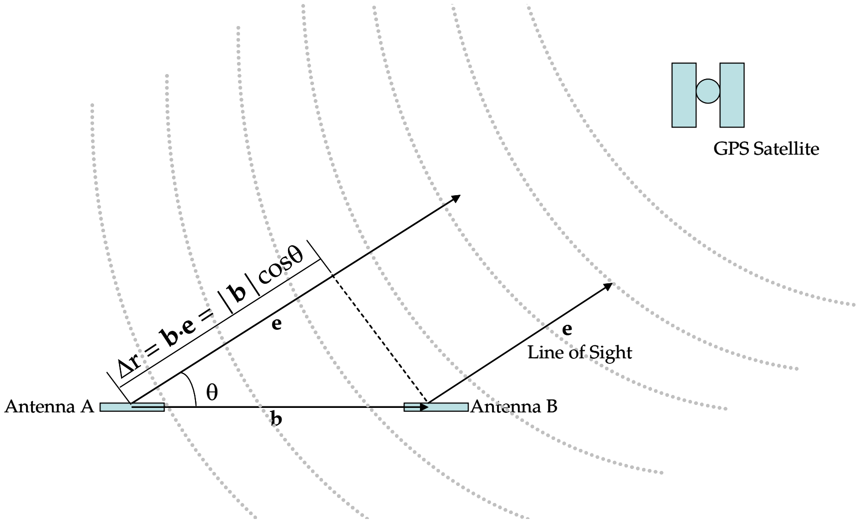

At each antenna, the receiver accumulates a measurement of the phase of the GPS signal from each satellite. The receiver measures a fraction of the signal cycle, and also keeps track of any full cycles accumulated since it started tracking the signal, unless there is a cycle-slip. This phase can be represented as a function of the range to the satellite. The initial integer number of cycles to the satellite is unknown and is referred to as the integer ambiguity, N. For a given satellite and receiver, the phase measurement is:

$$\phi_A = \frac{f}{c}(\rho_A + \beta_A) - N_A + \varepsilon. \tag{4.3}$$

Where ρ_A is the true range from the antenna A to a satellite, β is the clock bias of the receiver, and ε is any measurement errors (including satellite and receiver specific errors). The GPS L1 signal frequency is f, 1575.42 MHz (for a wavelength of 19.03 cm), and c is the speed of light.

The delta-range can also be formulated as a function of the difference of the phase measurements at each antenna, or the “delta-phase.” The delta-phase, expressed in Equation 4.4, is the difference in phase measurements from one particular satellite between two different antennas. The integer number of wavelengths as measured between the two antennas is k, and $\Delta\beta$ is the delta-clock bias or line bias between the two antennas. Note that the line bias is receiver pair dependent and not a function of the satellite. The line bias estimation or calibration procedure is detailed in Section 4.1.2.2. Section 4.1.2.3 describes methods to resolve the integer ambiguity, k.

$$\Delta\phi \equiv \phi_A - \phi_B = \frac{f}{c}(\rho_A - \rho_B + \beta_A - \beta_B) - N_A - N_B + \varepsilon = \frac{f}{c}(\Delta r + \Delta\beta) - k + \varepsilon \qquad (4.4)$$

The delta-range can also be expressed as the projection of the baseline vector, **b**, onto the line-of-sight vector, **e**, because the magnitude of **b** is small compared to the distance to the satellite.

$$\Delta r = \mathbf{b} \bullet \mathbf{e} \qquad (4.5)$$

The line-of-sight vector, **e**, is formed in the earth-referenced, local-level frame, while **b** is pre-determined in the frame of the antenna, or the body frame. Equation 4.5 can then be expressed as

$$\Delta r = (\mathbf{b}^B)^T(\mathbf{C}_L^B\mathbf{e}^L) . \qquad (4.6)$$

Substituting this definition of delta-range (expressed in units of phase), Equation 4.6, into Equation 4.4 for delta-phase gives:

$$\Delta\phi = (\mathbf{b}^B)^T(\mathbf{C}_L^B\mathbf{e}^L) + \Delta\beta - k + \varepsilon\,. \tag{4.7}$$

Equation 4.7 can be used to solve for $\mathbf{C}_L^B$ once enough measurements of $\Delta\phi$ are acquired as discussed in Section 4.1.2.

The delta-phase, $\Delta\phi$, is the GPS attitude observable required for GPS attitude determination. Refer to [28] and [29] for additional discussion of GPS attitude observables. The following section discusses the GIGET GPS receiver measurements of delta-phase and its unique advantages.

4.1.1.3 GPS Attitude Receivers

GIGET produces the delta-phase measurement by differencing a satellite's phase measurements as observed from two or more antenna/receiver sections. GIGET has up to five antennas so redundant measurements can be used for robustness to antenna outage or flexibility in baseline configuration as described in Chapter 3.

Previous attitude determination systems, such as the TANS Vector or Quadrex [23], have relied on fixed "master" and "slave" antenna pairs for the baseline vector definition. GIGET essentially has the advantages of a "roving" master and slave configuration, with varying antenna pair selections available from the GPS server and attitude client/server software described in Chapter 3. During operation, GIGET can change the baseline configuration as needed. That is, the master antenna can change from one GIGET antenna to another depending on signal quality or satellite availability. For example, if a designated master antenna fails, a second antenna can be used as a new master antenna on the next measurement epoch. With the five possible antennas available with the GIGET receiver, a minimum number of baselines can almost always be obtained. To completely solve for the attitude matrix, a minimum of three antenna pairs must observe at least two satellite delta-phase measurements [29].

Each time the baselines are reconfigured, meaning different antenna/receiver pairs are used for the delta-phase measurements, a new set of line bias terms (the $\Delta\beta$ term in Equation 4.7) must also be used.

A unique feature of the GIGET receiver is that each of its receiver sections has a common reference oscillator. This implies that the $\Delta\beta$ term in Equation 4.7 is truly only a line bias due to differing delays in the signal path to each receiver and not also a function of the different receiver's clock biases. That is, the clock bias of both receivers measuring the delta-phase is common, and subtracts out of the measurement equation, Equation 4.7. The remaining path delays can be pre-calibrated and removed from the equation as well. This makes the attitude solution much simpler, since the line bias does not need to be estimated along with the attitude. Without the pre-calibrated line bias removal, the delta-phase measurements must be "double-differenced" to eliminate the clock term, or the clock term must be directly estimated within the attitude solution. Both methods are explained in more detail in Section 4.1.2, but both require more measurements and provide a significantly noisier solution.

Of course the constant line bias term due to the common reference oscillator is only approximate, and this term does slowly drift over time due to temperature fluctuations in and around the receiver and other variations in the receiver design. Much care was taken to limit these variations in the receiver as discussed in Section 2.1.1, however, the GIGET line bias estimation techniques do account for any small drifts in the line bias (See Figure 4.2).

4.1.2 GPS Attitude Algorithms

There are two general methods to solve for the attitude matrix given an appropriate number of GPS delta-phase measurements. The first involves using the phase measurements to solve for the baseline vectors positions, then these vector estimates are combined to resolve the attitude matrix, $\mathbf{C}_L^B$. Another approach uses the phase measurements to directly solve for $\mathbf{C}_L^B$. GIGET utilizes both of these approaches, so both will be briefly summarized below. However, there are other documents which give much more detailed descriptions of these algorithms [23][7].

4.1.2.1 Attitude Solution

The attitude matrix, $\mathbf{C}_L^B$, is a non-linear function of Euler angles or quaternions and is not solved explicitly. Therefore, to solve, the matrix is linearized with respect to an initial estimate, $\overline{\mathbf{C}}_L^B$.

$\delta\mathbf{C}$ is defined as a transformation through a sequence of small angles, $\delta\boldsymbol{\theta}$, from this initial estimate, $\overline{\mathbf{C}}_L^B$, to the true $\mathbf{C}_L^B$. Where,

$$\mathbf{C}_L^B = \delta\mathbf{C}\,\overline{\mathbf{C}}_L^B\text{, and} \tag{4.8}$$

$$\delta\mathbf{C} \equiv \mathbf{C}_L^B(\delta\theta_1, \delta\theta_2, \delta\theta_3) = \begin{bmatrix} 1 & \delta\theta_3 & -\delta\theta_2 \\ -\delta\theta_3 & 1 & \delta\theta_1 \\ \delta\theta_2 & -\delta\theta_1 & 1 \end{bmatrix}. \tag{4.9}$$

Assuming small angles, $\delta\mathbf{C}$, can be approximated to first order as

$$\delta\mathbf{C} \approx \mathbf{I} + \{\delta\boldsymbol{\theta}\}, \tag{4.10}$$

where, $\{\bullet\}$,denotes a cross product operator and the skew-symmetric matrix of a vector, defined as:

$$\{\mathbf{v}\} \equiv \begin{bmatrix} 0 & v_3 & -v_2 \\ -v_3 & 0 & v_1 \\ v_2 & -v_1 & 0 \end{bmatrix}. \tag{4.11}$$

Substituting back into the delta-phase equation (Equation 4.7) reveals,

$$\Delta\phi = (\mathbf{b}^B)^T(\mathbf{I} + \{\delta\boldsymbol{\theta}\})\bar{\mathbf{C}}_L^B\mathbf{e}^L + \Delta\beta - k + \varepsilon. \tag{4.12}$$

Given estimates of the baseline vector, $\bar{\mathbf{b}}$, and the attitude matrix, $\bar{\mathbf{C}}_L^B$, the integer ambiguity, $\bar{k}$ (see Section 4.1.2.3), and line bias estimate, $\Delta\beta$, this delta-phase term can be estimated as:

$$\Delta\bar{\phi} = (\bar{\mathbf{b}}^B)^T\bar{\mathbf{C}}_L^B\mathbf{e}^L + \Delta\bar{\beta} - \bar{k}. \tag{4.13}$$

The difference in the estimated delta-phase, $\Delta\bar{\phi}$, from the actually measured delta-phase is the delta-phase residual, $\delta\phi$. That is,

$$\delta\phi \equiv \Delta\phi - \Delta\bar{\phi}. \tag{4.14}$$

Assuming small errors in the estimates of line bias and integer ambiguity, two general methods can be used to solve for the attitude matrix, $\mathbf{C}_L^B$. The first solves for the baseline vector components, $\bar{\mathbf{b}}$, in a least squares sense from Equation 4.13. The attitude matrix can be determined from the knowledge of the baseline vectors defined in inertial space. That is, the Euler angles or quaternions defining the attitude matrix can be estimated directly from the location in space of the baseline vectors [7]. The second technique is developed by Cohen [23] and manipulates the equation to solve for the attitude matrix directly. Cohen demonstrated that the equation for $\delta\phi$ can be rearranged as

$$\delta\phi = (\bar{\mathbf{C}}_L^B \mathbf{e}^L)^T \{\bar{\mathbf{b}}^B\} \delta\theta + \varepsilon , \tag{4.15}$$

with $\{\bar{\mathbf{b}}^B\}$ the skew symmetric representation of $\bar{\mathbf{b}}$ as defined in Equation 4.11. With a least squares approach and enough measurements of $\delta\phi$, this equation can be used to solve for $\delta\bar{\theta}$ where

$$\mathbf{H} = (\bar{\mathbf{C}}_L^B \mathbf{e}^L)^T \{\bar{\mathbf{b}}^B\} \ . \tag{4.16}$$

With an estimate of $\delta\theta$, Equation 4.8 and Equation 4.10 can be used to solve for a new estimate of the attitude matrix, $\bar{\mathbf{C}}_L^B$.

4.1.2.2 Line Bias Estimation

The description of both attitude solution techniques in the previous sections assumes a very good knowledge of the clock bias difference, $\Delta\beta$. This clock or line bias can be estimated or removed in several different ways [23][7][30]. This section briefly covers some of these techniques and summarizes the two ways GIGET solves for this line bias term.

The first method uses “double differencing” techniques to remove the clock bias term from the solution altogether. The delta-phase measurements described in previous sections are considered “single difference” measurements. They are the difference in measured phase from a single satellite between two antenna/receiver pairs. A double difference measurement is the difference across two satellites (satellites i and j in Equation 4.17) of the single difference measurements:

$$\nabla\Delta\phi_{ij} \equiv \Delta\phi_i - \Delta\phi_j = \frac{f}{c}(\Delta r_i - \Delta r_j + \Delta\beta - \Delta\beta) - k_i + k_j + \varepsilon_i - \varepsilon_j = \frac{f}{c}(\nabla\Delta r) - k_{ij} + \varepsilon_{ij}. \quad (4.17)$$

Given enough double difference measurements, the attitude matrix can be resolved with similar techniques as discussed in the previous section [30][29][31]. The double difference techniques completely eliminate the clock term from the attitude solution equation. This greatly benefits the attitude determination process when the receivers do not share a common clock base, and the line bias term is quite variable. However, double difference techniques both require more measurements and provide a significantly noisier solution. GIGET does not require the double differencing techniques because its receivers have a common reference oscillator, and the line bias term can be estimated directly using either of the two methods discussed below.

The second method assumes that the line bias term is constant and can be pre-determined through any of several surveying techniques of the baseline vectors. Once the line bias is determined, it can be removed from the attitude solution equations. This is discussed in detail in the literature [23]. The following section refers to this method as the “known line bias” technique.

A third method for estimating the line bias, or clock bias, between two receivers is to solve directly for this state along with the baseline position states. This is a traditional method similar to other GPS position solution techniques [32][7]. The following section refers to this method as the "unknown line bias" techniques. Like the double difference technique, it requires more measurements and provides an equally noisy attitude solution.

GIGET uses a combination of the known and unknown line bias techniques. That is, first the line biases for each potential baseline (several are possible with the multi-antenna GIGET system) are surveyed and estimated and assumed constant in the attitude solutions during GIGET operations. However, during attitude operations, GIGET also processes the unknown line bias method in the background. GIGET uses the background calibration to periodically update the line bias estimation in the primary attitude solution routine. The unknown line bias estimation results are averaged over a period of ten to twenty minutes before being used as the new calibrated line bias estimate. The averaging time can be varied depending on the drift of the line biases. However, the results in Section 4.2.6.1 show that the biases do not drift much for short periods of time and the known line bias technique is quite sufficient for most GIGET testing (usually under twenty minutes).

4.1.2.3 Integer Resolution

Numerous techniques resolve the integer ambiguity noted in Equation 4.13. These include motion based techniques [23], or processes that require several minutes of data collection, or those that search for likely integers out of a fixed volume of space [33][34][35]. All, however, can benefit from a good initial guess of the attitude of the baseline platform to reduce the search space for the integers. GIGET uses an integer ambiguity technique that first uses the *a priori* knowledge of attitude to essentially "back-out" the most probable integers. The GIGET algorithm passes these integer guesses through a series of very stringent tests using prior knowledge of baseline lengths and body frame orientation to verify that they are the correct integers. If not correct, the GIGET algorithm begins to search over a probable space around this first initial guess of attitude as opposed to the entire integer space. This sequential integer ambiguity determination is detailed in [7][36].

This integer resolution method is straight forward if GIGET initializes at a known location and attitude (this is how most of the GIGET system tests were initialized). But a more difficult situation occurs if there is a cycle-slip or total GPS outage during GIGET operations. How would GIGET know its current attitude to begin the search if it lost GPS? This is where a combined GPS/INS system such as GIGET can be most advantageous. The inertial navigation system (INS) in GIGET is also estimating the platform attitude. If there is a GPS outage or cycle-slip, the INS provides an ideal initial guess for the attitude and hence integer determination. This integer determination method is 100% reliable as long as the difference between the estimated and actual attitude is less than six degrees in all axes for the short baselines used by Hayward [7] of less than 50 cm. Therefore, this method is very good for short GPS outages, but once the INS attitude drifts away from truth too much, one of the other integer determination methods must be used. GIGET's tactical grade inertial sensor quality made such large drifts during outages unlikely. However, for other systems that use much lower grade sensors, other techniques may be needed for integer determination.

4.1.3 Testing and Evaluation

GIGET attitude systems were first tested on ground systems, then flown on the Queen Air test airplane of the GPS Laboratory to verify the receiver performance. For the testing, the

Queen Air airplane contained a Trimble TANS Quadrex receiver (sharing antenna inputs with GIGET) and also a navigation grade inertial navigation system, the Honeywell 1050. The Quadrex receiver is an early version of the TANS Vector receiver manufactured by Trimble Navigation for attitude determination. The following attitude results compare the TANS attitude receiver performance to the GIGET performance, and both use the INS solution as the "truth" attitude. Figure 4.2 demonstrates that the know line bias solution for both the TANS and the GIGET (black lines labeled as "multi"antenna system) are similar, and attitude error is less than 0.2 degrees (using baselines of 36 cm and 50 cm) compared to the INS solution.

Figure 4.2. Queen Air Flight Test Results

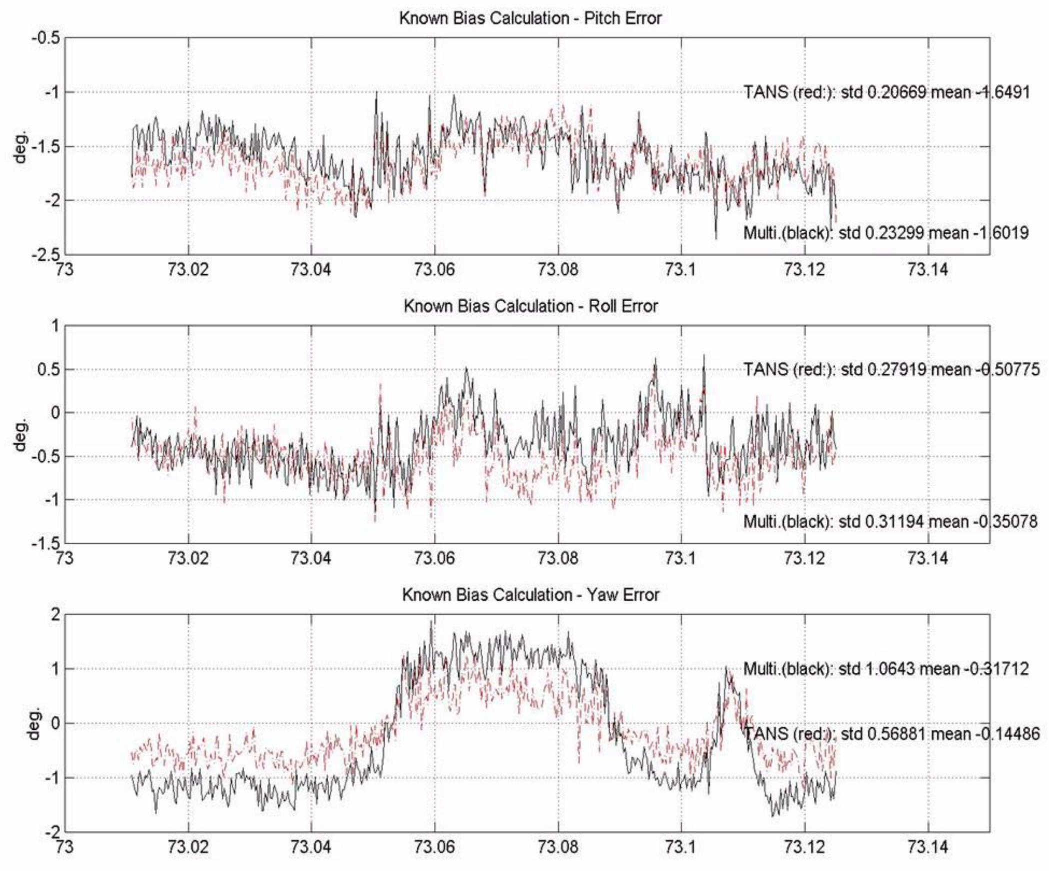

4.2 Inertial Navigation System

Inertial navigation is based on the implementation of Newton's laws of motion using the sensor measurements of force and rate. It is limited in accuracy by the quality of these sensor measurements. It is a self-contained system that provides angular and translational information: position, velocity, attitude, angular rate, and linear acceleration. Before an analysis or development of an inertial navigation algorithm, the sensor measurements and the translational and angular information must be defined in a series of reference frames relating the frame of the vehicle platform to an inertial frame.

This section begins with a short definition of the frames, then continues with the strap-down mechanization chosen to represent the inertial navigation system. A mechanization not only includes the frame in which the inertial equations are defined, but also the type and methods of defining the errors in the inertial navigation information. Perfect inertial sensors would lead to perfectly accurate navigation information, but since real sensors are degraded by error sources, techniques have been derived to estimate and compensate for these errors. GIGET uses a very widely used *Psi-Angle* mechanization of these navigation errors. Section 4.2.2 briefly presents these navigation error equations, but much more detail can be found in the literature [37][38][39]. The extended Kalman filter of Section 4.2.3 describes the blending of these error equations with GPS measurements for a more precise estimate of the navigation errors.

This chapter continues with a discussion of the loosely coupled and tightly coupled methods for blending the GPS and inertial information, and with the simulation and testing of both methods with GIGET. Chapter 4 concludes with a discussion of inertial aiding of GPS receivers, which is referred to a ultra-tightly coupled or deep integration.

4.2.1 Reference Frames

The following reference coordinate frames are used in describing the navigation algorithms of GIGET. The letters next to the frame name designate the frames when used in equations throughout this chapter. Refer to [37] or [39] for further discussion of the following frame definitions.

Body Frame (B) - an orthogonal coordinate system with an arbitrary orientation, but fixed inside the vehicle body, usually centered in the vehicle center of mass, or defined by the axes of an accelerometer or gyroscopic triad. Aircraft applications conventionally have the x_B axis point through the nose of the aircraft (the roll axis), the y_B axis out the right wing (the pitch axis), and the z_B axis pointing down (the yaw axis).

Local Level Frame (L or NED) - a coordinate frame with its origin defined similar to the body frame, but with one axis along the local geodetic frame. The x_L axis points towards geodetic north, the y_L axis completes a right-hand orthogonal frame (i.e. points to the east), and the z_L axis is orthogonal to the reference ellipsoid and points inward (or down).

Wander Frame (W) - a coordinate frame defined on the basis of the local level frame, but with the x_W axis not slaved to point in the north direction. The wander frame rotates with respect to the local level frame about its z_W axis. The angle between north and the x_W axis is called the wander angle, α. The local level frame (L) is precessed about its vertical axis to maintain the level axes pointing north and east; however, the amount of L frame precession becomes very large at high latitudes. The wander frame was derived to avoid this large precession rate if the Earth's poles are traversed. It is used with GIGET primarily because it is such a commonly used frame and mechanization in conventional inertial navigation systems. The wander angle is defined in terms of longitude (λ) and latitude (ϕ) as:

$$\dot{\alpha} = -\dot{\lambda}\sin\phi . \qquad (4.18)$$

Figure 4.3 more clearly shows the wander angle as an azimuth rotation relative to north.

Figure 4.3. Wander Angle

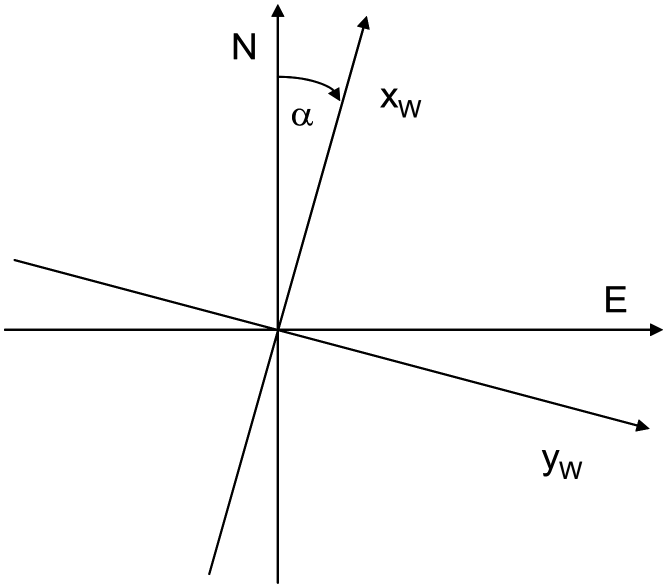

Earth Frame (E or ECEF) - an orthogonal coordinate frame with its origin at the center of mass of the Earth. The x_E axis points toward the meridian of Greenwich, the z_E axis lies along the mean spin axis of the Earth, and the y_E axis completes a right-hand orthogonal coordinate system.

Inertial Frame (I) - is a non-rotating and non-accelerating frame relative to inertial space (i.e. the "fixed" stars). By neglecting the motion of the Earth around the Sun, the frame center is assumed at the Earth center of mass. The x_I and y_I axes lie in the equatorial plane of the Earth, with the x_I axis pointing towards a star, and the z_I axis aligns with the Earth's spin axis.

4.2.2 Mechanization

GIGET algorithms use the wander frame to mechanize the inertial navigation equations. Although GIGET will not likely traverse the poles to make the wander frame mechanization a requirement, it is a very widely used and standard way of defining the navigation equations. With the wander frame as a basis, it is easier to compare algorithm development and resulting GIGET performance with many systems already in use today [38][40][41]. As previously mentioned, these algorithms are used as a baseline for performance evaluation, and GIGET is not limited to this mechanization. Many future studies may benefit from the comparison of additional GIGET mechanizations with the more standard ones presented in this document. However, in an effort to contain the size of the work, the trades presented in Chapter 5 all use the wander frame mechanization and consider trade-offs of measurement type.

4.2.2.1 Inertial Navigation Equations

From Newton's laws of motion the following equations can be derived to describe the motion of a vehicle in the wander frame. Many other references can be consulted for detailed proofs and derivations, such as [42][37][39]. Note that the brackets, $\{\bullet\}$, denote the skew-symmetric matrix of the enclosed vector, as in Equation 4.11.

$$\dot{\mathbf{C}}_B^W = \mathbf{C}_B^W\{\omega^B\} - \{\rho^W + \mathbf{\Omega}^W\}\mathbf{C}_B^W \tag{4.19}$$

$$\dot{\mathbf{v}}^W = (\mathbf{C}_B^W)\,\mathbf{a}^B - \{2\mathbf{\Omega}^W + \rho^W\}\mathbf{v}^W + \mathbf{g}^W \tag{4.20}$$

$$\dot{\mathbf{D}}_W^E = \mathbf{D}_W^E\{\rho^W\} \tag{4.21}$$

Where

$\mathbf{C}_B^W$ = the transformation matrix from the body frame to the wander frame

$\mathbf{D}_W^E$ = the transformation matrix from the wander frame to the earth frame

$\mathbf{v}^W$ = the vehicle velocity relative to the Earth expressed in the wander frame

$\mathbf{g}^W$ = plumb-bob gravity vector expressed in the wander frame

$\mathbf{\Omega}^W$ = Earth's angular velocity relative to an inertial frame

ρ^W = the angular velocity of the wander frame relative to the Earth. This is also known as the transport rate. For the wander frame mechanization, the vertical component of the transport rate, ρ_z, is set to zero.

ω^B = the angular velocity of the vehicle relative to an inertial frame.

$\mathbf{a}^B$ = the non-gravitational acceleration (or specific force) of the vehicle expressed in the body frame.

The following diagram in Figure 4.4 summarizes the method for solving these equations to determine position, velocity, attitude, attitude rate, and acceleration information.

Figure 4.4. Inertial Navigation Processing

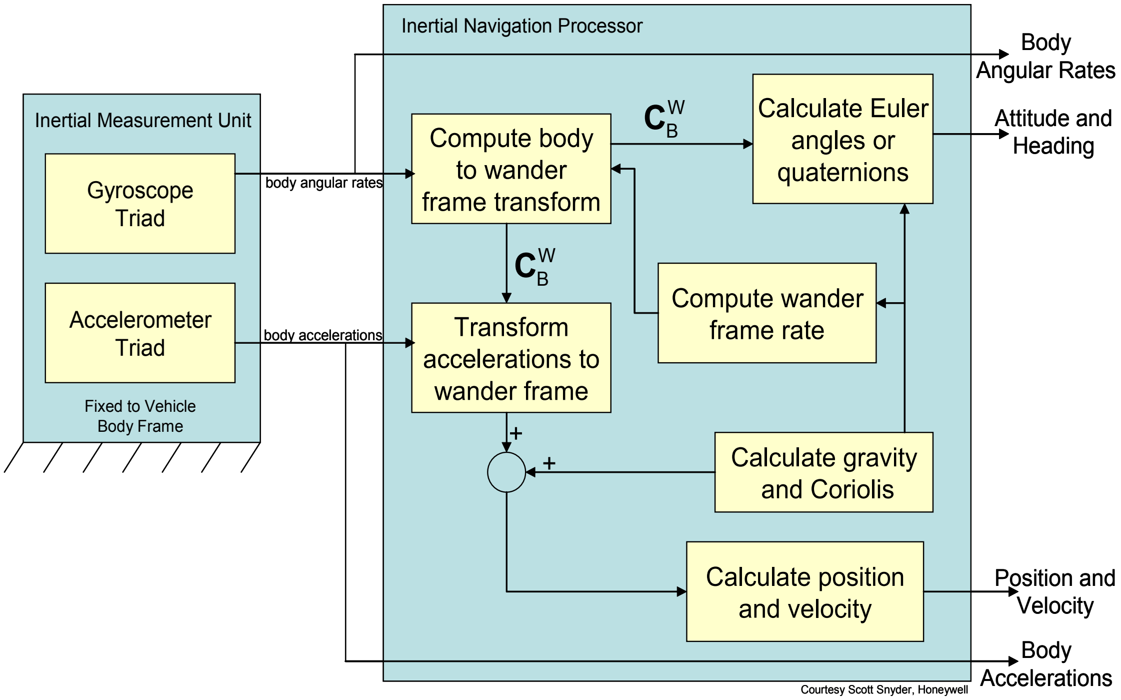
Inertial Navigation Processor
Inertial Measurement Unit
Gyroscope Triad
Accelerometer Triad
Fixed to Vehicle Body Frame
body angular rates
body accelerations
Compute body to wander frame transform
C_B^W
C_B^W
Calculate Euler angles or quaternions
Compute wander frame rate
Transform accelerations to wander frame
+
+
Calculate gravity and Coriolis
Calculate position and velocity
Body Angular Rates
Attitude and Heading
Position and Velocity
Body Accelerations

Courtesy Scott Snyder, Honeywell

A series of calculations occur in each of the blocks represented in Figure 4.4. For GIGET, these calculations are performed at a 50 Hz output rate. The following briefly summarizes these calculations. Refer to other documents for further details of these operations [39][43][37].

1. *Compute body to wander frame transform* - this calculation block takes in the gyroscope outputs of vehicle body angular rates (or Δθ's--delta-angle, the sensed change in angular position from one measurement epoch to the next), and the computed wander frame rate. With these inputs and the estimated position and wander angle, Equation 4.19 is numerically integrated and corrected for coning (error induced by incremental rotation over update period) and sculling (correlated angular and translational oscillation) [39]. The primary output is an updated transformation matrix from the body frame to the wander frame.

2. *Transform accelerations to the wander frame* - input to this calculation block include the measured accelerations (or Δv's--delta-velocity, the sensed change in velocity from one measurement epoch to the next) in the body frame. These are transformed to the wander frame before integration.

3. *Calculate gravity and Coriolis* - with an estimate of the vehicle's latitude, this block calculates a gravity estimate given a model for plumb-bob gravity [44]. The Coriolis acceleration is also calculated given the estimated position, wander frame rate and wander angle.

4. *Calculate position and velocity* - finally, the velocity is numerically integrated with the inputs of gravity, coriolis acceleration, and measured accelerations. A further integration of the latest velocity estimate calculates the position, given an update of the transformation matrix from the wander frame to the earth frame, **D**.

Before the navigation process begins, the INS solution is operationally initialized with a commanded initial position and the GPS attitude solution. Conceptually, the inertial system can be initialized by first sensing the gravitational acceleration in a stationary and surveyed position. With this sensed gravity vector, the pitch and roll of the vehicle platform can be coarsely resolved; however, there is an ambiguity in determining the heading of the platform. The tactical grade inertial sensor's quality is not sufficient to gyrocompass by sensing the Earth's rotation to detect the east direction. Therefore, the GPS attitude system heading is aligned with the inertial measurement unit yaw axis so that the INS attitude can be initialized with the GPS attitude solution. This initial condition is sufficient for a fine alignment Kalman filter procedure as described in [45].

The results of these calculations of position, velocity and attitude are subject to a variety of errors of the inertial sensors and the navigation system itself. These errors include sensor biases, scale factor and alignment errors, G sensitivity, quantization, thermal noise, round-off errors, vibration, and many more. The next section develops a model to describe and predict these errors. With additional GPS or other external navigation aids, these errors can be measured by comparing the INS outputs to these other navigation solutions. An extended Kalman filter described in Section 4.2.3, uses these measurements of navigation errors to correct the overall navigation system outputs.

4.2.2.2 Error Equations

The errors in the inertial navigation system are defined as the difference between the navigation output values such as position, velocity and attitude, and the actual values. There are many techniques to model the inertial navigation errors. GIGET implements the *Psi-Angle* error model method, derived in detail in [38][37][39] to formulate the transition matrix or plant matrix of an extended Kalman filter (See Section 4.2.3). The Psi-Angle method is widely used because the resulting differential equations for the angular errors are completely uncoupled from the resulting equations for the translational errors. This not only creates a numerical advantage, but can illustrate the fundamental dependence of the velocity results to the angular error accuracy (see Chapter 5). The Psi-Angle method defines three coordinate axes to derive the equations for the system error [37].

True (T) - This is the local level (wander) coordinate system that represents the true position of the system or platform.

Computed (C) - This is the local level coordinate system that the inertial system *computes* as the actual system, i.e. it is the computed estimate of the True system.

Platform (P) - This is the set of axes that specify the actual platform alignment. This differs from the True system by any unknown misalignment errors of the inertial sensors.

These three coordinate system sets differ by a series of small angle rotations. These angle vectors are $\boldsymbol{\phi}$, the angle error from the True axes to the Platform set (platform misalignment); $\delta\boldsymbol{\theta}$, the angle error from the True axes to Computed axes (computed position error); and $\boldsymbol{\psi}$, the angle error from the Computed axes to the Platform axes. The angle error vectors are related as:

$$\boldsymbol{\phi} = \boldsymbol{\psi} + \delta\boldsymbol{\theta} \tag{4.22}$$

Figure 4.5 is a two dimensional view of the angular errors, but the actual errors are in three dimensions.

These angular errors illustrate two contributing factors to the overall system error due to the gyroscope measurements. First, the gyroscopic drift contributes to errors directly in the sensor measurements.

$$\dot{\boldsymbol{\psi}} = -\boldsymbol{\varepsilon}, \tag{4.23}$$

where $\boldsymbol{\varepsilon}$ is the platform drift.

Second, angular errors contribute to the errors in the estimate of the local level coordinate frame, in which all the INS outputs are defined [38]. Thus, there is a computed error in position due to angular errors. This position error is related to the angular error as:

$$\delta\mathbf{R} = \delta\boldsymbol{\theta} \times \mathbf{R}, \tag{4.24}$$

where $\mathbf{R}$ is the position vector of the vehicle [37]. The δ term implies a perturbation from the true value, defining an error as estimate minus truth.

Figure 4.5. Angle Error Vector Illustration

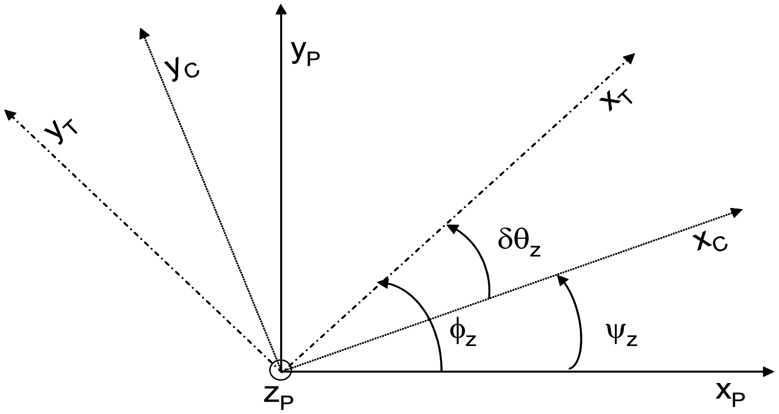

Given the above definitions for angular errors, and applying a perturbation in the navigation equations of Equation 4.19 through Equation 4.21, a complete set of error models for the INS outputs of position, velocity, and attitude are derived [37][39]. The perturbations result in the following Psi-Angle error equations to describe position, velocity, and angular error dynamics.

$$\dot{\psi} = -(\boldsymbol{\Omega}^{W} + \rho^{W}) \times \psi - \mathbf{C}_{B}^{W}\delta\omega^{B} \tag{4.25}$$

$$\delta\dot{\mathbf{v}} = -\psi \times \mathbf{a}^{W} - (2\boldsymbol{\Omega}^{W} + \rho^{W}) \times \delta\mathbf{v} - \mathbf{G}\delta\mathbf{R}^{W} + \mathbf{C}_{B}^{W}\delta\mathbf{a}^{B} + \delta\mathbf{g}^{W} \tag{4.26}$$

$$\delta\dot{\mathbf{R}}^{W} = \delta\mathbf{v} - \rho^{W} \times \delta\mathbf{R}^{W} \tag{4.27}$$

$$\mathbf{G} = \omega_s^2 \begin{bmatrix} 1 & 0 & 0 \\ 0 & 1 & 0 \\ 0 & 0 & -2 \end{bmatrix} \tag{4.28}$$

$$\omega_s^2 = \frac{g}{R_E} \tag{4.29}$$

Where,

$\delta\mathbf{v}$ = the vehicle velocity error relative to the Earth

$\delta\mathbf{R}$ = the vehicle position error

ψ = the vehicle angular error

$\delta\mathbf{g}^W$ = gravity deflection and anomaly errors expressed in the wander frame

$\mathbf{G}$ = gravity gradient matrix

ω_s = the Schuler frequency, approximately $2\pi/84.4$ minutes.

R_E = the distance from the Earth's center

$\mathbf{a}^W$ = the non-gravitational acceleration expressed in the wander frame

$\delta\mathbf{a}^B$ = the acceleration (accelerometer) errors expressed in the body frame

$\delta\boldsymbol{\omega}^B$ = the angular rate (gyroscope) errors expressed in the body frame

The gyroscope and accelerometer bias errors ($\delta\boldsymbol{\omega}^B$ and $\delta\mathbf{a}^B$) are modelled as a first-order Gauss Markov process:

$$\delta\dot{\bar{\boldsymbol{\omega}}}^B = -\frac{\delta\bar{\boldsymbol{\omega}}^B}{\tau_{\omega B}} + \eta \qquad (4.30)$$

$$\delta\dot{\bar{\mathbf{a}}}^B = -\frac{\delta\bar{\mathbf{a}}^B}{\tau_{aB}} + \eta \qquad (4.31)$$

4.2.3 GPS/INS KALMAN FILTER FORMULATION

The previous section defined the inertial navigation equations and described a model for INS errors. Assuming that the INS errors are small relative to the motion of the vehicle, the INS output can be used as a reference trajectory for a Kalman filter to optimally estimate the INS errors. The Psi-Angle error equations are used to formulate the transition matrix or plant matrix of an extended Kalman filter. Figure 4.6 illustrates the GIGET extended Kalman filter. When compared to the INS outputs, GPS measurements provide an external measure of the error in the INS, and hence act as the Kalman filter measurement updates. The type of GPS measurements define the style of GPS/INS blending, such as loosely coupled or tightly coupled. This section briefly describes the GIGET Kalman filter and the corresponding transition matrix with sensor error models. It also discusses the GPS measurements of position, velocity, attitude, range, and delta-range as defined in the loosely coupled and tightly coupled systems.

4.2.3.1 Kalman Filter Basics

This section briefly summarizes the extended Kalman filter equations and operations, but these are derived in much more detail in many other references such as [46][47]. The extended Kalman filter is a method to optimally estimate a state of the general form

$$\dot{\boldsymbol{x}}(t) = \boldsymbol{f}(\boldsymbol{x}(t),t) + g(\boldsymbol{x}(t),t)\boldsymbol{w}(t)\,, \tag{4.32}$$

where $\boldsymbol{x}$(t) is the state vector and $\boldsymbol{w}$(t) is the process noise: a Gaussian white-noise process with mean and covariance given by

$$E\{\boldsymbol{w}(t)\} = \boldsymbol{0} \text{ and } E\{\boldsymbol{w}(t), \boldsymbol{w}^T(t')\} = Q(t)\delta(t-t')\,. \tag{4.33}$$

The prediction of the state can be written approximately as

$$\dot{\bar{\boldsymbol{x}}}(t) = \boldsymbol{f}(\bar{\boldsymbol{x}}(t),t)\,. \tag{4.34}$$

Integrated, this equation gives

$$\bar{\boldsymbol{x}}(t) = \phi(t, \bar{\boldsymbol{x}}(t_0), t_0)\,. \tag{4.35}$$

The state error vector, δ$\boldsymbol{x}$, and the state covariance matrix, **P**(t) are defined as:

$$\delta\boldsymbol{x} \equiv \bar{\boldsymbol{x}}(t) - \boldsymbol{x}(t) \tag{4.36}$$

$$\mathbf{P}(t) \equiv E\{\delta\boldsymbol{x}(t), \delta\boldsymbol{x}^{\mathrm{T}}(t)\}\ . \tag{4.37}$$

Neglecting higher order terms, the state error vector can now be expressed by the differential equation:

$$\delta\dot{\boldsymbol{x}}(t) = \boldsymbol{F}(t)\delta\boldsymbol{x}(t) + G(t)\boldsymbol{w}(t), \tag{4.38}$$

where

$$\boldsymbol{F}(t) \equiv \frac{\partial}{\partial \boldsymbol{x}}\boldsymbol{f}(\boldsymbol{x}, t)\bigg|_{\bar{\boldsymbol{x}}(t))} \text{ and } G(t) \equiv g(\bar{\boldsymbol{x}}(t), t). \tag{4.39}$$

Equation 4.38 can be formally integrated to give

$$\delta\boldsymbol{x}(t) = \Phi(t, t_0)\delta\boldsymbol{x}(t_0) + \int_{t_0}^{t} \Phi(t, t')G(t')\boldsymbol{w}(t')dt'. \tag{4.40}$$

$\Phi(t,t_0)$ is the transition matrix, which satisfies

$$\frac{\partial}{\partial t}\Phi(t, t_0) = \boldsymbol{F}(t)\Phi(t, t_0) \text{ and } \Phi(t_0, t_0) = \boldsymbol{I}. \tag{4.41}$$

The predicted covariance matrix can be expressed as

$$\mathbf{P}(t) = \Phi(t, t_0)\mathbf{P}(t_0)\Phi^T(t, t_0) + \int_{t_0}^{\mathrm{t}} \Phi(t, t')G(t')Q(t')G^T(t')\Phi^T(t, t')dt'. \tag{4.42}$$

Discretizing the above equations describes the time update equations for the extended Kalman filter:

$$\delta\boldsymbol{x}^-(k + 1) = \Phi((k + 1), k)\delta\boldsymbol{x}^+(\mathrm{k}) \tag{4.43}$$

$$\mathbf{P}^-(k + 1) = \Phi((k + 1), k)\mathbf{P}^+(k)\ \Phi^T((k + 1), k) + \boldsymbol{Cd}, \tag{4.44}$$

where ***Cd*** is the discretized process noise, an estimate of the integral on the right-hand side of Equation 4.42.

The Kalman filter measurement updates are derived in Section 4.2.4 and Section 4.2.5 for the loosely coupled and tightly coupled cases.

4.2.3.2 Transition Matrix

Equation 4.25 through Equation 4.31 from the previous section define the INS error state vector so that the transition matrix, Φ, can be approximated with a second order power series expansion. See [39] for a detailed derivation of the transition matrix.

$$\Phi((k+1), k) = \mathrm{I} + \mathbf{F}\Delta \mathrm{t} + \frac{(\mathbf{F}\Delta \mathrm{t})^2}{2!} \qquad (4.45)$$

where, Δt is the time difference from epoch k to k+1, and **F** is defined as in Equation 4.38 for a δ***x*** error state of

$$\delta\boldsymbol{x} = \begin{bmatrix}\delta\mathbf{R} & \delta\mathbf{v} & \psi & \delta\bar{\boldsymbol{\omega}} & \delta\bar{\mathbf{a}}\end{bmatrix} \qquad (4.46)$$

From Equation 4.25 through Equation 4.31, the following represents the continuous transition matrix multiplied by Δt, **F**Δt as used in Equation 4.45.

$$\mathbf{F}\Delta \mathrm{t} = \begin{bmatrix} \begin{bmatrix} & & -\rho_y\Delta t \\ & & \rho_x\Delta t \\ \rho_y\Delta t & -\rho_x\Delta t & \end{bmatrix} & \begin{bmatrix} \Delta t & & \\ & \Delta t & \\ & & \Delta t \end{bmatrix} & & & \\ \begin{bmatrix} \frac{-g\Delta t}{RE} & & \\ & \frac{-g\Delta t}{RE} & \\ & & \frac{2g\Delta t}{RE} \end{bmatrix} & \begin{bmatrix} \left\{ -\begin{bmatrix} 2\Omega + \rho\Delta t \end{bmatrix} \right\} \end{bmatrix} & \begin{bmatrix} & -\Sigma\Delta v_z & \Sigma\Delta v_y \\ \Sigma\Delta v_z & & -\Sigma\Delta v_x \\ -\Sigma\Delta v_y & \Sigma\Delta v_x & \end{bmatrix} & & \begin{bmatrix} \text{Average} \\ \mathbf{C}_B^W\Delta t \end{bmatrix} \\ & & \begin{bmatrix} \left\{ -\begin{bmatrix} \Omega + \rho\Delta t \end{bmatrix} \right\} \end{bmatrix} & \begin{bmatrix} \text{Average} \\ -\mathbf{C}_B^W\Delta t \end{bmatrix} & \\ & & & \begin{bmatrix} \frac{-1}{\tau\omega B} & & \\ & \frac{-1}{\tau\omega B} & \\ & & \frac{-1}{\tau\omega B} \end{bmatrix} & \\ & & & & \begin{bmatrix} \frac{-1}{\tau a B} & & \\ & \frac{-1}{\tau a B} & \\ & & \frac{-1}{\tau a B} \end{bmatrix} \end{bmatrix} \qquad (4.47)$$

It is interesting to note the coupling between the error states when looking at the transition matrix. The angular errors, ψ, do not depend on the $\delta\mathbf{R}$ (position errors) or $\delta\mathbf{v}$ (velocity errors) states, while the $\delta\mathbf{v}$ error state equation *is* dependent on the angular errors. This is evident in the results presented in Chapter 5, where error growth in velocity does not quickly translate into error growth in attitude; however, even small error growth in attitude, can greatly affect and degrade the errors in velocity.

The performance specification of the Honeywell HG1700 for random walk (0.1 deg/$\sqrt{\text{hr}}$) and bias errors (1.0 deg/hr and 1 milliG) provides a good estimate for the extended Kalman filter process noise, while the initial covariance matrix values are based on typical error values for the initial position (either differential (1.0 m) or carrier-differential (0.2 m) GPS) [39].

4.2.3.3 Kalman Filter Feedback Configuration

The GIGET extended Kalman filter operates in a feedback configuration by using the estimates of sensor errors ($\delta\bar{\mathbf{a}}$ and $\delta\bar{\omega}$ of Equation 4.30 and Equation 4.31) to correct the raw inertial sensor measurements ($\Delta\theta$'s and Δv's) before they are integrated in the INS. Figure 4.6 illustrates the feedback configuration of the GPS/INS filter.

Figure 4.6. Closed Loop GPS/INS Kalman Filter Diagram

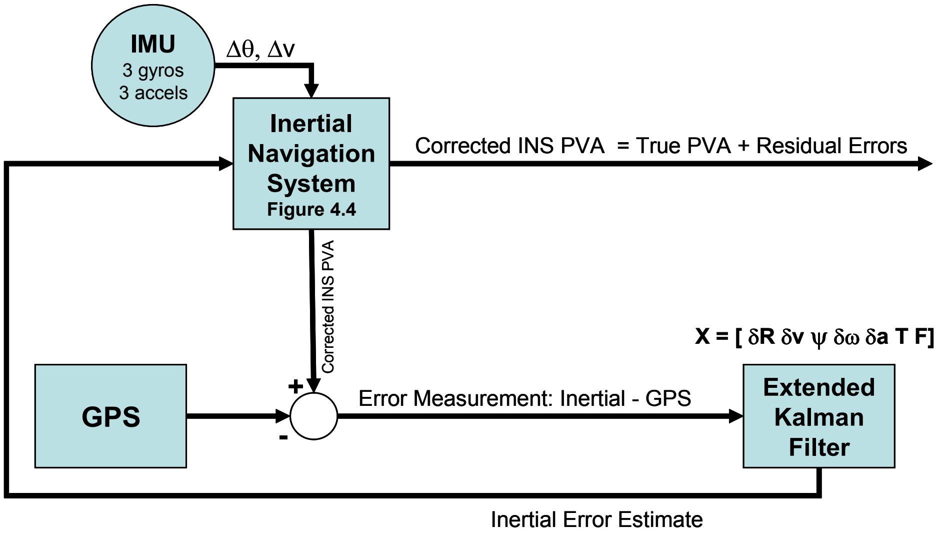

The GPS/INS extended Kalman filter presented here can be classified as either a loosely coupled or a tightly coupled filter, depending on the type of measurement updates it receives. The following sections will describe the two different types of filters and the formulation of the measurements corresponding to both. Both filter types use GPS measurements at 1 Hz to update the Kalman filter. References such as [39][48], and [47] describe and contrast these two system in further detail.

4.2.4 LOOSELY COUPLED

A loosely coupled GPS/INS system receives GPS measurement updates of position, velocity or attitude. In other words, it uses GPS *processed* measurements and not GPS *raw* measurements. A separate navigation filter within the GPS receiver formulates the processed measurements before they are output to the GPS/INS filter. The benefits of this type of system is that the GPS receiver can be treated as a “black box,” meaning that additional filter design to formulate a separate GPS solution is not necessary. The filter designer can benefit from the GPS measurements without a lot of modifications or knowledge of GPS. However, this lack of visibility into the GPS solution can also be considered a downside if there is a GPS outage (of less than four satellites) or fault. Once the GPS stops providing processed measurements, the inertial sensor calibration from the GPS/INS Kalman filter stops as well.

Another downside of a loosely coupled filter is that there *is* an additional filter involved. The processed GPS measurements are now a function of the dynamics and correlations of the GPS *internal* filter which are largely unknown to the GPS/INS filter designer. The loosely coupled system is essentially a cascade of filters and the estimated noise of the processed GPS measurements is not white noise, violating an initial assumption of the Kalman filter. The Kalman filter, therefore, is not optimal and requires additional tuning. Figure 4.7 shows the loosely coupled GPS/INS system concept.

Figure 4.7. Loosely Coupled GPS/INS System

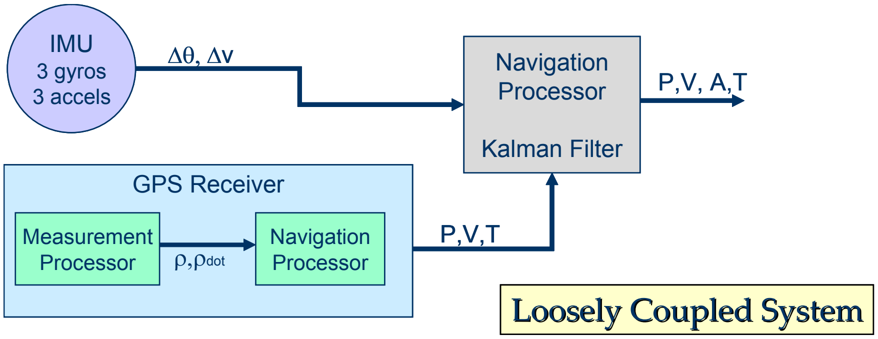

The GPS/INS filter incorporates the GPS measurements of position, velocity and attitude as follows.

Given the Kalman filter update equations as:

$$\boldsymbol{y}(k) = \boldsymbol{H}(k)\delta\boldsymbol{x}(k) + \boldsymbol{v}(k) \tag{4.48}$$

$$\delta\boldsymbol{x}^{+}(k+1) = \delta\boldsymbol{x}^{-}(k+1) + \boldsymbol{K}(k+1)[\boldsymbol{y}(k+1) - \boldsymbol{H}(k+1)\delta\boldsymbol{x}^{-}(k+1)] \tag{4.49}$$

The Kalman filter gain is computed by:

$$\boldsymbol{K}(k+1) = \mathbf{P}^{-}(k+1)\ \boldsymbol{H}^{T}(k+1)[\boldsymbol{H}(k+1)\mathbf{P}^{-}(k+1)\ \boldsymbol{H}^{T}(k+1) + \boldsymbol{R}(k+1)]^{-1} \tag{4.50}$$

with **R** as the matrix of measurement noise, and the covariance matrix update is:

$$\mathbf{P}^{+}(k+1) = [\boldsymbol{I} - \boldsymbol{K}(k+1)\boldsymbol{H}(k+1)]\mathbf{P}^{-}(k+1) \tag{4.51}$$

For GPS updates the measurements are:

$$\boldsymbol{y}(k) = \boldsymbol{y}_{\mathrm{INS}}(k) - \boldsymbol{y}_{\mathrm{GPS}}(k)\,. \tag{4.52}$$

For a GPS position measurement of latitude(ϕ), longitude(λ) and altitude (h), the update equations are:

$$\boldsymbol{y} = \begin{bmatrix} \phi_{\mathrm{INS}} \cdot (\mathrm{R_E} + \mathrm{h_{INS}}) \\ \lambda_{\mathrm{INS}} \cdot (\mathrm{R_E} + \mathrm{h_{INS}}) \\ \mathrm{h_{INS}} \end{bmatrix} - \left(\begin{bmatrix} \phi_{\mathrm{GPS}} \cdot (\mathrm{R_E} + \mathrm{h_{GPS}}) \\ \lambda_{\mathrm{GPS}} \cdot (\mathrm{R_E} + \mathrm{h_{GPS}}) \\ \mathrm{h_{GPS}} \end{bmatrix} - \mathbf{C}_{\mathrm{B}}^{\mathrm{NED}}\,\mathrm{l^B} \right) \tag{4.53}$$

and

$$\mathbf{H} = \begin{bmatrix} \cos\alpha & -\sin\alpha & 0 & 0 & 0 & 0 & 0 & 0 & 0 & 0 & 0 & 0 & 0 & 0 & 0 \\ \sin\alpha & \cos\alpha & 0 & 0 & 0 & 0 & 0 & 0 & 0 & 0 & 0 & 0 & 0 & 0 & 0 \\ 0 & 0 & 1 & 0 & 0 & 0 & 0 & 0 & 0 & 0 & 0 & 0 & 0 & 0 & 0 \end{bmatrix}, \tag{4.54}$$

where $\mathrm{l^B}$ is the lever arm, the vector from the GPS antenna location to the inertial measurement unit location, expressed in the body frame of the vehicle. The wander angle is α, $\mathrm{R_E}$ is the Earth's radius. $\mathbf{C}_{\mathrm{B}}^{\mathrm{NED}}$ is the transformation matrix from the vehicle body frame to the local level, NED reference frame.

For GPS velocity measurements expressed in the NED frame, the update equations are:

$$\boldsymbol{y} = \mathbf{v}_{\mathrm{INS}} - (\mathbf{B}\mathbf{v}_{\mathrm{GPS}}^{\mathrm{NED}} - \mathbf{C}_{\mathrm{B}}^{\mathrm{W}}(\omega^{\mathrm{B}} \times \mathrm{l}^{\mathrm{B}})), \tag{4.55}$$

$$\mathbf{B} = \begin{bmatrix} \cos\alpha & \sin\alpha & 0 \\ -\sin\alpha & \cos\alpha & 0 \\ 0 & 0 & 1 \end{bmatrix}, \tag{4.56}$$

where **B** is the transformation matrix from the NED frame to the wander frame. With the definitions of the velocity errors in the Psi-Angle formulation [39], the measurement matrix **H** becomes:

$$\mathbf{H} = \begin{bmatrix} \frac{(\mathrm{v_z} + \mathrm{v_y}\sin\alpha\tan\phi)}{(\mathrm{R_E} + \mathrm{h})} & \frac{(\mathrm{v_y}\cos\alpha\tan\phi)}{(\mathrm{R_E} + \mathrm{h})} & 0\ 1\ 0\ 0\ 0\ 0\ 0\ 0\ 0\ 0\ 0\ 0\ 0 \\ \frac{-(\mathrm{v_x}\sin\alpha\tan\phi)}{(\mathrm{R_E} + \mathrm{h})} & \frac{(\mathrm{v_z} - \mathrm{v_x}\cos\alpha\tan\phi)}{(\mathrm{R_E} + \mathrm{h})} & 0\ 0\ 1\ 0\ 0\ 0\ 0\ 0\ 0\ 0\ 0\ 0\ 0 \\ -\frac{\mathrm{v_x}}{(\mathrm{R_E} + \mathrm{h})} & -\frac{\mathrm{v_y}}{(\mathrm{R_E} + \mathrm{h})} & 0\ 0\ 0\ 1\ 0\ 0\ 0\ 0\ 0\ 0\ 0\ 0\ 0 \end{bmatrix}. \tag{4.57}$$

For measurements of GPS attitude, the update equations, assuming small errors in attitude Euler angles (roll (Φ), pitch(Θ), and yaw(Ψ)), are:

$$\boldsymbol{y} = \begin{bmatrix} \Phi_{\mathrm{INS}} - \Phi_{\mathrm{GPS}} \\ \Theta_{\mathrm{INS}} - \Theta_{\mathrm{GPS}} \\ \Psi_{\mathrm{INS}} - \Psi_{\mathrm{GPS}} \end{bmatrix} - [\text{GPS to INS attitude offset}], \tag{4.58}$$

where [GPS to INS attitude offset] is set of Euler delta-angles describing the offset from the GPS attitude system's antenna reference body frame to the INS body frame. With the conversion from attitude errors to Psi-Angle errors, the measurement matrix is

$$\mathbf{H} = \begin{bmatrix} 0 & \frac{1}{(\mathrm{R_E} + \mathrm{h})} & 0\ 0\ 0\ 0\ 1\ 0\ 0\ 0\ 0\ 0\ 0\ 0\ 0 \\ \frac{-1}{(\mathrm{R_E} + \mathrm{h})} & 0 & 0\ 0\ 0\ 0\ 0\ 1\ 0\ 0\ 0\ 0\ 0\ 0\ 0 \\ 0 & 0 & 0\ 0\ 0\ 0\ 0\ 0\ 1\ 0\ 0\ 0\ 0\ 0\ 0 \end{bmatrix}. \tag{4.59}$$

Measurement noise for the GIGET system is estimated at 0.5 m for the GPS positions, 0.05 m/s for velocity and 0.2 degrees for attitude. The values are derived from an accumulation of test data results discussed in following sections.

Because the loosely coupled system relies on a complete GPS solution to come from the GPS receiver, the Kalman filter receives *no* measurements unless the GPS receiver completes a full navigation solution. This means that if the GPS receiver does not have a confident view of at least four satellites, no GPS measurements will be processed, and therefore no updates to the GPS/INS performed. With a tightly coupled system, raw measurements are processed, so that even if fewer than four satellites are visible, the GPS/INS filter can still gather much information from the remaining satellite's raw measurement updates. The next section describes how these measurements are incorporated into the GPS/INS filter.

4.2.5 TIGHTLY COUPLED

A tightly coupled GPS/INS system receives *raw* GPS measurement of pseudo-range and Doppler or delta-range. The problems of cascading filters is avoided because the tightly coupled filter does not use a separate filter within the GPS receiver. The tightly coupled GPS/INS filter also benefits from GPS measurement updates, even if there are less than four satellites available for a complete GPS navigation solution.

One of the downsides of a tightly coupled filter is the complexity that raw measurements add to the GPS/INS filter. For instance, at least two more states must be added to the Kalman filter to estimate GPS clock bias and clock rate. Also, the Kalman filter performs a measurement update at every epoch, for every satellite in view, and not just for three measurements of position, velocity and attitude of a loosely coupled system. This additional processing of measurements adds a considerable computational load.

The filter complexity means additional work for the GPS/INS filter designer, and requires the designer to have a good understanding of the workings of GPS and how the GPS navigation solution is performed. The tightly coupled filter requires line-of-sight information to the satellites as well as potential information on GPS signal strength or elevation angle to improve the measurement noise estimates while incorporating the GPS updates.

Results presented in Chapter 5 demonstrate that the tightly coupled filter, in side-by-side comparisons with a loosely coupled system, responds more slowly to error growth in the inertial sensors. This is due to the fact that the tightly coupled Kalman filter does not receive as direct a measurement of sensor errors as a loosely coupled system does (a GPS measurement of velocity is a more direct measurement of INS velocity and delta-velocity errors than is a GPS delta-range measurement). The additional, tight coupling of the measurements means that, while the GPS/INS filter may be more robust in the long-term, for short-term disturbances in inertial errors, it responds more slowly.

Figure 4.8 shows a tightly coupled system concept.

Figure 4.8. Tightly Coupled GPS/INS System

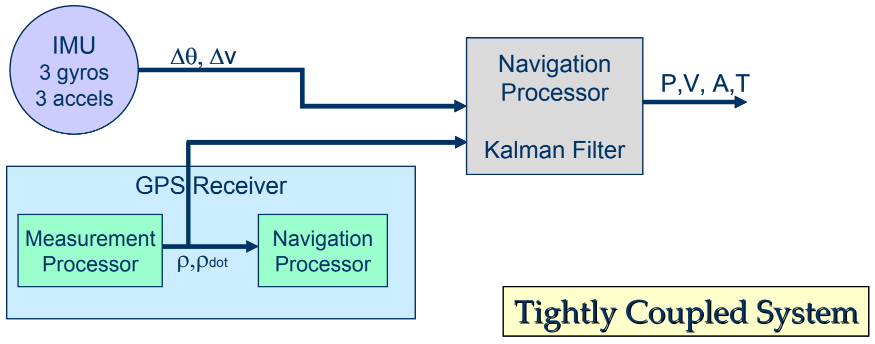

The Kalman filter update equations are listed below and are derived in further detail in [39].

To process pseudo-range measurement updates, first an estimate of the range to the satellite from the INS, $\bar{\rho}$, is generated with the INS position estimate and the line-of-sight vectors to the satellites.

$$\bar{\rho} = \left\| \mathbf{R}^{ECEF}_{SV} - \mathbf{R}^{ECEF}_{INS} - l^{ECEF} \right\| = \sqrt{\Delta x^2 + \Delta y^2 + \Delta z^2}, \tag{4.60}$$

$$l^{ECEF} = \mathbf{D}^{E}_{W} \mathbf{C}^{W}_{B} l^{B} , \tag{4.61}$$

$$\mathbf{e}^{ECEF} = \begin{bmatrix} \Delta x / \bar{\rho} \\ \Delta y / \bar{\rho} \\ \Delta z / \bar{\rho} \end{bmatrix} = \mathbf{D}^{E}_{W} \mathbf{e}^{W} , \tag{4.62}$$

where, $\mathbf{R}_{SV}$ is the satellite position, and **e** is the satellite line-of-sight unit vector. The Kalman filter measurement is now defined in terms of the pseudo-range estimate and the GPS measured pseudo-range.

$$\boldsymbol{y} = \bar{\rho} - \rho_{GPS} . \tag{4.63}$$

The measurement matrix, **H**, is

$$\mathbf{H} = \begin{bmatrix} -e^{L}_{x} & -e^{L}_{y} & -e^{L}_{z} & 0 & 0 & 0 & 0 & 0 & 0 & 0 & 0 & 0 & 0 & 0 & 0 & 1 & 0 \end{bmatrix} \tag{4.64}$$

where the 16th state is the GPS clock bias estimate and the 17th state is the GPS clock rate estimate.

The delta-range measurements are formulated by first differencing the pseudo-range estimated at the last epoch from the current:

$$\Delta\bar{\rho}(k+1) = \bar{\rho}(k+1) - \bar{\rho}(k)\,. \tag{4.65}$$

The delta-range measurement update is then defined by:

$$\boldsymbol{y} = (\Delta\bar{\rho} - \Delta\rho_{\mathrm{GPS}})/\Delta\mathrm{t}\,, \tag{4.66}$$

with Δt the time from the last epoch to the current. The measurement matrix follows as

$$\mathbf{H} = \begin{bmatrix} 0 & 0 & 0 & -\mathrm{e}_{\mathrm{x}}^{\mathrm{L}} & -\mathrm{e}_{\mathrm{y}}^{\mathrm{L}} & -\mathrm{e}_{\mathrm{z}}^{\mathrm{L}} & 0 & 0 & 0 & 0 & 0 & 0 & 0 & 0 & 0 & 0 & 1 \end{bmatrix}\cdot \tag{4.67}$$

The measurement noise values on the pseudo-range measurements and delta-range measurements are typically 0.5 m and 0.03 m/s respectively.

4.2.6 Testing and Evaluation

The algorithms and integration methods presented in the previous sections were tested with data collected in the GIGET avionics box mounted on a roof-top test-bed and in an automobile for ground testing. The results were compared to simulations to develop a complete set of simulation and testing tools to use in the trade studies presented in Chapter 5. The following sections describe the testing and simulation development.

4.2.6.1 Roof-Top Testing

As with most navigation test platforms, a key challenge involves the comparison of measurements from a sensor package versus a known truth source. A roof-top test-bed acts as a truth source and provides an accurate test of GIGET navigation system performance. The platform consists of an antenna array mounted rigidly to a remote-controlled camera mount on top of the Durand building on Stanford's campus. The camera mount can be rotated slowly on two axes. The commanded camera mount’s platform angle gives a rough estimate and comparison of the antenna array's attitude.

The roof-top system is ideal for algorithm testing and verification. The following plot show results from a static attitude test on the roof-top platform.

Figure 4.9. Typical GIGET Roof-Top Testing Results

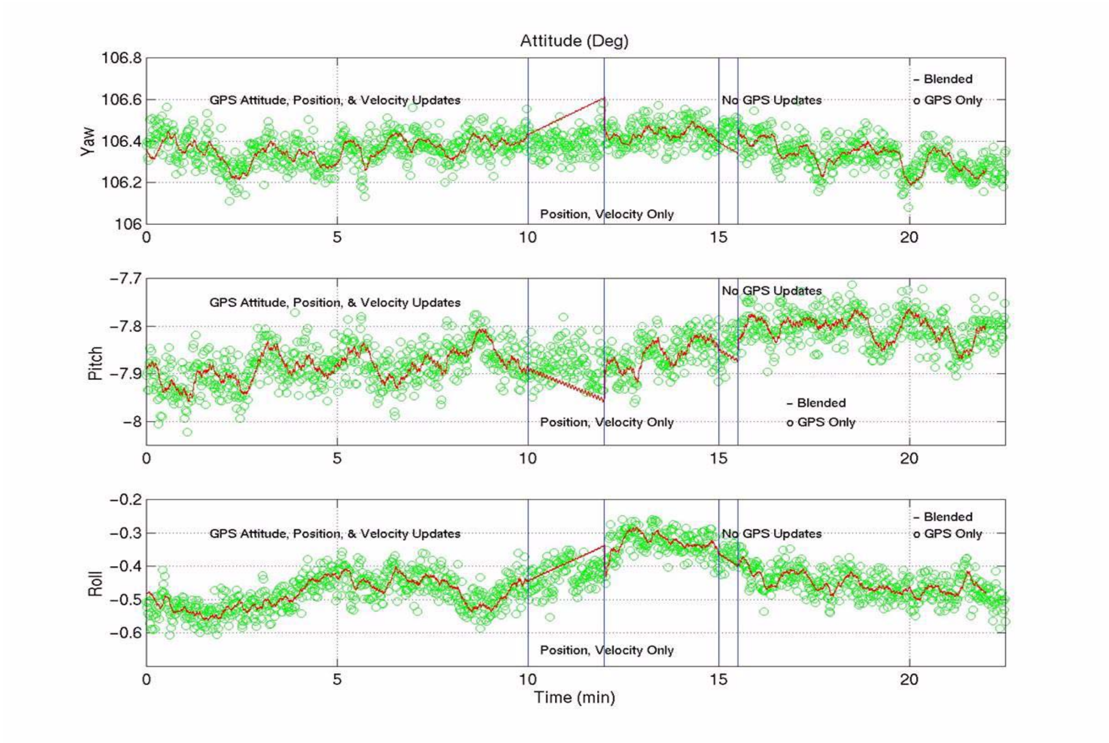

The green circles in Figure 4.9 represent the GPS updates at 1 Hz; the red line represents the GPS/INS filter outputs. In the time periods indicated by the vertical bars, the filter experiences a simulated GPS outage of attitude, velocity or position, meaning that the GPS/INS filter does not receive a GPS Kalman filter update. The resulting drifts in the red lines indicate the blended filter's performance.

Several tests on the roof-top test-bed, such as the one represented in Figure 4.9, help to tune the GPS/INS filters and to verify and compare with GIGET simulations. Although the vibration-free, roof-top test-bed is very useful for attitude testing, there is no translational motion to get an rigorous sense of GIGET filter velocity and position performance.

Therefore, ground testing in a car provides additional testing and verification of GIGET performance.

4.2.6.2 Ground Vehicle Testing

An antenna array with an attached brace for the GIGET avionics box provides an excellent portable platform for ground testing. The entire array structure, of approximately seven feet by six feet, fits on top of a vehicle either rigidly or semi-rigidly. If semi-rigidly mounted on a car, the array can be rolled during the ground testing to more accurately simulate the dynamics of an aircraft. The truth system for the ground testing is post-processed carrier differential results of the gathered GPS measurements from the ground vehicle and from a known reference station.

The antenna array is pre-calibrated and can be quickly and easily moved, in whole, from one vehicle to another, but most of the GIGET testing is performed on the small car seen in Figure 4.10. This portable array structure gives GIGET a very fast set-up time even when moved to a completely new vehicle. And because the array is pre-calibrated and aligned, data collection can begin almost immediately after set-up. For instance, the set-up time to move GIGET from the car to the farm tractor discussed in Chapter 7 was only around one hour.

Figure 4.10. GIGET Ground Testing Set-Up

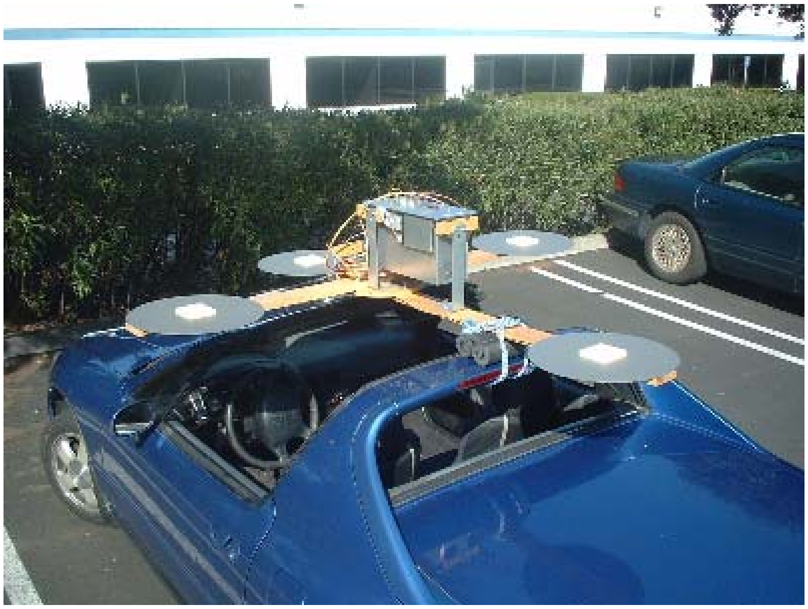

Figure 4.11 shows a typical GIGET ground test. The test starts in a parking lot in Sunnyvale, CA and proceeds down Hwy 237 to Hwy 85 with several passes through the cloverleaf at Hwy 85 and El Camino Real before heading back via Hwy 237 to Sunnyvale.

Figure 4.11. Typical GIGET Ground Test Trajectory

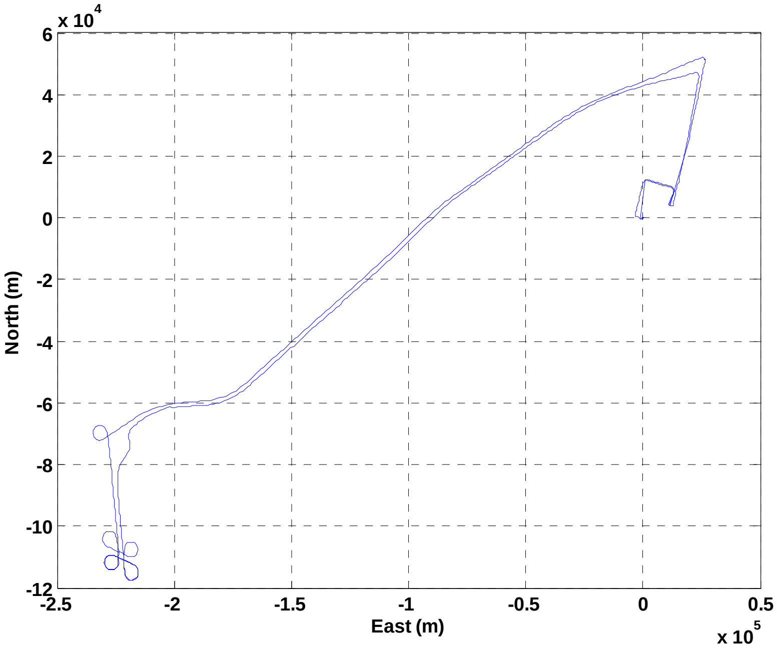

4.2.6.3 Simulation and Analysis

The ground and flight testing resulted in a tremendous amount of data using the GIGET tactical grade inertial measurement unit. However, the goal of GIGET is not just to analyze the tactical grade performance in a particular car or aircraft, but to expand, as a generalized tool for analysis, to many levels of integration and sensor quality. The challenge is to take these tactical IMU data and formulate the simulation tools to map a much wider GPS/INS integration space.

GIGET uses the navigation and attitude client/servers as a model for post-processing actual test data, modified test data, or simulated data. A suite of GIGET analysis tools take simulated tactical grade data, generated through simulated trajectories, and tunes them to match the real-time results. GIGET tools generate automotive grade inertial data by either adding simulated errors to actual test data, or by using automotive grade error characteristics with simulated trajectories.

Generating navigation grade data proves to be more difficult. While it is possible to add noise to tactical grade data to degrade its quality to automotive grade, it is not possible to remove error sources from test data to generate higher quality, navigation grade data. Therefore, GIGET interpolates the post-processed, carrier phase differential GPS solution from test data, converts it to rates and accelerations, and adds navigation grade error sources. This interpolation is a cumbersome process but gives a good comparison check on test data results. The simulated error sources for each inertial grade are developed from the literature [43][49] and summarized in Table 4.1.

Table 4.1. Sensor Quality in GIGET Simulation

Sensor Quality	Gyro Bias	Gyro Noise	Accel Bias	Accel Noise
Navigation Grade	0.01 deg/hr	0.005 deg/ $\sqrt{\text{hr}}$	50 microG	0.001 m/s^2
Tactical Grade	1 deg/hr	0.125 deg/ $\sqrt{\text{hr}}$	0.5 milliG	0.01 m/s^2
Automotive Grade	100 deg/hr	0.3 deg/ $\sqrt{\text{hr}}$	30 milliG	0.05 m/s^2

The combination of test data and trajectory simulation provides a complete set of tools to analyze GPS/INS integrated navigation systems. Chapter 5 summarizes several trades using these GIGET tools. The GIGET results map out a wider view of GPS/INS combinations than what has been previously studied.

4.3 Inertial Aiding of GPS Receiver

The previous sections of this chapter generally describe the use of GPS to aid and calibrate an inertial navigation system, i.e. GPS aiding of INS. Another approach to GPS/INS integration is INS aiding of GPS. This section will define the different types of inertial aiding to GPS receivers, explain the motivation for such aiding, describe some results, and discuss the difficulties in the implementation.

4.3.1 Methods

An INS can aid a GPS receiver on a variety of different levels. INS outputs of position, velocity and attitude, used as external inputs to a GPS receiver can: aid in pre-positioning calculations for faster signal acquisition and tracking; provide interference rejection during signal tracking; and aid in cycle-slip detection. These aiding methods vary in complexity and implementation. They also vary greatly in the terminology used to describe them in the literature [19][18][47]. The next section describes the terminology used in this document to clarify the definitions of the aiding levels.

4.3.1.1 Terminology

Terms such as "tightly coupled", "ultra-tightly coupled", "inertial aiding", "deep integration", have all been used in the past to describe the aiding of a GPS receiver by an inertial system. However, the definitions of these terms have migrated over the years to refer to different types of aiding.

Historically, the aiding of the GPS receivers with inertial systems was always anticipated [1], and the first use of the term "tightly coupled" referred to tracking loop aiding of the GPS receivers [11][14][32]. The tight coupling also referred to the use of a large internal GPS tracking and navigation filter to blend the external inertial aiding measurements with the raw GPS observables [17][18]. This type of tracking filter is best described by Spilker as a vector-delay-locked-loop (VDLL) [32]. But now the term "tightly coupled" has migrated [50][47][48] to refer to a GPS/INS blending that uses raw GPS observables, but not necessarily as aiding inside the GPS receiver. This is the "tightly coupled" definition used in the previous sections in this chapter.

The term "ultra-tightly coupled" has entered the vernacular to replace the original use for the term "tightly coupled" [51]. However, even this term is interchanged with other aiding descriptors such as "deep integration." I choose to use the term "ultra-tightly coupled" to indicate a GPS receiver using a "vector-locked-loop" such as the VDLL that is aided by inertial measurements. "Deep integration" then refers to any aiding of the GPS tracking loops with inertial measurements, including the vector-locked-loop concept, but also including aiding of more traditional tracking loop designs. The remaining term, “inertial aiding,” is used more broadly to refer to *any* aiding of the GPS receiver, not limited to tracking loop aiding, but also including acquisition and integer search aiding (by reducing initial search volume).

4.3.1.2 Tracking Loop Example

GPS receivers traditionally track the GPS signal carrier with Costas-type phase-locked-loops (PLL) or frequency-locked-loops (FLL); delay-locked-loops (DLL) track the GPS code. The design of these tracking loops generally require the trade-off between good performance under high user dynamics (requiring higher tracking loop bandwidth), and good performance under interference and noise (requiring lower tracking loop bandwidth). However, if the tracking loops are aided with an external estimate of the user’s dynamics, the tracking loop bandwidth can be significantly reduced for interference rejection while still maintaining the good performance under high user dynamics.

Figure 4.12 illustrates this external aiding with typical GPS tracking loops. The bottom loop represents the carrier tracking loop. The carrier signal measurement enters the tracking loop through the phase discriminator to generate a phase error estimate. This phase error drives the carrier loop filter which outputs an estimate of the signal Doppler to drive the carrier NCO (numerically controller oscillator). The NCO duplicates the phase of the incoming signal, and this phase estimate is fed back to the phase discriminator. The tracking loop is usually said to be “locked” if the phase error is less than five degrees.

In a coherent tracking receiver, the Doppler estimate of the carrier loop is also fed into the code loop to aid in the tracking of the code as an additional range-rate estimate. Similarly, an external estimate of Doppler can be fed into the carrier loop to aid in its estimation of signal's phase-rate. The blue box labeled "External Aiding" is the external Doppler aiding. The user's velocity (converted to units of cycles/second) can be projected onto the line-of-sight to a satellite being tracked to become the estimate of the phase-rate or Doppler of that satellite's signal. If this aiding signal is added to the Doppler estimate coming from the carrier loop filter, it drives the NCO to the user's dynamics, leaving only the residual satellite, oscillator and signal dynamics to be tracked by the carrier loop filter. With the elimination of the user's dynamics as a design constraint, the loop filter's bandwidth can be reduced by almost a factor of ten.

As seen in Figure 4.12, by aiding the carrier loop with a Doppler estimate, the code loop automatically receives the external aiding through the coherent carrier-code aiding signal. Even if the carrier loop looses lock, the external Doppler estimate continues to feed into the delay-locked-loop to aid code tracking, and the aided DLL can continue to operate at very low signal levels. However, the requirements on the aiding signal are much more strict for the carrier loop (on the order of a few centimeters) than for the code loop (on the order of a few meters) [19]. Therefore, the following discussion focuses on the aiding requirements and challenges for the phase-locked-loop.

Figure 4.12. GPS Tracking Loops with External Aiding

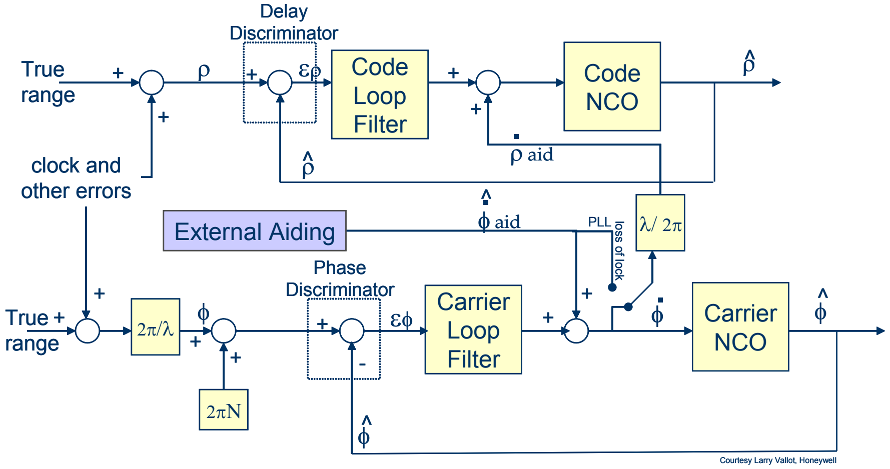

4.3.1.3 Benefits

With the external estimate of the user's velocity steering the carrier loop NCO, the residual dynamics that the carrier loop filter needs to track is significantly reduced. Therefore, the PLL can operate with a much reduced bandwidth, and receiver designers avoid the usual trade-off between dynamic performance and receiver bandwidth. The reduction of bandwidth leads to increased resistance to interference and jamming. The bandwidth reduction, however, is limited by constraints such as oscillator jitter and aiding signal quality. The next section discusses these error sources, but the following summarizes the benefits of reducing the tracking loop bandwidth.

Equation 4.68 relates the carrier phase tracking loop jitter (σ_{PLL} in radians), receiver tracking loop bandwidth (B_n in Hz) and signal carrier to noise ratio (C/N_0 in dB-Hz where $c/n_0 = 10^{C/N_0/10}$) for a Costas-type PLL. T is the prediction integration time, which for this research is limited to 20 milli-seconds due to the data bit boundaries of the GPS satellite data message modulated onto the current GPS signals [15].

$$\sigma_{PLL} = \sqrt{\frac{B_n}{c/n_0}\left(1+\frac{1}{2T(c/n_0)}\right)} \tag{4.68}$$

Using this relation, Figure 4.13 illustrates that, for a one sigma requirement in phase error of five degrees, a tracking loop with a bandwidth of 10 Hz requires a C/N_0 of 32 dB-Hz or greater.

Figure 4.13. Phase Error v. Signal Level for Various Bandwidths

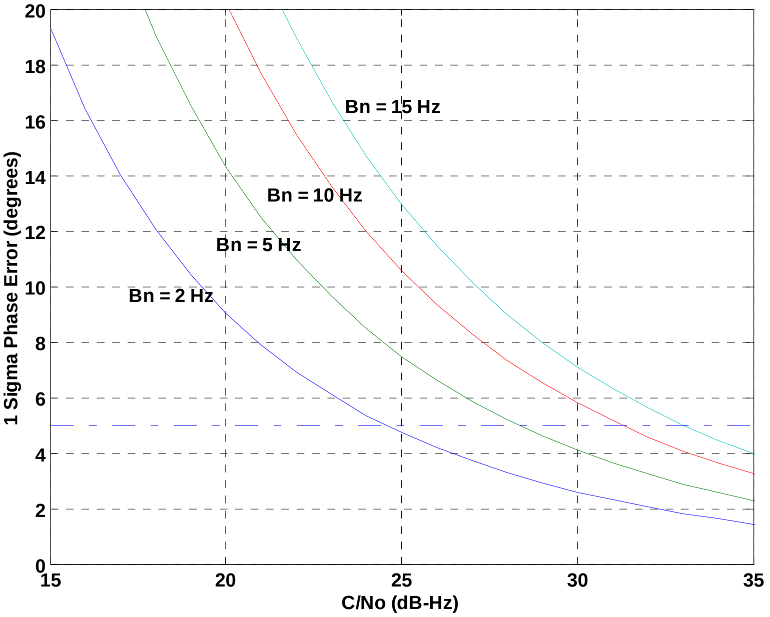

Figure 4.13 also illustrates that a receiver with a reduced bandwidth of 2 Hz can tolerate a reduced signal level of 24 dB-Hz for the same phase error. With this reduction in acceptable signal level, the receiver can maintain lock and avoid cycle-slips in the presence of increased interference.

These results are theoretical results for phase error only. However, there are many other error sources affecting the tracking loop performance, including aiding signal errors and oscillator jitter, that present challenges for the design of any externally aided receiver. The following section highlights a few of these challenges.

4.3.1.4 Challenges

The benefits discussed in the previous section assumed a perfect external aiding source for the GPS receiver. However, inertial aiding information can induce its own errors into the receiver's tracking loops. Errors arise from aiding data accuracy, latency, time-tag jitter, lever-arm calculations, or oscillator jitter and g-sensitivity. These error sources increase with higher speed and dynamics of the user, but all must remain within the tolerable error limits of the tracking loops.

Aiding Data Accuracy - Although a PLL must track to less than one quarter of a wavelength (less than 5 cm for L1), the inertial aiding does not necessarily have to be accurate to 5 cm. A restriction on *positioning* accuracy to 5 cm would limit the inertial systems capable of aiding GPS receivers to only extremely expensive, navigation grade systems, or better. Unfortunately, this positioning accuracy requirement has been considered the limiting constraint for inertial aiding for several years [11][14]. However, the aiding signal is in the form of velocity; therefore, limits on the velocity errors determine acceptable aiding accuracy. In addition, most modern PLL designs are third-order systems, meaning that they can track ramps in frequency (velocity) with zero steady-state error; hence, as long as the velocity errors induced by the inertial aiding signals are within the bandwidth of the tracking loops, the receivers can maintain lock on the signal.

These constraints intersect as the receiver bandwidth is decreased and the user dynamics are increased. As the bandwidth is reduced, the tracking loop becomes more dependent on the aiding signal to steer the NCO, and therefore is more sensitive to errors in the aiding signal. At the same time, as the user dynamics increase, the INS is more dependent on the GPS for its error calibration, and the inertial aiding signal quality begins to degrade. The feedback due to the deep integration begins to become unstable. At some limit, the INS can no longer depend on the GPS for calibration; inertial errors begin to drift; inertial aiding quality to the GPS receiver begins to degrade, eventually leading to the loss of lock in GPS tracking. This is therefore the "worst-case" scenario for inertial aiding. The INS receives no GPS updates and errors begin to degrade as shown in the trade studies in Chapter 5. How long can the tracking loops maintain lock on the GPS signal if they depend on an aiding signal from the INS that includes a error source that acts just like a frequency ramp? The answer depends on the tracking loop filter design and the amount of drift in the aiding data. The following section on GIGET implementation discusses this in more detail.

Aiding Data Latency and Time-tag Error - Another challenge for inertial aiding is the very strict timing requirements. Latency in the aiding data can induce large errors into the tracking loops; but again, this all depends on the dynamics of the user and on the tracking loop filter design. If the user is static or if velocity is constant, latency in the aiding signal does not contribute to tracking loop error at all. However, as a user accelerates, the aiding data errors will grow. These latency errors are due to the transport delay from the INS time of computation to the GPS tracking loop time of application. An estimate of user acceleration in the aiding data can limit errors if the acceleration is used to extrapolate to the time of application.

The update rate of the aiding data also directly affects the timeliness of the signal. If the transport delay is assumed to be the length of one aiding update interval, then the average data latency would be one half the update interval. This could give an overall latency 1.5 times the update interval.

Time-tag errors also contribute to the aiding data errors, but this too is a function of user dynamics. If the time-tag is incorrect by 50 micro-seconds at a time of user acceleration of 100 m/s^2, the overall error in velocity would be 0.005 m/s (50 μsec * 100 m/s^2). An error of this size should not induce large phase errors in the tracking loops; but with larger time-tag errors, larger accelerations, or more sensitive tracking loop filters, these errors become more significant [19].

Aiding Data Continuity - As the tracking loop bandwidth decreases and the dependence on the aiding data to steer the NCO increases, the tracking loop becomes more sensitive to any discontinuities or jumps in the aiding data. The aiding signal must be very smooth and continuous to avoid adding any jerk or accelerations that the tracking loop filter must track through.

Lever-arm Errors - Errors in the calculation of the lever-arm from the INS position to the GPS antenna contribute to errors in the aiding data. The contribution to the velocity error estimate can be seen in Equation 4.55 as being on the order of $\omega \mathbf{x} \delta \mathrm{l}$, with $\delta \mathrm{l}$, the lever arm error, and ω, the angular rate of the user. While the aiding error is clearly a function of the estimate of the lever-arm, the overall size of the aiding error is again a function of the user’s dynamics. The larger the angular motion of the user, the larger the error due to lever-arm calculations. Because smaller lever-arms are usually more accurately measured, they contribute less to lever-arm errors.

Oscillator Errors - Errors and jitter due to the receiver's oscillator present a fundamental limit to the reduction of tracking loop bandwidth. Depending on the quality and type of oscillator used, the frequency errors can range from 0.1 Hz to 3 Hz [22]. These errors are also affected by user dynamics; acceleration and vibration of the GPS receiver's oscillator directly increase its error characteristics [52].

Systems that have used inertial aiding in the past have been for military purposes and therefore require extremely high jamming resistance as well as extremely high dynamic performance (certain cases require a maximum velocity of 12,000 m/s with 100 G acceleration and 13 G/second jerk [20]). Navigation grade inertial systems are used in these extreme conditions to reduce the errors in the aiding signal as much as possible. Will tactical (or lower) grade systems be sufficient for lower dynamic environments? Can GIGET be used to determine the commercial applicability for inertial aiding? The next section on GIGET implementation addresses these questions.

4.3.2 GIGET Implementation

GIGET is uniquely designed to implement inertial aiding to the GPS receiver at several different levels. The PCI high-speed bus interface with the single board computer (see Chapter 2), eliminates many of the aiding data error sources due to latency between INS calculations an transport into the GPS receiver. The high resolution timer (HRT) server (see Chapter 3) eliminates much of the time-tag errors in the aiding signal. The tactical grade inertial measurement unit provides an aiding signal with sufficient accuracy for the moderate dynamics of a commercial user. The navigation client/server places inertial aiding packets of position, velocity, attitude, time-tag, and acceleration information into a dual-ported RAM in the GPS receiver at a 50 Hz rate. While these data can be most easily utilized for acquisition aiding, pre-positioning, and even FLL pull-in range reductions, the goal of PLL aiding remains un-obtained in GIGET. The additional load of a 50 Hz signal to be input into the existing tracking loop receiver firmware, in real-time, proved too difficult without a complete redesign of the underlying embedded GIGET firmware. Ideally, receiver designers will build new systems from scratch with the concept of external aiding as a requirement. Embedded firmware with a legacy of add-ons and modifications will not be able to handle the additional computational load or the real-time throughput requirements of an externally aided receiver (at least at the PLL level). Figure 4.14 presents the proposed state transitions for the GIGET aided receiver.

The external aiding data are received and passed through a series of acceptance tests for quality and consistency. The receiver generates the Doppler estimate from the aiding data by projecting the user's velocity along the line-of-sight vectors to the satellites. If the aiding data are acceptable, it then transitions to aid in the search mode of the receiver. Once a signal is acquired, the receiver state transitions to a series of frequency-locked-loops to pull in the signal further. The Doppler estimate in the FLL helps to reduce the initial frequency range estimate on the signal. Once the FLLs have locked on the signal, and the edge transition of the GPS data bit is known, the receiver transitions to a PLL. Traditionally, the receiver will remain in this state unless the signal is lost due to low signal level or multiple cycle-slips. However, with the addition of the aiding signal, a further state may be achieved. If the tracking loop aiding is available and of good quality, the receiver can transition into an *aided* PLL state. The bandwidth of this PLL is reduced for interference rejection. In addition, the C/N$_0$ at which this aided PLL considers a signal lost is much lower (potentially, at least 10 dB-Hz lower). If the signal quality continues to degrade, eventually the aided PLL will lose the signal and will have to transition back to one of the search states.

The aiding data begin to degrade after long periods in the aided PLL state with a lack of strong GPS signal strength. The INS can no longer depend on the GPS for error calibration; with a GPS outage, the aided PLL relies too much on the aiding signal. The resulting output from the GPS receiver is almost purely inertially steered, and can therefore not be used to calibrate the inertial sensors. The feedback would drive the errors in the inertial system unstable. This is the "worst-case" inertial aiding scenario, where the inertial sensors errors drift as in a total GPS outage.

Figure 4.14. GIGET Receiver Aiding State Transitions

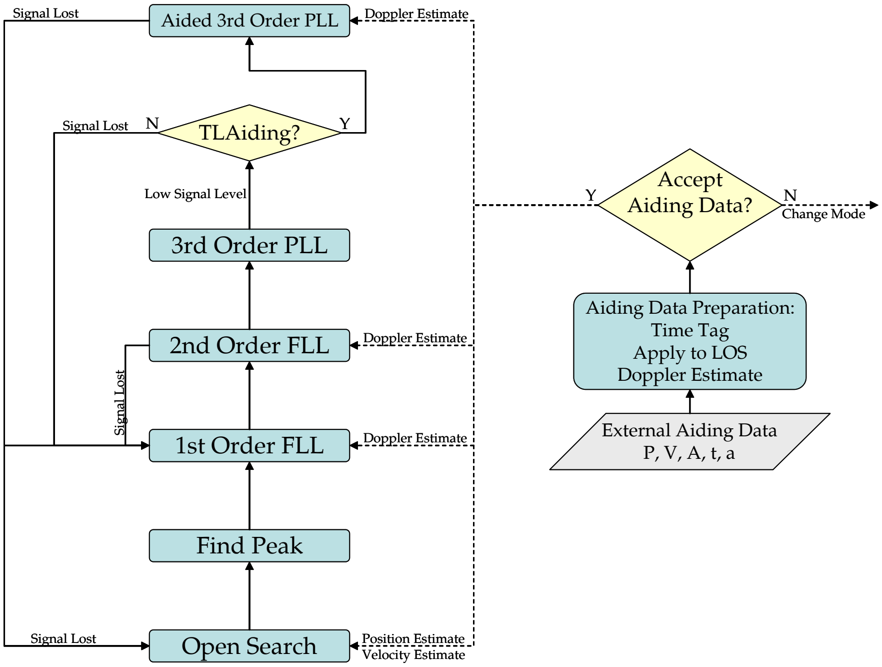

Although GIGET receivers proved too difficult to modify for PLL aiding, other GIGET tool sets did aid in the analysis of the "worst-case" aiding scenario. GIGET trajectory simulations, as described in the trade studies of Chapter 5, provided inputs to a Trimble Navigation tracking loop simulation [53]. The tracking loop simulation was modified to incorporate the aided PLL as described previously. The details of the tracking loop design is Trimble proprietary information; however, it is a third-order tracking loop with a second-order, Jaffe-Rectin [54] filter design of the form:

$$F(z) = \frac{4X}{TK_dK_{NCO}}\left[\frac{C_0z^0 + C_1z^{-1} + C_2z^{-2}}{z^0 - 2z^{-1} + z^{-2}}\right] \tag{4.69}$$

Where,

B = loop bandwidth,

T = sampling period,

W = 6B/5

X = tan(WT/2)

$C0 = 0.5X^2 + X + 1$

$C1 = X^2 - 2$

$C2 = 0.5X^2 - X + 1$

Derived from the results presented in Chapter 5, the worst-case (no continued GPS calibration of INS) error growth in the inertial aiding signal roughly translates to a velocity ramp of 0.1667 m/s/s for the automotive grade system, 0.03 m/s/s for the tactical grade system, and 0.001 m/s/s for the navigation grade system. The tracking loop is able to maintain lock with the navigation grade inertial aiding signal with a bandwidth as low as 2

Hz. With the tactical grade inertial aiding signal, the tracking loop only maintains lock for a few seconds with a reduced bandwidth of 5 Hz. The automotive grade system seems to only make the tracking loop unstable.

4.3.3 AIDING CONCLUSIONS

The GIGET results are helpful in determining future, minimum design requirements for inertially aided systems of both the GPS receiver and the inertial sensor quality. Given that these results are worst-case scenario, they clearly indicate that under better aiding conditions, where the INS is still using GPS to calibrate errors, a tactical quality inertial sensor should be sufficient for PLL aiding.

Operationally, PLL aiding is difficult to manage. Even with the GIGET hardware improvements to incorporate this level of aiding, its legacy embedded firmware does not handle the additional computation load or the real-time throughput well. For efficient tracking loop aiding, receiver firmware must be designed with external aiding inputs in mind from its conception.

Chapter 5:
Trade Study Results

The previous chapters have described the development of GIGET; this chapter shows the application of GIGET for a trade study. Figure 5.1 shows some of the previously uncharted territory (blue circle) of the GPS/INS space that trades accuracy and expense versus complexity of design. The following results demonstrate how GIGET explores this space with a wide combination of GPS/INS integration methods.

Figure 5.1. GPS/INS Trade Space

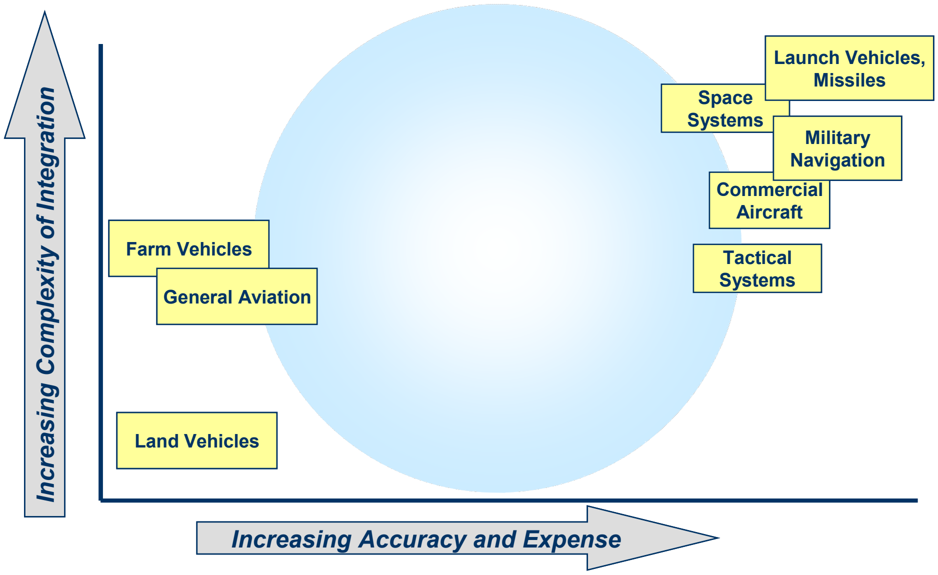

The yellow boxes in Figure 5.1 illustrate existing point designs such as: military and space systems using tightly coupled algorithms in sensor packages costing over $100,000; and land vehicles using loosely coupled methods with very inexpensive (<$100) sensor systems. The space represented by the blue circle includes GPS/INS combinations of tightly coupled systems with moderately priced sensors, or loosely coupled systems with tactical grade sensors. The cases presented in this chapter demonstrate these combinations and others that range from the expensive and complex, to the simple and inexpensive. Each study trades the performance for a GPS/INS blending method against sensor quality through a range of GPS data outages. The blending methods include tightly coupled cases, loosely coupled cases with GPS attitude, and loosely coupled cases without GPS attitude. The inertial sensor quality ranges from navigation grade to tactical grade and automotive grade.

5.1 Test Scenario

The ground and flight testing results using the GIGET hardware were used to formulate and tune a *generalized* set of analysis and simulation tools, not only for tactical grade system analysis, but also for navigation and automotive grade system analysis (see Chapter 4, Section 4.2.6). The following trade study uses these tools to make generalized conclusions using a test trajectory with moderate to high dynamics.

Each result represents over 60 simulated GPS outages over a ten-minute, simulated flight profile that contains three 90 degree turns. The GPS outages occur for 10 seconds, 30 seconds and 60 seconds. Figure 5.2 shows an example GPS outage for a velocity profile in the east direction. The blue circles represent GPS velocity updates at 1 Hz; the green line shows the resulting GPS/INS filter velocity output; and the red line is the true velocity. At around 100 seconds, the GPS/INS filter stops incorporating the GPS updates and the solution output begins to drift. In this example, the resulting errors in east velocity can be measured at 10 seconds, 30 seconds, or 60 seconds.

The following table repeats Table 4.1 for convenience and describes the general performance characteristics of the inertial sensors used in the trade study.

Table 5.1. Sensor Quality in GIGET Trade Study

Sensor Quality	Gyro Bias	Gyro Noise	Accel Bias	Accel Noise
Navigation Grade	0.01 deg/hr	0.005 deg/$\sqrt{hr}$	50 microG	0.001 m/s^2
Tactical Grade	1 deg/hr	0.125 deg/$\sqrt{hr}$	0.5 milliG	0.01 m/s^2
Automotive Grade	100 deg/hr	0.3 deg/$\sqrt{hr}$	30 milliG	0.05 m/s^2

Figure 5.2. GPS Outage Example

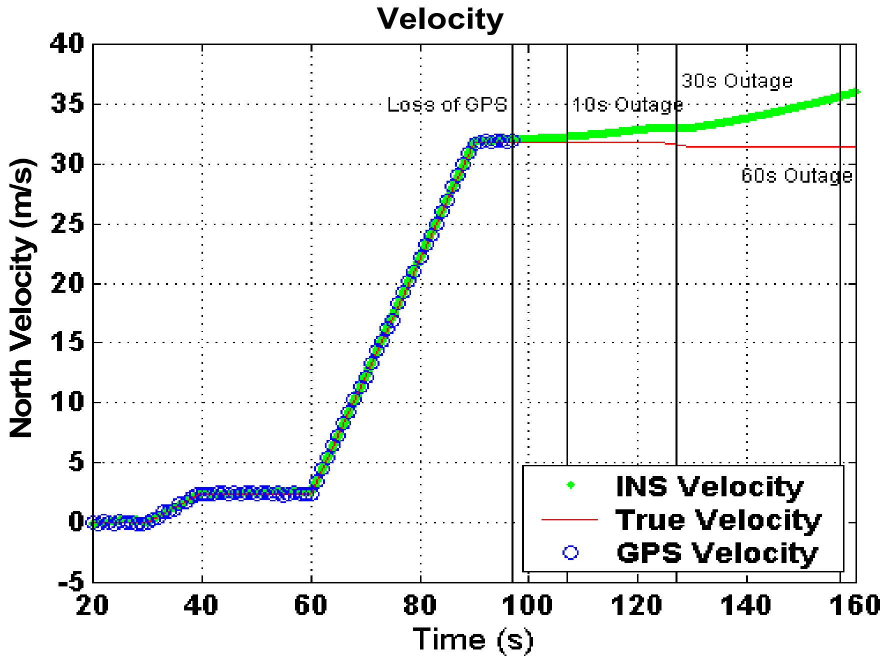

5.2 Example Trades

In each of the following plots, the red bars represent GPS/INS filter outputs using a loosely coupled system with no GPS attitude updates. The grey bars represent GPS/INS filter outputs using a loosely coupled system *including* GPS attitude updates. The yellow bars represent tightly coupled GPS/INS filter output (including GPS attitude updates). The complexity of the filters move from least complex (red) to most complex (yellow).

The height of each bar marks the average error accumulated over the sixty or more data runs for each of three simulated GPS outage lengths: 10 seconds, 30 seconds, and 60 seconds. The standard deviation of these errors in noted on the top of the bars.

The results are grouped for comparison with the nominal tactical grade results. That is, the plots first relate tactical grade results to navigation grade results, then tactical grade results to automotive grade results. In some cases, the comparative magnitude of the errors is so large, that a "zoomed-in" view is included to highlight the difference.

5.2.1 Position Results

Figure 5.3. Tactical Grade v. Navigation Grade Position Results

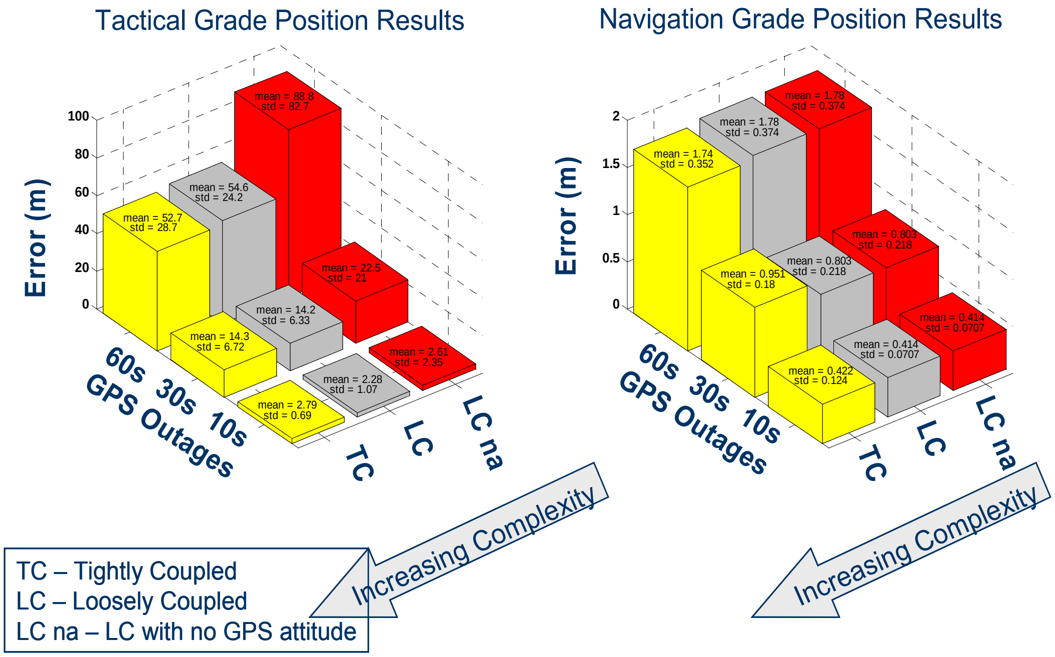

Figure 5.3, as expected, demonstrates the order of magnitude greater performance of the navigation grade systems when compared to the tactical grade systems. The zoomed-in view in Figure 5.4 illustrates this more closely.

The tactical versus navigation position results show a general trend in improvement from the loosely coupled with no attitude (88.8 m error in 60 s, tactical; 1.78 m error in 60 s, navigation) to the tightly coupled (52.7 m error in 60 s, tactical; 1.74 m error in 60 s, navigation). The filter with greater complexity (tightly coupled) is expected to out-perform the less complex filter (loosely coupled). However, note that, for shorter outages in particular, the loosely coupled system beats the tightly coupled system performance for both the navigation (0.80 m, LC in 30 s versus 0.95 m, TC in 30 s) and tactical grade (14.2 m, LC in 30 s versus 14.3 m, TC in 30 s). This is because the tightly coupled filter tends to respond more slowly to disturbances in the system; these variations are most evident near turns. A better model for the accelerometer errors, including misalignment and scale factor errors, would compensate for the differences.

The variations are not as evident in the tactical grade systems because noise on the accelerometers outweigh modeling errors. With the navigation grade sensors, however, the noise is reduced, leaving residual modeling errors to contribute a greater percentage to the overall error result.

Figure 5.4. Tactical Grade v. Navigation Grade Position Results--Zoomed-In View

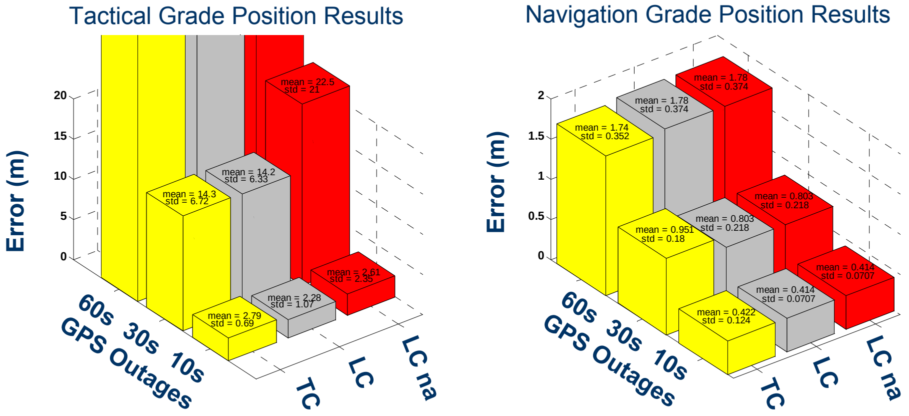

Similar results follow in Figure 5.5 for the tactical grade versus automotive grade sensors. Again the plots show an order of magnitude difference in position errors, as expected, between the tactical grade systems and the automotive grade systems. Figure 5.6 show this more clearly in a zoomed-in view.

Figure 5.5. Tactical Grade v. Automotive Grade Position Results

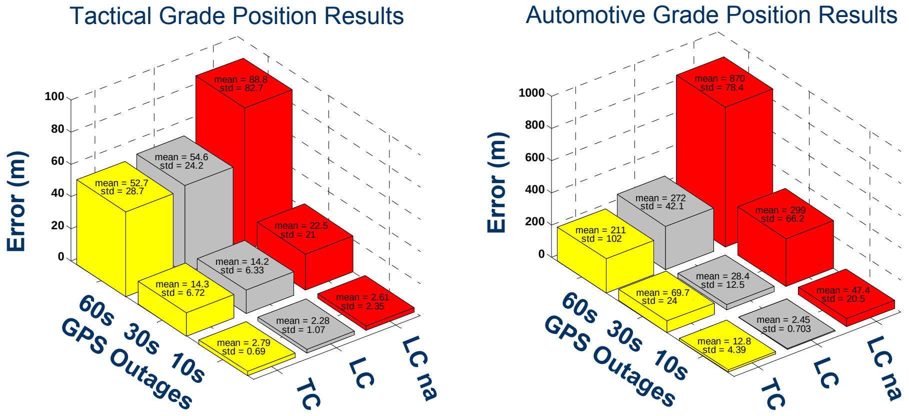

Tactical Grade Position Results

Automotive Grade Position Results

The tactical versus automotive position results show a general trend in improvement from the loosely coupled with no attitude (88.8 m error in 60 s, tactical; 870 m error in 60 s, automotive) to the tightly coupled (52.7 m error in 60 s, tactical; 211 m error in 60 s, navigation). However, as in the tactical versus navigation grade results, there is a discrepancy in this expected trend for the shorter GPS outages--the loosely coupled system outperforms the tightly coupled system. In the automotive case, the loosely coupled systems show a dramatic relative improvement over the tightly coupled systems. For short-term disturbances, the response time of the tightly coupled filter is much slower, resulting in more rapid errors growth.

These position errors may also be more noticeable in the automotive grade systems because of the poor performance of the automotive grade gyroscopes. The velocity and position solutions are very sensitive to errors in the attitude solution. The rapid error growth in attitude due to the lower quality automotive grade gyroscopes (see Figure 5.12) translates into the more rapid velocity and position error growth.

Figure 5.6. Tactical Grade v. Automotive Grade Position Results--Zoomed-In View

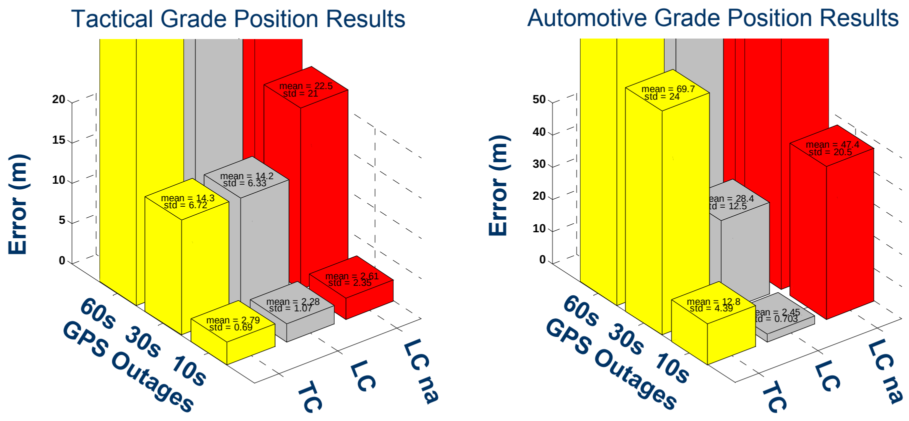

5.2.2 Velocity Results

Figure 5.7 and Figure 5.8 show the velocity results for the tactical grade systems versus the navigation grade systems. As expected, the trends in the velocity results correspond to trends in the position results, discussed in the previous section.

Figure 5.7. Tactical Grade v. Navigation Grade Velocity Results

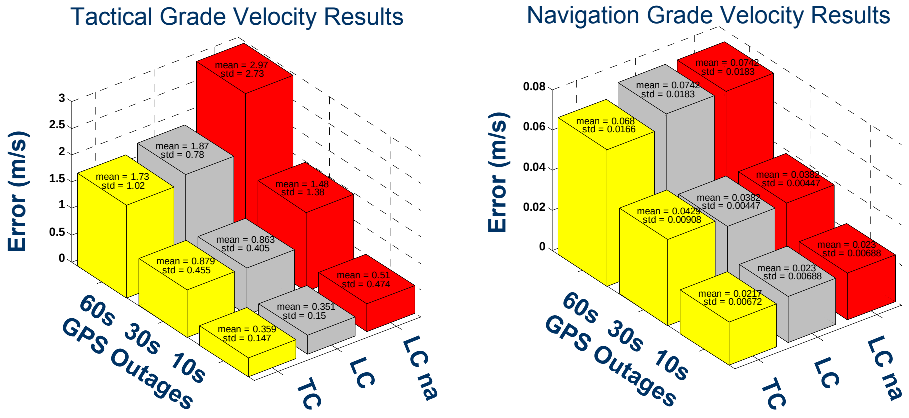

Figure 5.8. Tactical Grade v. Navigation Grade Velocity Results--Zoomed-In View

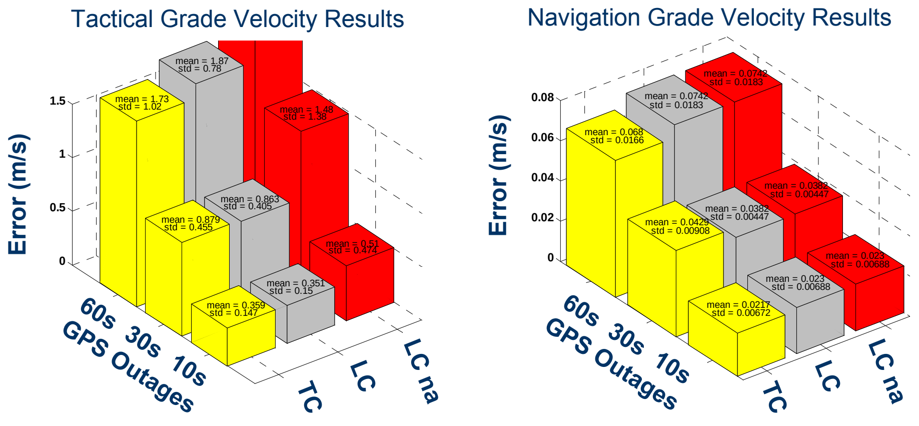

Figure 5.9 and Figure 5.10 show the velocity results for the tactical grade systems versus the automotive grade systems. Again, the trends in the velocity results correspond to trends in the position results, discussed in the previous section.

Figure 5.9. Tactical Grade v. Automotive Grade Velocity Results

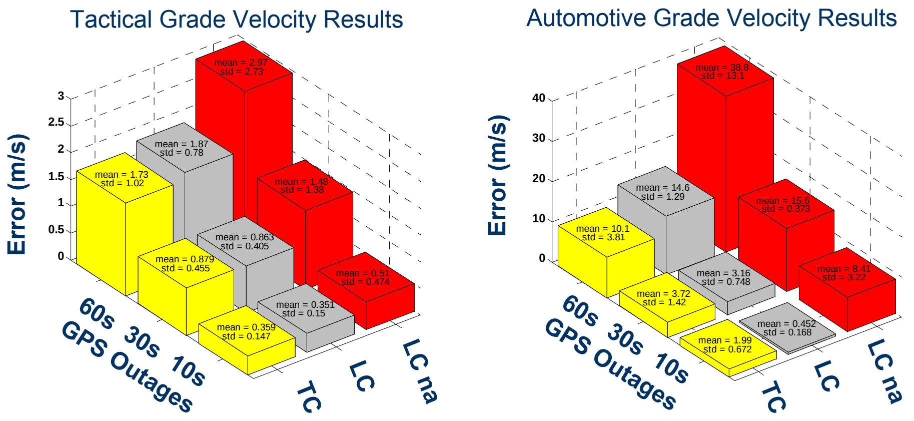

Figure 5.10. Tactical Grade v. Automotive Grade Velocity Results--Zoomed-In View

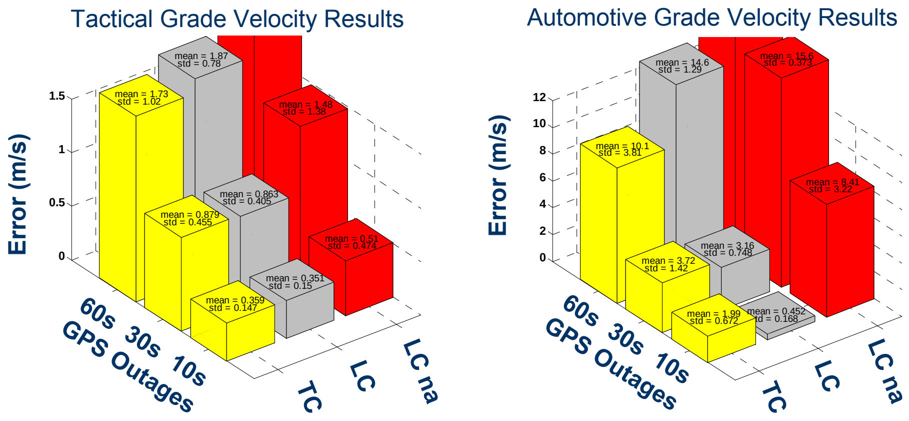

Tactical Grade Velocity Results

Automotive Grade Velocity Results

5.2.3 Attitude Results

Figure 5.11 shows the tactical grade attitude results versus the navigation grade attitude results. The navigation grade errors are an order of magnitude better than the tactical grade errors. Because of the high accuracy in the navigation grade gyroscopes, the attitude errors are small even for the loosely coupled systems with no GPS attitude updates.

The slight improvement in the loosely coupled systems over the tightly coupled systems in the tactical grade case point out the slow response of the tightly coupled filter as seen in the velocity and position results.

Figure 5.11. Tactical Grade v. Navigation Grade Attitude Results

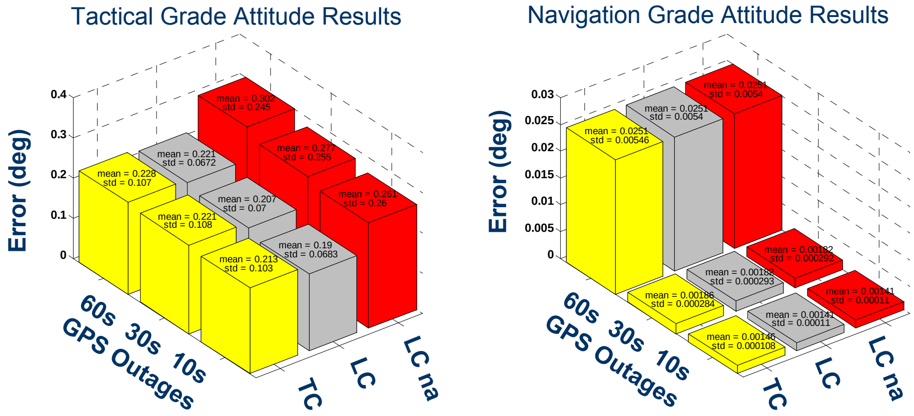

Tactical Grade Attitude Results

Navigation Grade Attitude Results

Figure 5.12 shows the tactical grade attitude results versus the automotive grade attitude results. The tactical grade errors are an order of magnitude better than the automotive grade errors.

As seen in the velocity and position results, the loosely coupled systems (0.22 deg error in 60 s, tactical; 3.68 deg error in 60 s, automotive) slightly outperforms the tightly coupled systems (0.23 deg error in 60 s, tactical; 3.84 deg error in 60 s, automotive). The zoomed-in view of Figure 5.13 shows this more clearly. Even though these error differences are small (~0.2 deg, automotive), they have a large effect on the velocity and position results; the velocity and position solutions are very sensitive to errors in the attitude solution. The rapid error growth in attitude due to the lower quality automotive grade gyroscopes translates into the more rapid velocity and position error growth (see Figure 5.9).

Figure 5.12. Tactical Grade v. Automotive Grade Attitude Results

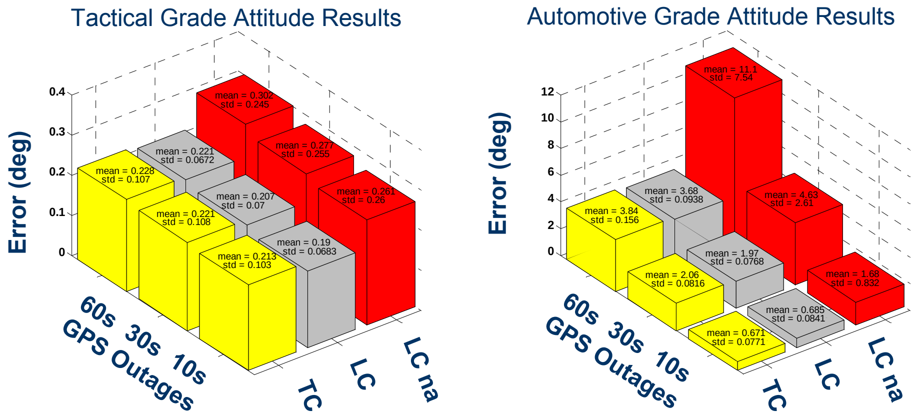

Tactical Grade Attitude Results

Automotive Grade Attitude Results

Figure 5.13. Tactical Grade v. Automotive Grade Attitude Results--Zoomed-In View

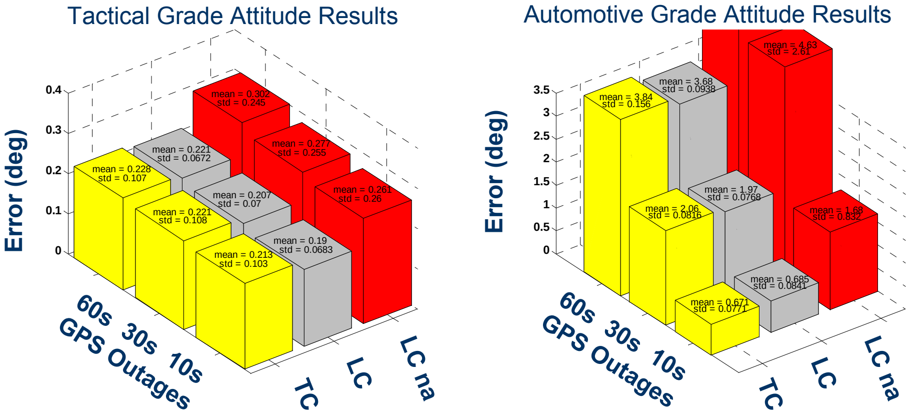

5.3 Summary and Conclusions

Figure 5.14 shows the GPS/INS trade space of accuracy and expense versus complexity of design after charting the results of the trade studies presented in this chapter. GIGET has mapped much of the previously uncharted territory represented by the blue circle. This figure graphically illustrates how GIGET aids in the selection of GPS/INS combinations for any *general* application. The trades presented can be translated to any general set of requirements; the results are not limited to costly point designs for a *specific* application.

The GIGET results of these newly charted integrated navigation systems lead to some general conclusions about GPS/INS combinations. First, the loosely coupled systems generally outperform the tightly coupled systems for short GPS outages. These are side-by-side comparisons of the two systems with similarly tuned Kalman filters and with the same relatively simple sensor error model. The tightly coupled systems may perform better if more complicated error models were introduced; however, the tightly coupled filter is *already* a more complicated filter to implement. When, therefore, is a tightly coupled system recommended? The answer lies in the fundamental advantage of the tightly coupled system--the filter can continue to calibrate INS errors even with less than four satellites in view. The results presented in this chapter include only full GPS outages; once the outage begins, no Kalman filter updates occur for either the tightly coupled or loosely coupled systems. However, if three or less satellites are visible, the tightly coupled system will continue to update, while the loosely coupled system will experience a full GPS outage. Therefore, if the GPS/INS system will be used in an environment where there may be several blocked GPS satellites--such as an urban environment--a tightly coupled system has the advantage. But in general, for less restrictive environments with only rare, short GPS outages, a loosely coupled system would suffice.

Second, the GIGET trades point to conclusions about GPS attitude. GPS attitude adds great complexity of hardware and software to any system. It does, however, give very stable, reliable and accurate attitude information. The addition of attitude measurements acts as a tremendous benefit in GPS/INS systems--especially in lower quality systems. Any GPS/INS system needs an additional heading reference to calibrate yaw gyroscope bias errors [43]. A two-antenna GPS attitude system delivers heading measurements and is much less complicated to operate than a full GPS attitude system. A two-antenna GPS system is a good compromise between its added complexity and its benefits.

Figure 5.14. GPS/INS Trade Space after GIGET Testing

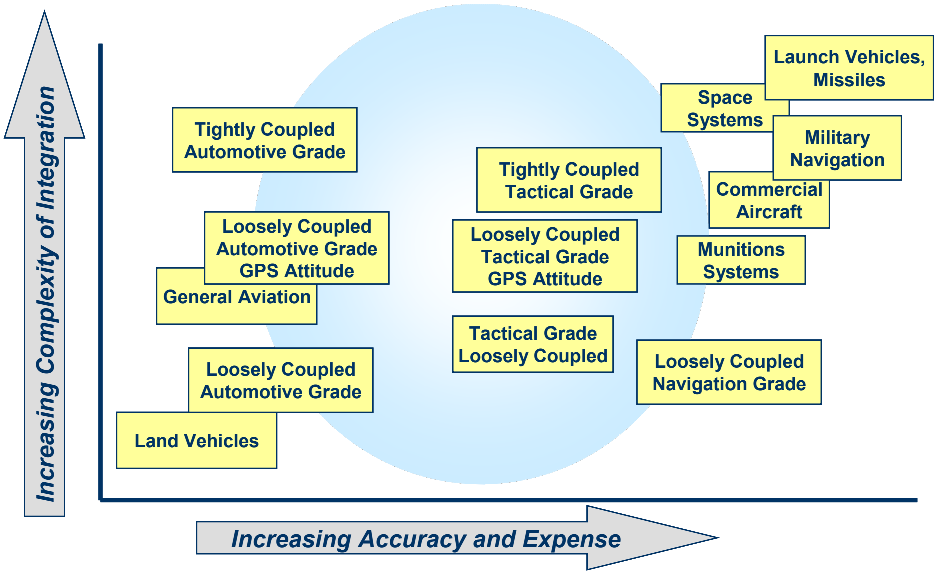
Increasing Complexity of Integration
Tightly Coupled Automotive Grade
Loosely Coupled Automotive Grade GPS Attitude
General Aviation
Loosely Coupled Automotive Grade
Land Vehicles
Tightly Coupled Tactical Grade
Loosely Coupled Tactical Grade GPS Attitude
Tactical Grade Loosely Coupled
Space Systems
Launch Vehicles, Missiles
Military Navigation
Commercial Aircraft
Munitions Systems
Loosely Coupled Navigation Grade
Increasing Accuracy and Expense

Third, the navigation grade systems clearly outperform the lower grade systems. When is the additional cost of a navigation grade system justified? The GIGET results in this document use code-based, differential GPS in all the systems presented. Carrier differential GPS (CDGPS) would deliver even better performance with GPS updates in position on the order of only a few centimeters. If a system requires this level of position accuracy, a navigation grade system combined with CDGPS is the best option, even though this is an expensive combination.

Chapter 6: Case Study: DragonFly UAV

The GIGET comparisons in the previous chapter lead to some strong indicators of GPS/INS integrated systems performance. However, one of the strongest benefits of GIGET is that it is indeed a *hardware* tool set for GPS/INS evaluations. It is flexible, modular and portable enough to be transferred from vehicle to vehicle for real-time GPS/INS testing in the exact environment requiring the integrated navigation design. This is a unique and distinct feature of GIGET that supplies excellent verification for its GPS/INS design recommendations. The DragonFly Unmanned Air Vehicle (UAV) case study presented in this chapter provides an extreme example of the portable utility of GIGET. Not only is the DragonFly environment challenging, but its navigation requirements are strict.

The DragonFly Unmanned Air Vehicle (UAV) Project supports new research and innovations in navigation, fault tolerant control, and multiple vehicle coordination. It is an experimental test-bed that consists of multiple UAVs with modular onboard avionics packages. The DragonFly is an excellent vehicle platform to demonstrate the utility of the GIGET system. This application presents a difficult set of design constraints--issues such as size, power, weight, and structural integrity emerge as driving design factors. Once airborne, the flight test environment itself is harsh and demands a robust system; one that is built to withstand high and low frequency vibration, electromagnetic interference, temperature variations, and the occasional high descent rate landing. Although the DragonFly flight environment is very challenging, it still requires a very accurate and reliable navigation system for the support of multiple controls experiments. GIGET was flown on the DragonFly UAV and used as a tool to design and recommend an appropriate GPS/INS navigation package.

This chapter describes the DragonFly UAV in more detail and presents the GIGET results from DragonFly flight testing. A brief summary of the results and some recommendations for the DragonFly Project are included. These recommendations for the DragonFly address some of the UAV specific challenges for a navigation system that only could have been evaluated with a hardware tool set, such as GIGET, flown in the exact UAV environment.

Figure 6.1. DragonFly UAV Project

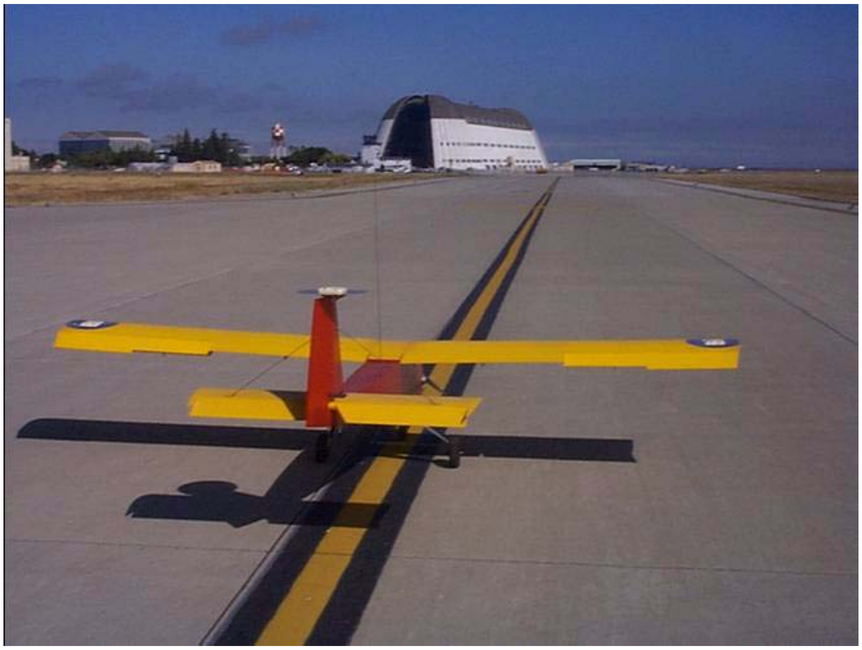

6.1 Project Motivation

Currently, unmanned air vehicles (UAVs) are attracting a large degree of interest in the navigation and control communities. Not only do UAVs provide excellent low-cost test-beds for navigation system experiments [55][56], but their design and control facilitate the exploration of many exciting new research areas in control theory, ranging from low-level flight control algorithm design and mode switching experiments [57][58] to high-level multiple aircraft coordinated mission planning [59][55]. Applications of UAVs include remote monitoring of traffic, search and rescue operations, weather prediction, and use as a test-bed for new algorithms and technologies for automated air traffic control, such as airborne navigation and surveillance using GPS and VHF datalink.

A core benefit of the use of a UAV test-bed is the reduced risk of harm to the operators. Safety issues are dramatically reduced when the human is removed from the cockpit. Advanced autopilot systems that may one day be FAA approved for airline use can be developed and tested with much lower risk on UAVs. Unusual aerodynamic configurations and distributed control systems may be implemented quite easily on a UAV, but can become prohibitive due to cost and complexity when applied to larger aircraft. The DragonFly UAV provides a unique and versatile test-bed for these advanced control technologies.

The DragonFly Project is managed by the Hybrid Systems Lab at Stanford University. The Hybrid Systems Lab is uniquely qualified to take full advantage of the DragonFly test-bed. The lab has tremendous experience with distributed control systems, air traffic management, flight simulation, etc. [55]. The DragonFly test-bed offers a complete package with software development capability and tools, aircraft controls development and modeling experience, and experimental hardware test platforms.

Figure 6.2. DragonFly UAV

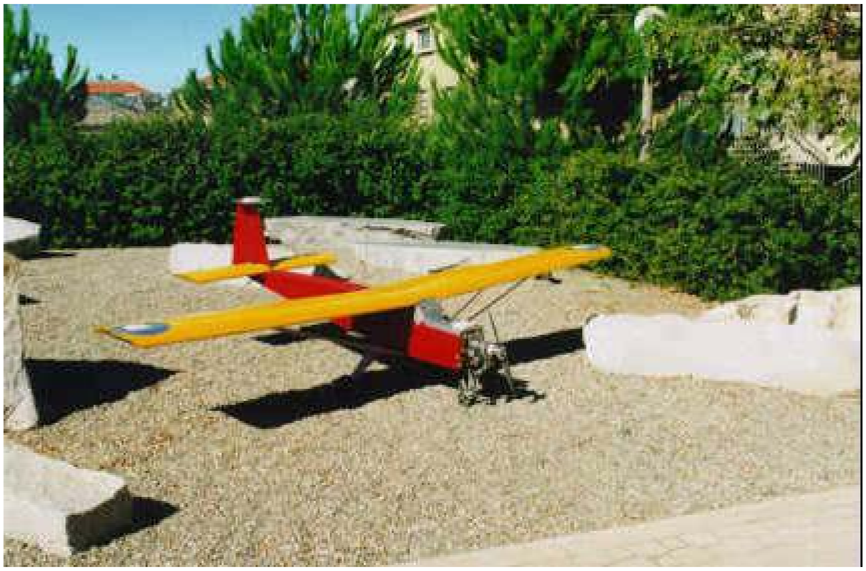

6.2 Aircraft Description

The GIGET system was tested and flown on the first DragonFly UAV, DragonFly I, or “Big Red.” The DragonFly I aircraft is 8 feet long with a twelve-foot wingspan. It is radio-controlled and constructed primarily of plywood with a fabric covering. It features the standard wing-tail configuration with tricycle landing gear. The airplane is powered by a 4.5 horsepower two-stroke, single cylinder engine on which is mounted a single-piece 20 inch diameter propeller and spinner. A single, 10 Hz actuator, actuates each control surface [25].

The GIGET avionics box was fitted into the forward section of the fuselage as seen in Figure 6.3. The DragonFly can carry approximately ten pounds of electronics and sensors as payload. Fully aerobatic, the DragonFly has a full suite of unique equipment not normally found on your typical model airplane. Four Trimble Navigation GPS patch antennas have been installed--one on each wing tip, one on the top of the vertical tail, and one on the top of the forward fuselage. A fifth, mounted on the underside of the airplane, could be used for GPS satellite tracking even during aerobatic maneuvers. The four GPS antennas on top of the aircraft connect to the GIGET receiver to provide GPS position, velocity and attitude measurements during flight operations.

Figure 6.3. GIGET Avionics Box and DragonFly Fuselage

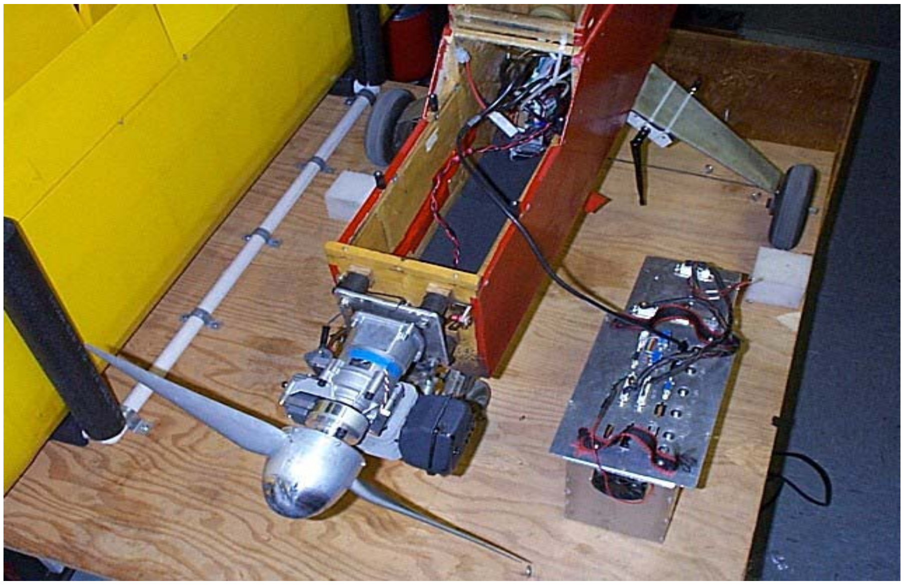

Also included are a radio modem antenna installed on the fuselage underneath the horizontal tail, a well-shielded and isolated 50.82 MHz radio receiver used for pilot inputs with a whip antenna installed on top of the fuselage, and a 2.4 GHz onboard video system installed on the main landing gear struts. Figure 6.4 presents an overall view of the location of the radio frequency (RF) equipment. Additional equipment installed on the aircraft, but not used by GIGET include a variometer used for airspeed measurement, an engine RPM sensor, and an angle-of-attack/beta vane used to determine attitude of the airplane relative to the oncoming air. These analog inputs can be routed through an onboard A/D converter and combined with the other sensor data for flight control experiments.

Figure 6.4. DragonFly Radio Frequency Equipment Locations

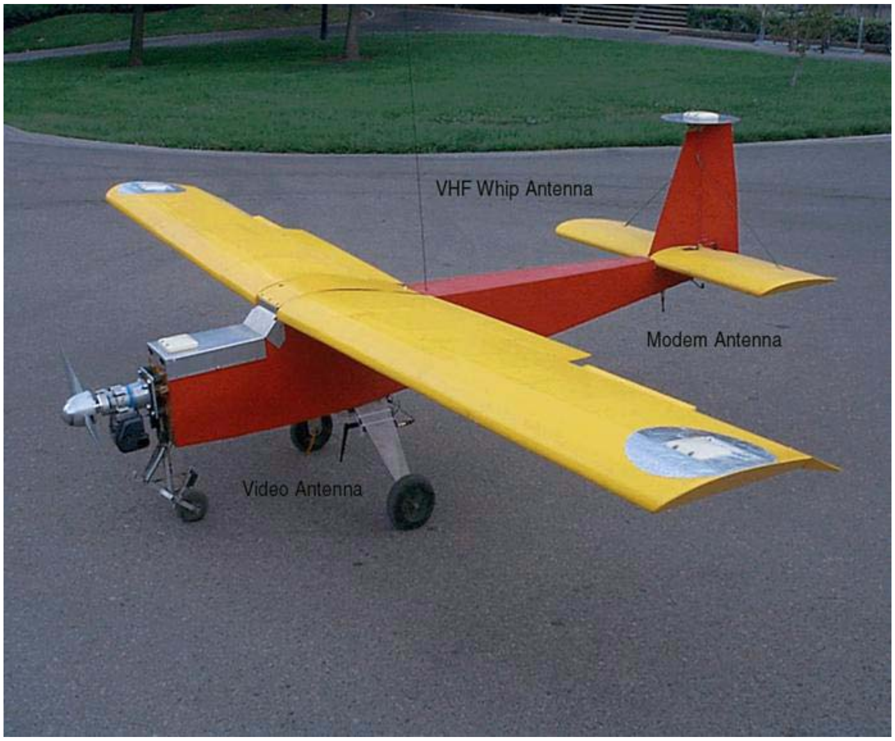

One of the many uses of the new avionics will be to enable fully autonomous flight of the DragonFly. In order for the airplane to function both autonomously and as a normal remotely piloted vehicle, an embedded processor was designed to control the actuators with commands originating from either the onboard computer or the onboard radio receiver. Designated as the Actuator Control Computer (ACC), and based on a PIC 16C76 microprocessor, the Stanford-designed and fabricated ACC monitors the pulse width modulated (PWM) signal that originates from the pilot. The pilot can switch to either manual or autonomous flight through the transmitter. The ACC is shown in Figure 6.5. The ACC will only pass the PWM to the actuators if the pilot is controlling the airplane. If the ACC senses the switch to autonomous mode, the ACC will read the actuator commands from a standard serial input from the onboard flight control computer, convert the commands to PWM, and then send these signals to the actuators. The pilot can take over from the computer at any time. The ACC was designed to be compact in size and frugal with the power, without unnecessary functionality. The ACC is a point design for a very specific function, but may easily adapt from one UAV platform to the next.

Figure 6.5. Actuator Control Computer

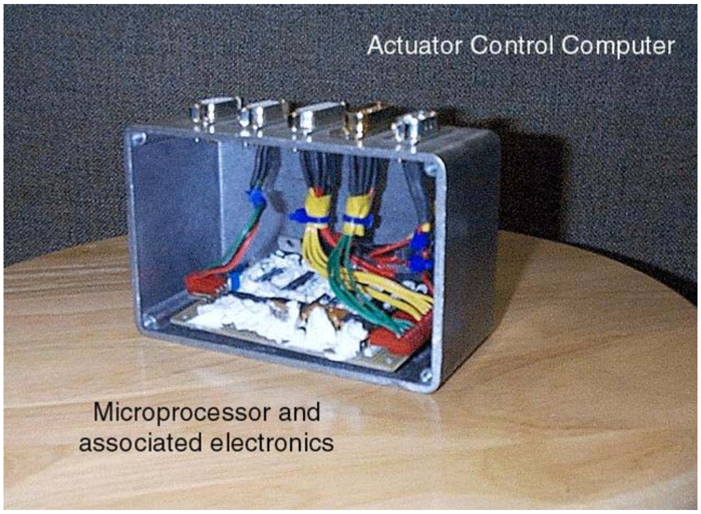
Actuator Control Computer
Microprocessor and associated electronics

With all of this electronic equipment onboard, the power requirements can be a limiting factor; however, only two battery packs are required to power all of the above mentioned RF transmitters, the ACC, and GIGET avionics package. One battery pack consists of five, D-cell sized NiCad batteries providing a nominal 6 VDC to the ACC, the actuators, and the 50.82 MHz radio receiver. The second battery pack consists of 10 D-cell sized NiCad batteries providing a nominal 12 VDC for the remainder of the onboard electronics. With all systems up and operating, the batteries will provide approximately two hours of flight time. This more than exceeds the normal 20-minute flight duration provided by the onboard fuel.

In order to reduce electromagnetic interference (EMI) caused by the magneto ignition system, a shielded spark plug cap has been installed on the engine. No EMI is apparent when the system is operating.

6.3 DragonFly Project Requirements

The DragonFly project requires a very accurate and reliable navigation system for the support of multiple controls experiments to test real-life air traffic scenarios such as closely spaced parallel approaches (CSPA) [60][61], or cooperative flight path planning, approach traffic alerting, blunder recovery, and the testing escape maneuvers. Although a navigation system using GPS alone may be suitable for some testing, more complicated control system experiments may need a more robust system that benefits from the blending of GPS with inertial sensors [6].

However, the environmental challenges of the DragonFly project combined with its strict navigation sensor error requirements make the selection of the best GPS/INS package difficult. GIGET is uniquely suited for this GPS/INS selection task because it is a *hardware* evaluation tool as well as a software tool set. There are difficulties and challenges due to the DragonFly test environment that no software-only tool set for the navigation system selection could evaluate. Because GIGET can be flown in the exact DragonFly environment, the design evaluation process is more complete.

Because the DragonFly Project is a platform for research in control systems and autopilot design, a primary measure of its test performance should be in flight technical error and total system error. The navigation sensor error should be as small a contributing factor as possible to the total error. DragonFly researchers should be able rely on an accurate navigation system and focus efforts on the control design and the reduction of flight technical errors.

6.3.1 Dynamic Performance

The DragonFly UAV is capable of relatively high dynamics, and its control systems will require navigation sensor updates at a high enough rate to compensate. Although it has been demonstrated that a navigation update rate of 10 Hz is sufficient for automatic landings [6], higher dynamic modes may become more evident in other DragonFly control systems testing. It is difficult or impossible to find a reliable GPS only system for complete navigation with more than a 10 Hz output. Therefore, a blended GPS/INS sensor package is required. Most GPS/INS systems have an update rate of at least 50 Hz and even up to 600 Hz or higher.

6.3.2 Accuracy

The DragonFly UAV currently only needs an navigation system with accuracy of less than 2 meters. The control experiments currently being tested are single aircraft tests that do not require automatic landings. However, for future testing with multiple aircraft in close proximity, or for research in automatic landing systems [6], the DragonFly will require a navigation sensor error of 0.5 meters (one sigma).

6.3.3 Availability, Continuity and Integrity.

Although the DragonFly projects are too varied and experimental in nature to give precise requirements in availability, continuity and integrity, its performance must be stable and consistent through outages of GPS of 10 seconds or less. The current flight testing for the DragonFly does not include aerobatics or any radical maneuvers or dynamics, so outages or blockages in GPS satellite visibility should be rare. However, the navigation system should seamlessly provide the required sensor performance during any short GPS outages.

6.3.4 Maintainability

The DragonFly Project is primarily a platform for research in controls and UAV operations. The navigation system needs to be consistent and reliable, and not a difficult system to maintain and expand. The hardware should be easily adapted for multiple UAVs and a variety of system tests. DragonFly researchers should not have to redesign the navigation package for every different flight controls experiment explored. They also should not be required to be navigation system experts to use, adapt, or upgrade the GPS/INS avionics and software systems.

6.3.5 Environment

The DragonFly UAV presents an extremely harsh physical environment for electronic systems. Not only are the systems required to be small and lightweight (less than 2500 cubic centimeters and less than ten pounds), but they must also survive in high temperature, high vibrations, and potentially high electromagnetic interference (EMI). The avionics must fit into a small section of the fuselage (Figure 6.3) or an adjacent pod (DragonFly III pod in Figure 7.3). The aircraft engine generates considerable vibration and EMI and is in close proximity to the avionics package.

6.3.6 Power

The DragonFly UAV can only carry enough batteries to provide 20 Watts of power to the navigation system (not including additional electronics) for one to two hours (see Chapter 6.2).

6.3.7 Cost

The DragonFly Project is funded through university grants and an extremely expensive navigation system is not feasible. However, given all the other challenging requirements, a navigation system cost of around $15,000 is still practical and economical.

6.4 DragonFly UAV Testing

Algorithms for cooperative flight path planning, approach traffic alerting, blunder recovery, and design of escape maneuvers will be designed and tested on the DragonFly UAV test-bed. The project goals are to test several real-life air traffic scenarios such as closely spaced parallel approaches (CSPA) in the DragonFly test-bed. Flight testing of the DragonFly UAVs takes place at Moffett Federal Airfield. Moffett provides a protected yet expansive area to test the vehicle.

Figure 6.6. DragonFly UAV Flying at Moffett Federal Airfield

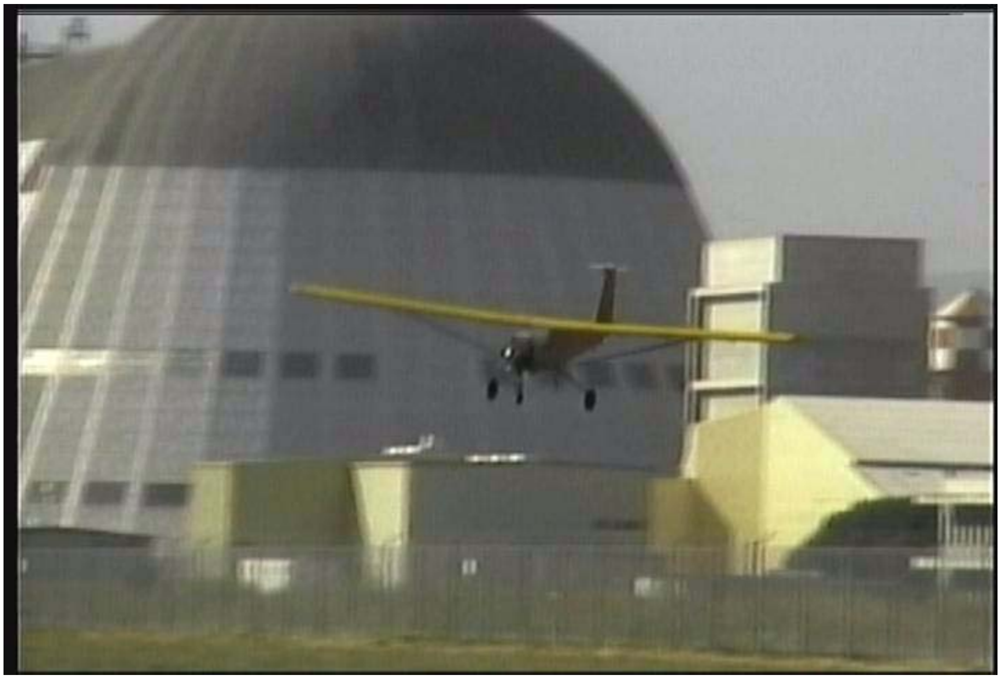

6.4.1 GROUND SYSTEMS

During flight testing, GIGET sends collected data down through the on-board radio modem to the GIGET ground station. The telemetered data include inertial measurement unit data, raw GPS observables, computed navigation and attitude solutions, timing information, and other sensor packets. The ground reference receiver sends code-based, differential GPS corrections to GIGET through the radio modem link at a 1 Hz rate. All ground components are packaged in a large portable suitcase with a battery and power distribution system for easy transport and use in the field. Figure 6.7 shows the ground station suitcase and ruggedized laptop.

Figure 6.7. Ground System Suitcase and Laptop

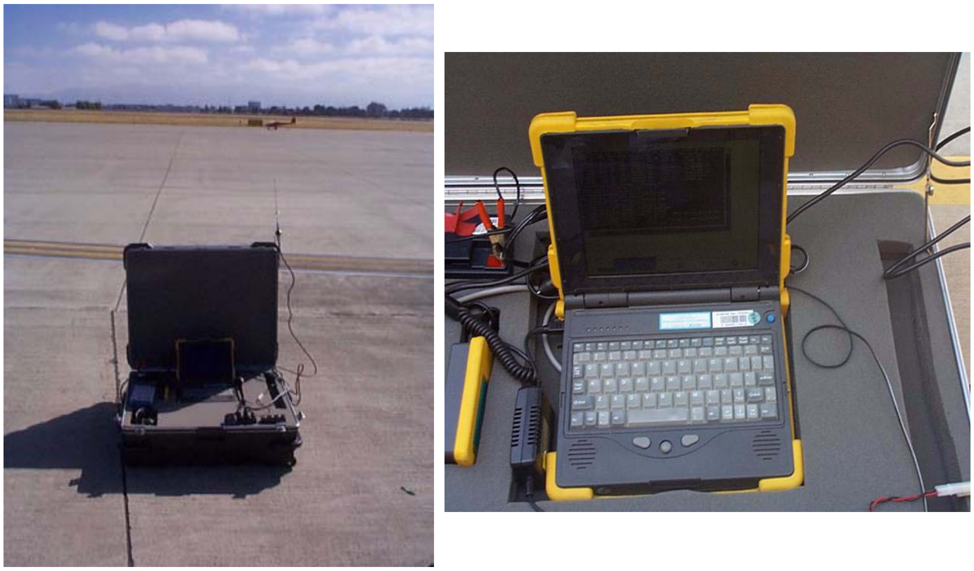

6.4.2 Flight Test Profile

Figure 6.8 shows a profile from a typical test flight for the DragonFly with the GIGET onboard. For the GIGET experiments, the remote RC pilot is in control of the UAV at all times. The pilot flies the airplane to altitude and trims to level flight. He then flies several passes overhead the airfield. Limited by the onboard fuel, the DragonFly aircraft can remain in flight for around 20 minutes. Even during these short flights with relatively low dynamics, GPS satellites can come in and out of view during steeply banked turns.

Figure 6.8. DragonFly Flight Profile

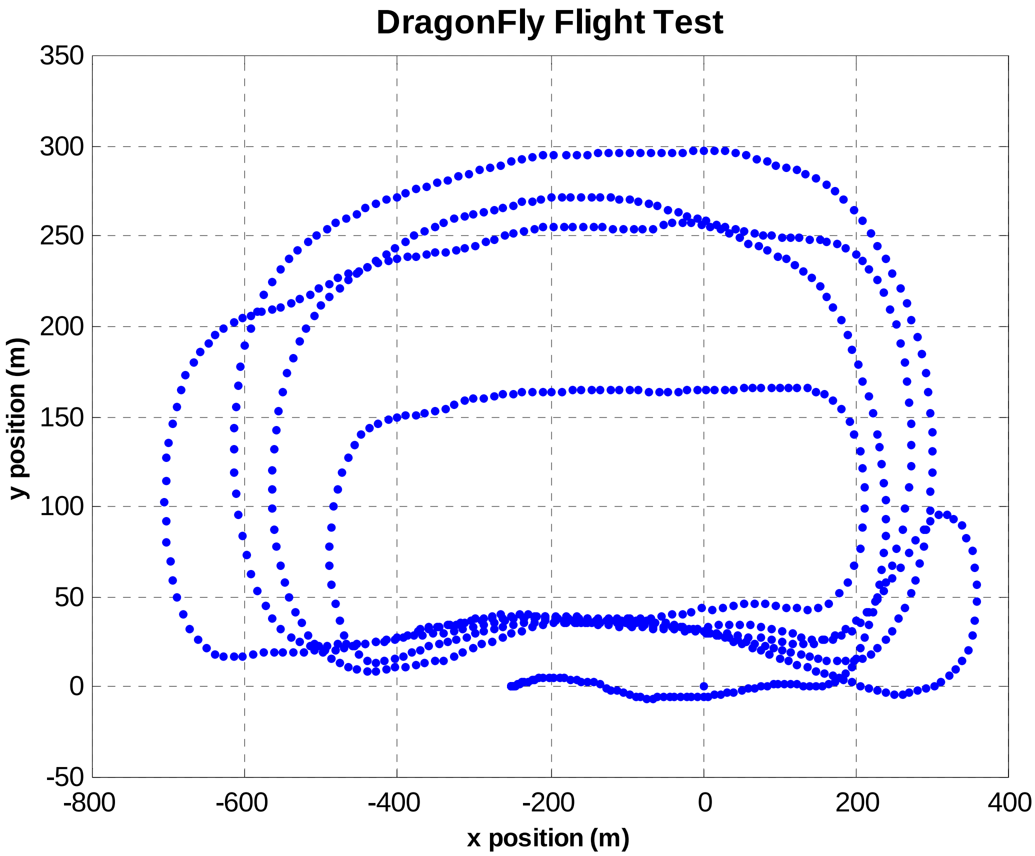

6.5 Experimental Results

The following charts represent typical performance of three GIGET navigation system solutions during the DragonFly flight testing. The GIGET outputs from all three filters are position, velocity and attitude. The following charts display the error in these navigation solution outputs given an induced GPS outage for 10 seconds, 30 seconds, and then 60 seconds. To determine the error in the solutions, the GIGET outputs are measured against a post-processed carrier differential GPS solution that acts as the system "truth." To generate the GIGET outputs, each navigation filter discussed uses the Psi-Angle mechanization method for the integration of the inertial measurements. Chapter 4 describes this inertial navigation solution method in more detail. The three filter outputs are all initialized at a known position and attitude at the start of the flight test.

The differences in the three filters lie in the measurements used. The first filter, represented by the dark-green color bars in Figure 6.9, Figure 6.10 and Figure 6.11, is a loosely coupled filter using GPS position, velocity and attitude to update an extended Kalman filter as described in Chapter 4, Section 4.2.3. The second filter, represented by the light-green color bars, is identical to the first loosely coupled filter, but has only GPS position and velocity updates provided to the extended Kalman filter. The third set of solutions, represented by the yellow bars, is also identical to the first filter, except that it incorporates *unfiltered* inertial measurements. The vibration environment of the DragonFly is extremely high, and the GIGET avionics box is located very close to the source of the vibration--the DragonFly 2-stroke engine. Even with extensive vibration isolation of the inertial measurement unit, the IMU could easily sense the vibration noise of the engine. The raw acceleration data from the IMU clearly indicated a noise source at exactly the engine rpm. To remove the engine noise, the raw inertial data were filtered with a simple Butterworth filter. This third set of navigation solutions (yellow bars) is included to demonstrate just how application and environment specific the performance of a GPS/INS system can be.

6.5.1 Attitude Results

Since there is no “truth” system for the attitude results, other than GPS attitude solutions or post-processed CDGPS solutions for each antenna, the absolute results presented in Figure 6.9 are less informative than the relative results between the three filter systems tested. In comparing the green bars (loosely coupled with and without GPS attitude) to the yellow bars (pre-filtered IMU inputs), there is not a large difference in performance between the filtered or unfiltered systems. The high performing gyroscopes in the tactical grade IMU are not as affected by engine vibration as are the accelerometers. Although the velocity results *are* greatly affected by the vibration, the INS attitude solution is not heavily dependent on the velocity errors (see Chapter 4, Section 4.2.3.2); therefore, the GIGET attitude solutions remain very similar. The results also indicate that for the typical DragonFly flight scenario and for short outages, the loosely coupled solution with a single antenna performs almost as well as the loosely coupled solution using GPS attitude. At a minimum, however, any INS system will need a external heading reference (either GPS derived or other) to maintain calibration on the yaw gyroscopes [43].

Figure 6.9. DragonFly Attitude Results

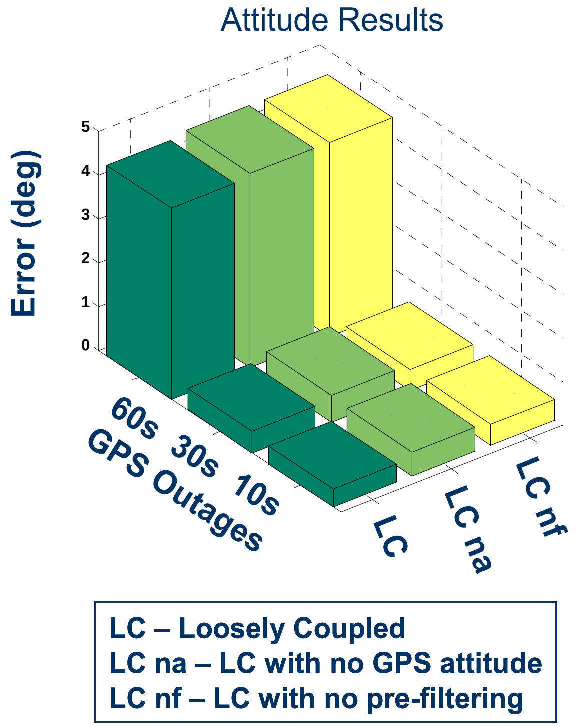

6.5.2 Velocity Results

Figure 6.10 shows the GIGET velocity solution results. The loosely coupled solution (dark-green bars) gives the best results with the velocity errors growing to 7.3 m/s after 60 seconds of a GPS outage. The loosely coupled velocity solution without GPS attitude (light-green) errors tend to grow much faster to around 9.5 m/s. This points to the dependence of the velocity results on an accurate estimate of attitude; the small errors in attitude quickly degrade velocity errors. Even during the short flight duration, the addition of a direct measurement of the attitude greatly benefits the estimation of the gyro-biases and hence attitude errors.

Figure 6.10. DragonFly Velocity Results

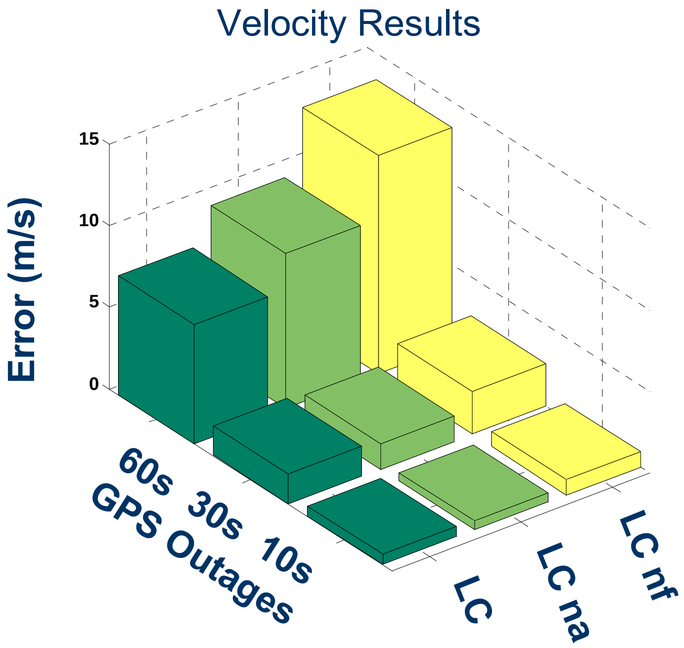

6.5.3 Position Results

The DragonFly position results in Figure 6.11 show similar trends to the velocity results. However, the affect of pre-filtering the IMU measurements becomes even more apparent in the position results. In the case of a 60 second GPS outage, the position errors for the non-filtered case (yellow) are almost 3 times the size of both pre-filtered cases.

Figure 6.11. DragonFly Position Results

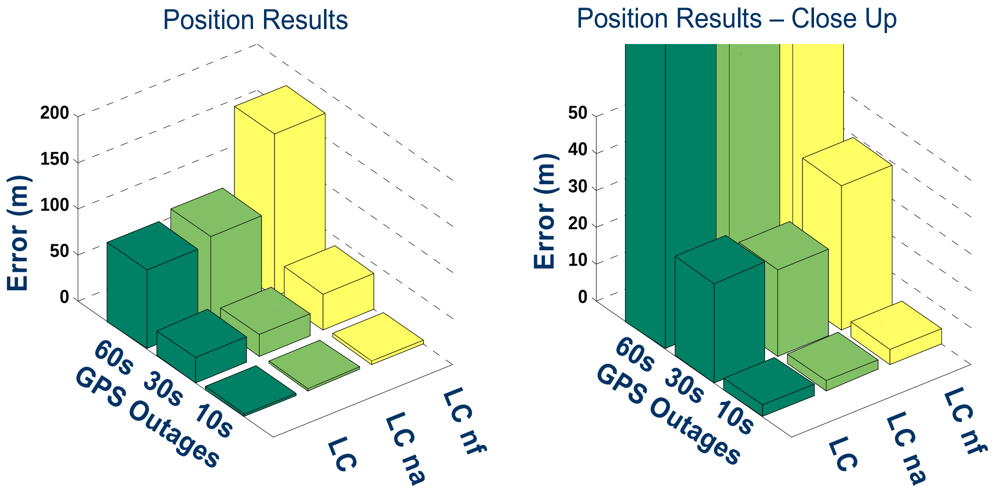

6.6 DragonFly Conclusions and Recommendations

With the DragonFly requirement of less than two meters of accuracy, and flight conditions that demand a sturdy, reliable, easy-to-maintain system, I recommend a loosely coupled GPS/INS package with a single GPS antenna. The loosely coupled algorithms require less processing power and do not require sophisticated knowledge of GPS raw observables to implement. A tightly coupled system is preferable for areas where partial GPS outages occur frequently; however, the DragonFly typically does not experience many GPS outages during the short flight times of its current flight test profile.

With only rare GPS outages greater than 10 seconds, an IMU of tactical grade quality provides more than enough accuracy. A lower quality IMU may be appropriate, but an automotive grade sensor package would not perform well in the challenging DragonFly environment.

A single GPS antenna is sufficient for the DragonFly, as long as another sensor is used as a heading reference. The DragonFly is easily initialized at a known, surveyed location before flight testing. GPS attitude and multiple antennas add a level of complexity to the system and would be difficult to maintain or expand to additional aircraft.

These recommendations are sufficient for the current DragonFly flight testing scenarios. However, if the DragonFly experiments expand to include automatic landing system design, or multiple-aircraft close formations, the navigation accuracy requirements would be much more strict (less than 0.5 meters); therefore, the GPS/INS system would need to be of higher performance. For these high-accuracy cases, I recommend a carrier differential GPS system for centimeter-level GPS accuracy, providing much improved GPS/INS calibration and tuning.

Chapter 7:
Future Work and Conclusions

The previous chapters have discussed the development of each of three tiers of GIGET (see Figure 7.1), its applications in a trade study, and its use as a hardware evaluation tool in the DragonFly UAV. This chapter summarizes the GIGET conclusions and presents some future uses, applications, and improvements.

Figure 7.1. Three GIGET Tiers

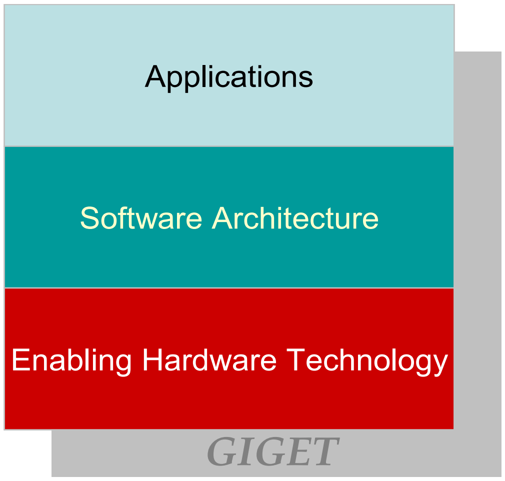

7.1 Summary of Conclusions

GPS and INS are complimentary navigation systems. Blending GPS with INS can remedy the performance issues of both; however, the many types of integration methods and sensors have made it difficult to determine the best GPS/INS combination for any desired application. Most of the integrated systems built to date have been point designs for very *specific* applications. GIGET aids in the selection of sensor combinations for any *general* application or set of requirements; hence, GIGET is the generalized way to evaluate the performance of integrated navigation systems.

GIGET can be described by three distinct levels or tiers. The first tier of GIGET involves the building and assembly of the innovative hardware that creates the foundation for the remaining GIGET levels. It is this enabling technology that gives the underlying modularity and flexibility of GIGET. The enabling technology includes a unique, five-antenna, forty-channel GPS receiver providing GPS attitude, position, velocity, and timing. An embedded computer with modular real-time software blends the GPS measurements with sensor information from a Honeywell HG1700 tactical grade inertial measurement unit. GIGET is quickly outfitted onto a variety of vehicle platforms to experimentally test and compare navigation performance.

The second GIGET tier covers the flexible software architecture that delivers the real-time capability to support the multiple GIGET, GPS/INS applications. GIGET comprises not only avionics hardware and ground systems, but also a vast array of lab equipment and computers for testing, simulation, and analysis. GIGET's software architecture enables the transparent networking between all these components, and it delivers the real-time capability to support the simultaneous, multiple GIGET experiments. The flexible nature of the software architecture allows for the seamless real-time switching of antenna inputs for roving master GPS attitude solutions and multiple-antenna GPS for INS integration.

The third GIGET level is the application layer where algorithms demonstrate various uses of GIGET. Loosely coupled and tightly coupled algorithms are examples of GPS aiding of INS calibration. GIGET is uniquely designed to implement INS aiding of GPS: the ultra-tightly coupled or deep integration algorithms. However, INS aiding of GIGET receivers is currently limited to pre-positioning and acquisition aiding, and requires a firmware redesign to include carrier tracking loop aiding.

7.1.1 The Evaluation Tool

In side-by-side experiments, GIGET compares loosely coupled and tightly coupled integrated navigation schemes that blend navigation, tactical, or automotive grade inertial sensors with GPS. These results formulate a trade study to map previously uncharted territory of the GPS/INS space that trades accuracy and expense versus complexity of design. Figure 7.2 shows this GPS/INS trade space after the GIGET trade study; the blue circle represents the previously uncharted territory. These GIGET results can be used to determine acceptable sensor quality in these integration methods for a variety of dynamic environments.

The GIGET results of these newly charted integrated navigation systems lead to some general conclusions about GPS/INS combinations. First, the loosely coupled systems generally outperform the tightly coupled systems for short GPS outages. However, a fundamental advantage of the tightly coupled system is that the filter can continue to calibrate INS errors even with less than four satellites in view. Therefore, if the GPS/INS system will be used in an environment where there may be several blocked GPS satellites--such as an urban environment--a tightly coupled system has the advantage. But in general, for less restrictive environments with only rare, short GPS outages, a loosely coupled system would suffice.

Figure 7.2. GPS/INS Trade Space after GIGET Testing

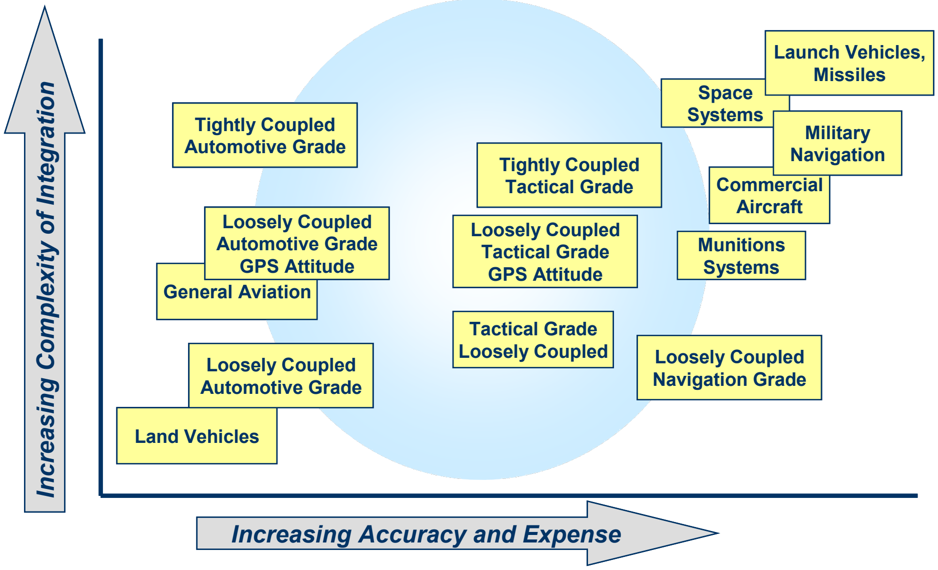

Increasing Complexity of Integration
Increasing Accuracy and Expense
Tightly Coupled Automotive Grade
Loosely Coupled Automotive Grade GPS Attitude
General Aviation
Loosely Coupled Automotive Grade
Land Vehicles
Tightly Coupled Tactical Grade
Loosely Coupled Tactical Grade GPS Attitude
Tactical Grade Loosely Coupled
Space Systems
Launch Vehicles, Missiles
Military Navigation
Commercial Aircraft
Munitions Systems
Loosely Coupled Navigation Grade

Second, the GIGET trades point to conclusions about GPS attitude. GPS attitude adds great complexity of hardware and software to any system; however, a two-antenna GPS system is a good compromise between its added complexity and its benefits.

Third, the navigation grade systems clearly outperform the lower grade systems. If a system requires position accuracy on the order of a few centimeters, a navigation grade system combined with CDGPS is the best option, even though this is an expensive combination.

7.1.2 DragonFly UAV

As a demonstration of its utility as a hardware evaluation tool, GIGET is used to design a navigation system on the DragonFly Unmanned Air Vehicle (UAV). The GIGET recommendations for the DragonFly address some of the UAV specific challenges for a navigation system that only could have been evaluated with a hardware tool set, such as GIGET, flown in the exact UAV environment.

The DragonFly UAV is a test-bed for autonomous control experiments. It is a small, lightweight, highly maneuverable aircraft that requires smooth, continuous navigation information. GIGET was flown on the DragonFly to evaluate different integrated navigation combinations in the UAV's dynamic environment. GIGET shows that a loosely coupled, single-antenna GPS system with a moderately priced inertial unit will provide the consistent navigation currently needed on the DragonFly.

Future applications of the DragonFly test-bed involve the flying of multiple DragonFlies. Figure 7.3 shows the latest UAV additions to the DragonFly test-bed: DragonFly II, and DragonFly III. Both are outfitted with the new avionics systems that incorporate GIGET navigation system recommendations.

Figure 7.3. DragonFly II and III

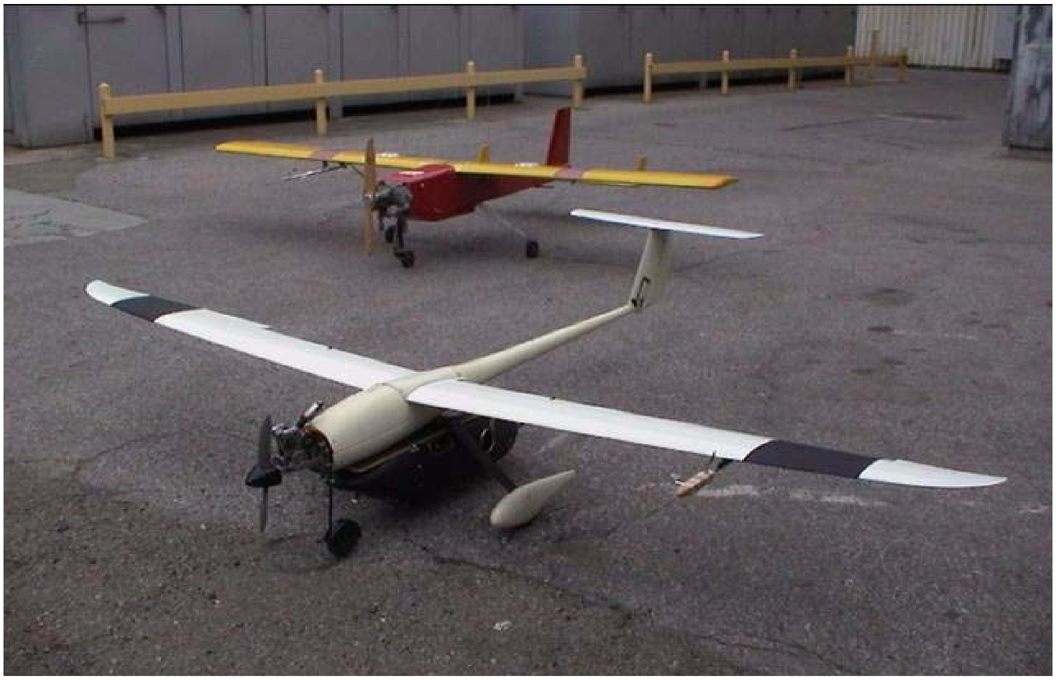

7.2 Future Work

Because GIGET is easily transported and quickly outfitted onto a variety of vehicle platforms, there are many future experiments where GIGET can test and compare navigation performance.

There are also several improvements that may be considered to make GIGET an even better evaluation tool.

7.2.1 Farm Tractor

The most recent use of GIGET is on the Trimble Navigation farm vehicle. Trimble markets equipment for the guidance and autonomous control of farm vehicles. The Trimble system uses high-precision GPS combined with fairly low-cost inertial sensors. Recently, Trimble was selecting new gyroscopes to place in the farm tractor autopilot system. GIGET was outfitted on the tractor in a set of experiments and used to compare the competing gyroscope replacements. Figure 7.4 shows some of the tractor testing results.

Figure 7.4. Farm Tractor Testing with GIGET

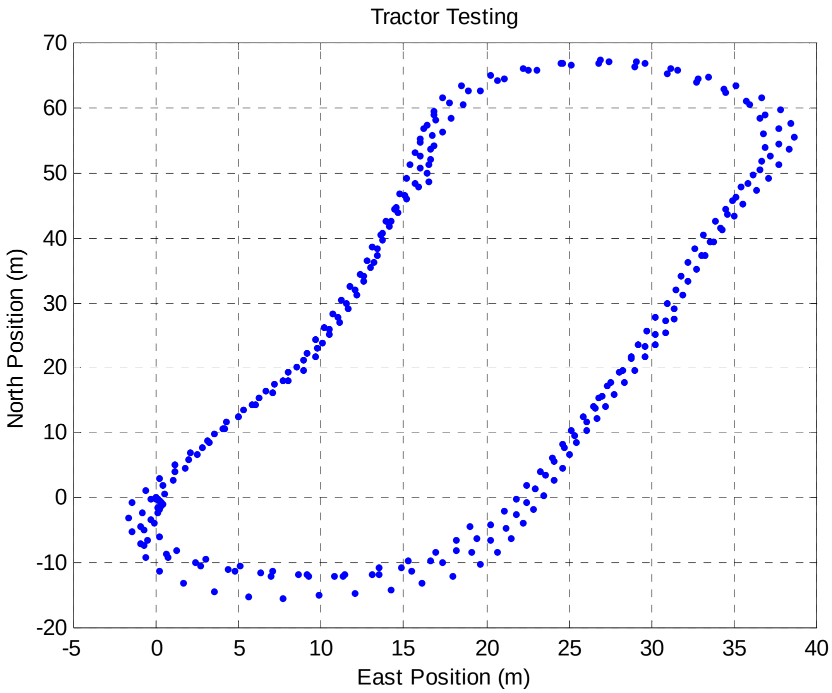

Figure 7.5 shows GIGET "on the farm," after being mounted on the Trimble tractor. The test set-up was easy, and the entire GIGET avionics and pre-calibrated antenna array was mounted and ready to collect data within an hour.

Figure 7.5. Trimble Navigation Farm Tractor with GIGET

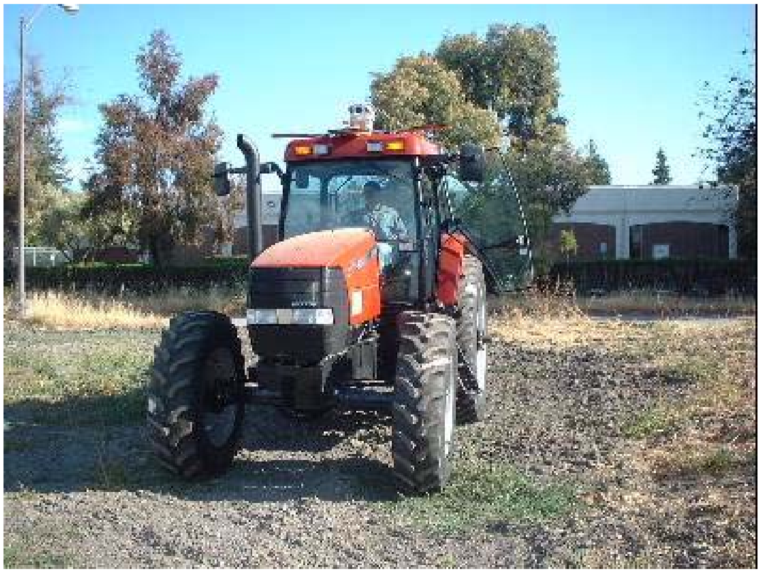

7.2.2 IMPROVEMENTS

GIGET has proven to be a unique and useful tool for the evaluation of GPS/INS integrated navigation systems. There are, however, improvements to make GIGET's performance and utility even better. I recommend the following:

- Completely re-write the GIGET receiver firmware to incorporate inertial aiding. Currently, the inertial aiding options in GIGET are limited, and the legacy software inside the receivers make it difficult to integrate aiding at the carrier tracking loop level.
- Use a high quality inertial measurement unit that is not ITAR (International Traffic in Arms Regulations) restricted. The tactical grade IMU currently used with GIGET performs very well, but it is export controlled, limiting its portability.

References

[1] H. Shoemaker. NAVSTAR Global Positioning System. In *Proceedings of the IEEE 1975 National Aerospace and Electronics Conference*, Dayton, OH, June 1975, pp. 351-4.

[2] D. Knight. The Rapid Development of Tightly-Coupled GPS/INS Systems. In *Proceeding of the IEEE Position Location and Navigation Symposium,* Atlanta, GA, April 1996, pp. 300-5.

[3] K. P. Schwarz, N. El-Sheimy. *KINGSPAD User's Manual*. University Technologies International, Inc., Calgary, Alberta, Canada, April 2000.

[4] CAST Navigation LLC. *CAST-4000 Specifications*. August 2001.

[5] H. Gelderloos, S. Sheikh, B. Schipper. GPS Attitude System Integrated with an Inertial System for Space Applications. In *Proceedings from the 20th Annual AAS Guidance and Control Conference*. Breckenridge, Colorado, February 1997, AAS 97-001.

[6] P. Y. Montgomery. *Carrier Differential GPS as a Sensor for Automatic Control.* Ph.D. Thesis, Stanford University, August 1996.

[7] R. C. Hayward, D. Gebre-Egziabher, M. Schwall, J. D. Powell, J. Wilson. Inertially Aided GPS-Based Attitude Heading Reference System (AHRS) for General Aviation Aircraft. In *Proceedings of the Institute of Navigation GPS Conference*, Kansas City, MO, September 1997, pp. 1415-24.

[8] D. Gebre-Egziabher, R. C. Hayward, J. D. Powell. A Low-Cost GPS/Inertial Attitude Heading Reference System (AHRS) for General Aviation Applications. In *Proceeding of the IEEE Position Location and Navigation Symposium,* Rancho Mirage, CA, April 1998, pp. 518-25.

[9] D. Bevly. *High Speed, Dead Reckoning, and Towed Implement Control for Automatically Steered Farm Tractors Using GPS*. Ph.D. Thesis, Stanford University, September, 2001.

[10] S. Alban. An Inexpensive and Robust GPS/INS Attitude System for Automobiles. In *Proceedings of the Institute of Navigation GPS Conference*, Portland, OR, September 2002, pp. 1075-87.

[11] E. Martin. Aiding GPS Navigation Functions. In *Proceedings of the IEEE 1976 National Aerospace and Electronics Conference*, Dayton, OH, May 1976, pp. 849-56.

[12] R. W. Carroll, W. A. Mickelson. Velocity Aiding of Noncoherent GPS Receiver. In *Proceedings of the IEEE 1977 National Aerospace and Electronics Conference*, Dayton, OH, May 1977, pp. 311-8.

[13] H. L. Jones, T. J. MacDonald. Comparisons of High Anti-Jam Design Techniques for GPS Receivers. In *Proceedings of the IEEE 1978 National Aerospace and Electronics Conference*, Dayton, OH, May 1978, pp. 39-46.

[14] W. S. Widnall. Alternate Approaches for Stable Rate Aiding of Jamming Resistant GPS Receivers. Presented at *The IEEE 1979 National Aerospace and Electronics Conference,* Dayton, OH, May 1979.

[15] P. Ward. GPS Receiver RF Interference Monitoring, Mitigation, and Analysis Techniques. *Navigation: Journal of the Institute of Navigation*, Vol. 41, No. 4, Winter 1994-1995, pp. 367-91.

[16] J. W. Sennott, D. Senffner. The Use of Satellite Geometry for Prevention of Cycle Slips in a GPS Processor. *Navigation: Journal of the Institute of Navigation*, Vol. 39, No. 2, Summer 1992, pp. 217-35.

[17] J. W. Sennott, D. Senffner. *Navigation Receiver with Coupled Signal Tracking Channels*. U.S. Patent 5,343,209, August 1994.

[18] R. E. Phillips, G. T. Schmidt. GPS/INS Integration. In *Advisory Group for Aerospace Research and Development Lecture Series-207*, Paris, France, July 1996, pp. 9-1-17.

[19] L. Vallot. *Requirements on Inertial Aiding Signals for GPS Receivers*. Honeywell Correspondence, Minneapolis, MN, January 1996.

[20] C. T. Bye, G. L. Hartmann. Development of a FOG-based GPS/INS. In *Proceeding of the IEEE Position Location and Navigation Symposium*, Rancho Mirage, CA, April 1998, pp. 264-71

[21] Northrop Grumman Navigation Systems. *LN-270 Specifications*. Retrieved from http://www.ngnavsys.com/Html/LN-270, May 2003.

[22] S. Alban, D. M. Akos, S. M. Rock, D. Gebre-Egziabher. Performance Analysis and Architectures for INS-Aided GPS Tracking Loops. In *Proceedings of the Institute of Navigation National Technical Meeting*, Anaheim, CA, January 2003.

[23] C. E. Cohen. *Attitude Determination Using GPS*. Ph.D. Thesis, Stanford University, December 1992.

[24] Carnegie Mellon Software Engineering Institute. *Client/Server Software Architectures--An Overview*. Retrieved from http://www.sei.cmu.edu/str/descriptions/clientserver_body.html, May 2003.

[25] J. Evans, S. Houck, G. McNutt, and B. Parkinson. Integration of a 40 Channel GPS Receiver for Automatic Control into an Unmanned Airplane. In *Proceedings of the Institute of Navigation GPS Conference*, Nashville, TN, September 1998, pp. 1173-80.

[26] G. Wahba. A Least-Squares Estimate of Spacecraft Attitude. *SIAM Review*, Vol. 7, No. 3, July, 1965, p. 409.

[27] Markley, F. L. Attitude Determination Using Vector Observations and the Singular Value Decomposition. *Journal of the Astronautical Sciences,* Vol. 36, No. 3, July-Sept., 1988, pp. 245-58.

[28] L. M. Ward. *Spacecraft Attitude Estimation Using GPS: Methodology and Results*. Ph.D. Thesis, University of Colorado, Boulder, 1996.

[29] P. Axelrad. GPS-Based Attitude Determination. In *The Institute of Navigation GPS Tutorial*, Nashville, TN, September 1998.

[30] R. Fuller, S. Gomez, L. Marradi, J. Rodden. GPS Attitude Determination From Double Difference Differential Phase Measurements. In *Proceedings of the Institute of Navigation GPS Conference*, Kansas City, MO, September 1996, pp. 1073-9.

[31] F. Van Graas, M. Braasch. GPS Interferometric Attitude and Heading Determination: Initial Flight Test Results. *Navigation: Journal of the Institute of Navigation*, Vol. 38, No. 4, Winter 1991-1992, pp. 297-316.

[32] B. Parkinson, J. J. Spilker. *Global Positioning System: Theory and Applications,* Vol. 1 and Vol. 2. AIAA, Washington, DC, 1996.

[33] C. Park, I. Kim, J. G. Lee, G. I. Jee. Efficient Ambiguity Resolution Using Constraint Equation. In *Proceeding of the IEEE Position Location and Navigation Symposium*, Atlanta, GA, April 1996, pp. 277-84.

[34] D. Knight. A New Method of Instantaneous Ambiguity Resolution. In *Proceedings of the Institute of Navigation GPS Conference,* Salt Lake City, UT, September 1994, pp. 707-16.

[35] D. Knight. *Method and Apparatus for Maximum Likelihood Estimation Direct Integer Search in Differential Carrier Phase Attitude Determination Systems*. U.S. Patent 5,296,861, March 1994.

[36] C. D. Hill, H. J. Euler. An Optimal Ambiguity Resolution Technique for Attitude Determination. In *Proceeding of the IEEE Position Location and Navigation Symposium*, Atlanta, GA, April 1996, pp. 262-69.

[37] G. M. Siouris. *Aerospace Avionics Systems: A Modern Synthesis*. Academic Press, Inc., San Diego, CA, 1993.

[38] A. Weinred, I. Y. Bar-Itzhack. The Psi-Angle Error Equation in Strapdown Inertial Navigation Systems. *IEEE Transactions on Aerospace and Electronic Systems*, Vol. AES-14, No. 3, May, 1978.

[39] S. I. Snyder. Integration of Satellite Navigation Systems (GPS) with Inertial Navigation Systems. In *Advisory Group for Aerospace Research and Development Lecture Series*, Ankara, Turkey, September, 1997, AGARD Contract # 2C78210.

[40] Y. C. Lee, D. G. O'Laughlin. A Performance Analysis of a Tightly Coupled GPS/Inertial System for Two Integrity Monitoring Methods. In *Proceedings of the Institute of Navigation GPS Conference*, Nashville, TN, September 1999, pp. 1187-200.

[41] M. Wei, K. P. Schwarz. A Strapdown Inertial Algorithm Using an Earth-Fixed Cartesian Frame. *Navigation: Journal of the Institute of Navigation*, Vol. 37, No. 2, Summer 1990, pp. 153-67.

[42] K. R. Britting. *Inertial Navigation Systems Analysis*. Wiley-Interscience, New York, NY, 1971.

[43] D. Gebre-Egziabher. *Design and Performance Analysis of a Low-Cost Aided Dead Reckoning Navigator*. Ph.D. Thesis, Stanford University, December 2001.

[44] D. Titterton, J. Weston. *Strapdown Inertial Navigation Technology*. Peter Peregrinus Ltd. on behalf of the Institution of Electrical Engineers, London, England, 1997.

[45] I. Y. Bar-Itzhack, N. Berman. Control Theoretic Approach to Inertial Navigation Systems. *AIAA Journal of Guidance, Control, and Dynamics*, Vol. 11, May-June 1988, pp. 237-45.

[46] A. Gelb. *Applied Optimal Estimation*. MIT Press, Cambridge, MA, 1974.

[47] E. D. Kaplan. *Understanding GPS Principles and Applications*. Artech House, Norwood, MA, 1996.

[48] J. A. Farrell, M. Barth. *The Global Positioning System & Inertial Navigation*. McGraw-Hill, New York, NY, 1998.

[49] M. Braasch. *Inertial Navigation System (INS) Toolbox for Matlab Manual*. GPSoft, Athens, OH, 2000.

[50] K. P. Schwarz, M. Wei. Aided Versus Embedded A Comparison of Two Approaches to GPS/INS Integration. In *Proceeding of the IEEE Position Location and Navigation Symposium*, Las Vegas, NV, April 1994 pp. 314-23.

[51] R. DiEsposti, S. Saks, L. Jocic, A. Abbott. The Benefits of Integrating GPS, INS, and PCS. In *Proceedings of the Institute of Navigation GPS Conference*, Nashville, TN, September 1998, pp. 327-331.

[52] J. M. Przyjemski, P. L. Konop. Limitations on GPS Receiver Performance Imposed by Crystal-Oscillator g-Sensitivity. In *Proceedings of the IEEE 1977 National Aerospace and Electronics Conference*, Dayton, OH, May 1977, pp. 319-22.

[53] G. Lennen. *Higher Order Carrier Tracking Loop Design for Enhanced Enigma Operation During Increased Solar Cycle Activity*. Trimble Navigation Report, October, 1998.

[54] R. Jaffe, E. Rechtin. Design and Performance of Phase-Lock Circuits Capable of Near-Optimum Performance Over a Wide Range of Input Signal and Noise Levels. *IRE Transactions on IT*, March 1955, pp.66-76.

[55] J. Evans, G. Inalhan, J.S. Jang, R. Teo, and C. Tomlin. DragonFly:A Versatile UAV Platform for the Advancement of Aircraft Navigation and Control. In *Proceedings of the 20th IEEE Digital Avionics Systems Conference*, October 2001.

[56] J. Evans, W. Hodge, J. Liebman, C. Tomlin, and B. Parkinson. Flight Tests of an Unmanned Air Vehicle with Integrated Multi-Antenna GPS Receiver and IMU: Towards a Testbed for Distributed Control and Formation Flight. In *Proceedings of the Institute of Navigation GPS Conference*, Nashville, TN, September 1999, pp 1799-808.

[57] E. Hallberg, I. Kaminer, A. Pascoal. Development of a Flight Test System for Unmanned Air Vehicles. *IEEE Control Systems Magazine*, Vol. 19, No. 1, February 1999, pp. 55-65.

[58] H. Shim, T. J. Koo, F. Hoffmann, S. S. Sastry. A Comprehensive Study on Control Design of Autonomous Helicopter. In *Proceedings of the IEEE Conference on Decision and Control*, Florida, December 1998.

[59] D. F. Chichka, J. L. Speyer. Solar Powered Formation-Enhanced Aerial Vehicle Systems for Sustained Endurance. In *Proceedings of the IEEE American Control Conference, Philadelphia*, June 1998.

[60] S. Houck. *Multi Aircraft Dynamics, Navigation and Operation*. Ph.D. Thesis, Stanford University, December 2001.

[61] R. Teo, C. J. Tomlin. Provably Safe Evasive Maneuvers against Blunders in Closely Spaced Parallel Approaches. In *Proceedings of the AIAA Guidance, Navigation and Control Conference*. Montreal, Canada, August 2001, AIAA 2001-4293